UNIVERSIDAD AUTÓNOMA DE BAJA CALIFORNIA

FACULTAD DE CIENCIAS MARINAS

INSTITUTO DE INVESTIGACIONES OCEANOLÓGICAS

PAPEL DE LOS MICROORGANISMOS PLANCTÓNICOS EN EL FLUJO DE CARBONO EN UNA REGIÓN DE SURGENCIA FRENTE A LA COSTA NORTE DE BAJA CALIFORNIA, MÉXICO

T E S I S

QUE PARA CUBRIR PARCIALMENTE LOS REQUISITOS NECESARIOS PARA OBTENER EL GRADO DE

DOCTOR EN CIENCIAS EN OCEANOGRAFIA COSTERA

PRESENTA

LORENA PATRICIA LINACRE ROJAS

ENSENADA, BAJA CALIFORNIA, MEXICO. ENERO DEL 2011.

RESUMEN

El presente documento de tesis es la evidencia del trabajo de investigación desarrollado durante aproximadamente 4 años y medio dentro del programa de doctorado en Oceanografía Costera de la Facultad de Ciencias Marinas/Instituto de Investigaciones Oceanológicas, de la Universidad Autónoma de Baja California. En este escrito se muestran las principales técnicas utilizadas, los resultados generados provenientes de observaciones de campo y las conclusiones que permitieron evaluar el papel de las comunidades de microorganismos planctónicos en el ciclo del carbono de las aguas costeras de la parte norte de la Península de Baja California, México. Este documento científico ha sido organizado de la siguiente manera: un capítulo introductorio que presenta al lector los principales antecedentes científicos relacionados al ciclo del carbono, como también la justificación de éste trabajo que conllevaron al planteamiento de los objetivos de este trabajo. El capítulo 1 donde se caracterizaron físico y químicamente las aguas costeras frente a Ensenada, Baja California, México, con el objetivo de establecer los principales procesos oceanográficos relacionados a los flujos de carbono, como asimismo, el marco ambiental que modula las interconexiones del ecosistema pelágico en esta región costera. El capítulo 2, donde se hace referencia a la componente específica de las tramas tróficas microbianas, denominada "el enlace microbiano", particularmente, la dinámica temporal de sus poblaciones autótrofas y heterótrofas y su contribución dentro del ciclo del carbono en esta región costera. El capítulo 3, donde se determinó la dinámica temporal de la producción primaria taxonómicamente específica y su impacto por el pastoreo del microzooplancton como una vía de transferencia de carbono dentro de la zona eufótica de esta región costera. Finalmente, un capítulo de conclusiones que permitió establecer una idea global sugerida por los principales resultados científicos encontrados a lo largo de éste estudio.

Palabras claves: flujo de carbono, microorganismos planctónicos, surgencia.

FACULTAD DE CIENCIAS MARINAS
INSTITUTO DE INVESTIGACIONES OCEANOLÓGICAS
POSGRADO EN OCEANOGRAFIA COSTERA

PAPEL DE LOS MICROORGANISMOS PLANCTÓNICOS EN EL FLUJO DE CARBONO EN UNA REGIÓN DE SURGENCIA FRENTE A LA COSTA NORTE DE BAJA CALIFORNIA, MÉXICO

T E S I S

QUE PARA CUBRIR PARCIALMENTE LOS REQUISITOS NECESARIOS PARA OBTENER EL GRADO DE

DOCTOR EN CIENCIAS

PRESENTA

LORENA PATRICIA LINACRE ROJAS

Aprobada por:

Dr. Jose Martin Hernández Ayón
Director

Dr. José Rubén Lara Lara
Sinodal

Dr. Michael R. Landry
Sinodal

Dr. Ramón Cajal Medrano
Sinodal

Dra. Rosa Reyna Mouriño Pérez
Sinodal

DEDICATORIA

A mis dos amores, mi esposo Reginaldo y mi hija Isabella, por caminar junto a mi con amor y paciencia este sendero lleno de aprendizaje y de experiencias valiosas. Los amo!!

AGRADECIMIENTOS

Gracias mi familia por su apoyo incondicional y por estar siempre a mi lado en las buenas y en las malas!!! Sin su ayuda jamás lo habría podido lograr, muchas gracias, los quiero mucho!!!!

Agradezco enormemente a todo mi comité de tesis conformado por los co-directores, Dr. J. Martín Hernández-Ayón y Dr. J. Rubén Lara-Lara, como asimismo los sinodales, Dr. Michael Landry, Dr. Ramón Cajal-Medrano y Dra. Rosa Reyna Mouriño Pérez, por ser parte fundamental en mi formación académica a lo largo de este doctorado y por el tiempo invertido en las correcciones realizadas a este documento de tesis.

Particularmente, agradezco al Dr. J. Martín Hernández-Ayón, por su apoyo incondicional en todo momento y por siempre alentarme a trabajar pese a todos los tropiezos que hubo en el andar. Gracias Martín por tu amistad!!!

Agradezco especialmente al Dr. Michael Landry de Scripps, UCSD, por abrirme las puertas de su laboratorio y brindarme la oportunidad de aprender técnicas novedosas, trasmitiéndome su experiencia en campo y laboratorio que fue fundamental para el desarrollo de este trabajo de tesis. Gracias además por su gran contribución al artículo científico publicado en JPR y a los valiosos comentarios hechos al primer borrador del manuscrito correspondiente al Capítulo 3 de ésta tesis. Asimismo, agradezco a su estudiante de doctorado Andrew Taylor como a su técnico Daniel Wick por el entrenamiento otorgado en el procesamiento y análisis de imágenes de muestras nano y microplanctónicas obtenidas con microscopía de epifluorescencia.

Agradezco a la técnica de CICESE, Oc. Carmen Bazán-Guzmán, por su apoyo fundamental en todas las actividades de campo y laboratorio, por su gran disposición de ayuda y por sobre todo su amistad. Gracias Carmen!!!

Agradezco a los técnicos de CICESE, Oc. Martín de la Cruz-Orozco y Oc. César Almeda-Jáuregui como también, al técnico de IIO-UABC, Oc. Arturo Siqueiros-Valencia por su gran ayuda en todas las actividades de campo a bordo del B/O Francisco de Ulloa.

Agradezco a las “chicas del CO_2”, Gaby, Ana, Norma, Candy y Daniela, por su valioso trabajo en campo y laboratorio en la generación de los datos químicos utilizados en este trabajo y sobre todo por su alegría y amistad!!! Gracias Chicas!!

Agradezco a la Biol. Patricia García-García de la Facultad de Ciencias, UABC, por el análisis de muestras de fitoplancton mediante microscopía invertida, en las instalaciones del IIO.

Agradezco al Dr. Víctor Camacho-Ibar del IIO, UABC, por el análisis de nutrientes en las instalaciones del IIO.

Agradezco al grupo del seminario de Oceanografía Química del Cuerpo Académico de Oceanografía Química, Biogeoquímica y Contaminación del Medio Ambiente Marino del IIO, UABC, en especial al Dr. Francisco Delgadillo y el Dr. Miguel Ángel Huerta, por brindarme la oportunidad de participar en éste constructivo foro de discusión que significó un aporte a mi trabajo de tesis.

Agradezco al Laboratorio de Microbiología Experimental de CICESE, por el apoyo brindado a través de la Dra. Rosa Reyna Mouriño-Pérez y sus estudiantes, en el entrenamiento y la utilización del microscopio invertido de epifluorecencia para el análisis de muestras de fitoplancton.

Agradezco al Laboratorio Húmedo de Acuicultura de CICESE, en especial a la Dra. Beatriz Cordero-Esquivel y la Dra. M. del Pilar Sánchez-Saavedra, por brindarme un espacio en su laboratorio para la realización de experimentos biológicos que formaron parte de esta tesis. Asimismo, agradezco a los técnicos Adrián Celaya-Ortega y Norberto Flores-Acevedo, por su gran apoyo brindado en la implementación de materiales requeridos en estos experimentos.

Agradezco al Dr. Ernesto García-Mendoza, y a todos los miembros de su laboratorio, Héctor, Lupita, Carolina, Luis, Patty, Jenny, por brindarme la oportunidad de aprender y utilizar la técnica de HPLC, y que me permitió generar los datos mostrados en el Capítulo 3 de este documento de tesis.

Agradezco a la tripulación del B/O Francisco de Ulloa por el tiempo y esfuerzo dedicado durante todos los cruceros, y en especial a los marineros de la embarcación menor GENUS, Luis Demetrio Arce-Valenzuela e Iván Castro-Navarro, por su grandísima ayuda en la recuperación de los experimentos realizados en el mar. Asimismo, agradezco enormemente a todos los investigadores, técnicos y estudiantes de CICESE y UABC que participaron en todas las campañas del proyecto FLUCAR, cuyo trabajo fue crucial para el éxito no solo de éste proyecto sino también, de mi trabajo de tesis. En especial agradezco a todos aquellos que me ayudaron en las filtraciones de los experimentos de campo y laboratorio, Leonardo, Lupita, Víctor, Edwin y Anita, sinceramente gracias sin su apoyo no lo habría logrado!!!

A mis amigos, César Barragán y Elena Enríquez por abrirme incondicionalmente las puertas de su casa con alegría y diversión, pero por sobre todo por brindarme su hermosa amistad, gracias!!!

A mis compañeros de cubículo, Ricardo Cruz y Nancy Saavedra por brindarme su amistad y compañerismo a lo largo de todo este tiempo, sinceramente gracias!!!

A mi amiga y compatriota Susana Zambra por su amistad y su gran ayuda en todo momento que lo necesité, gracias de todo corazón!!!

A la Sra. Maribel porque sin ella no habría podido seguir este camino, gracias por su ayuda en todo momento!!!

A mis amigos de siempre, César, Elena, Adriana, Paula, que independiente de la distancia siempre estuvieron conmigo apoyándome incondicionalmente, gracias por su confianza y amistad!!!

A todos mis compañeros y amigos que vivieron solidariamente conmigo esta etapa de mi vida!!! En especial, gracias a mi compañero Guillermo, su esposa María y su hija Lucía por su apoyo y amistad, a mi amigo y vecino Nacho por su siempre buena disposición y amistad de años, a mis ex-vecinos Lum y Paola por su apoyo cuando lo necesitamos y amistad, a Mary Carmen y Anita por su compañerismo, amistad y por permitirme compartir con Uds. unos ricos desayunos, uhmmm!!!

Agradezco al proyecto FLUCAR, financiado por CONACyT (SEP-2004-C01-45813/A-1 y 25339), por el apoyo económico brindado para la realización de mi proyecto de tesis, sin el cual, no hubiera sido posible la generación de los resultados mostrados en este documento de tesis.

Agradezco al proyecto IMECOCAL, y en particular al Dr. Reginaldo Durazo-Arvizu, por los datos hidrográficos proporcionados que fueron utilizados en el Capítulo 1 de este documento de tesis y por la ayuda brindada en el artículo científico publicado en CSR. Asimismo, agradezco a todos los co-autores de éste artículo, por sus valiosos comentarios que permitieron mejorar notablemente éste producto científico.

Agradezco al CONACyT por el financiamiento otorgado durante mi periodo de doctorado a través del Programa de Becas Nacionales.

Agradezco al programa de doctorado en Ciencias en Oceanografía Costera del IIO/FCM, UABC, por brindarme la oportunidad de superarme académicamente. Asimismo, agradezco a todos los maestros de este posgrado, en especial al Dr. Ramón-Cajal por enseñarme la belleza del mundo microscópico, como también a todas las autoridades y administradores de éste posgrado, en especial, a la secretaria Angélica Arce por su siempre buen trato y disposición con todos los estudiantes.

Al posgrado en Ecología Marina de CICESE, por otorgarme un espacio de trabajo durante los últimos años y en especial a la secretaria Elizabeth Farías, por su siempre disposición a ayudar! Asimismo, agradezco a los estudiantes y compañeros de éste posgrado, a las secretarias, técnicos, telefonistas, intendentes, que de alguna u otra manera contribuyeron al desarrollo de esta tesis e hicieron más grata mi estancia en esta Institución vecina.

GRACIAS A TODOS AQUELLOS QUE DE ALGUNA U OTRA MANERA CONTRIBUYERON A LA CONCLUSIÓN DE ESTE PROCESO!!!

I. ÍNDICE

ANEXOS:

II. LISTA DE TABLAS

III. LISTA DE FIGURAS

primarios en la trama trófica hacia sus consumidores heterótrofos y mixótrofos, y la vía llamada “fixed carbon recovery” es transferencia trófica de fuentes de carbono disuelto y particulado por organismos heterótrofos y bacterias (Figura tomada de Sherr y Sherr, 1988).

Capítulo I. Figura 1. Grilla de muestreo de IMECOCAL (panel superior), posición geográfica de la estación ENSENADA y de las estaciones de la línea 100 de IMECOCAL (panel inferior). Note la cercanía de la estación ENSENADA (8km) de la estación 100.30. Se muestran en el mapa las isóbatas 50, 100, 500 and 1000 m.

Capítulo I. Figura 2. Ocupación estacional de la línea 100 utilizada en el análisis armónico realizado en el periodo 1998-2008.

Capítulo I. Figura 3. Contornos de temperatura climatológica (°C) de la línea 100 generada a partir de 11 años de datos de IMECOCAL. (a) Promedio, (b) amplitud del ciclo anual (°C), (c) fase (meses) del ciclo anual que indica el tiempo en el cual el ciclo es máximo, (d) porcentaje de la varianza explicada para el ciclo anual. Se indican las isopicnas de 25.5 y 26.5 kg m^{-3} en líneas gruesas y blancas, las cuales representan las aproximaciones del límite inferior del núcleo de la CC (SAW) y del núcleo de la CU (ESsW), respetivamente.

Capítulo I. Figura 4. Contornos de salinidad climatológica de la línea 100 generada a partir de 11 años de datos de IMECOCAL. (a) Promedio, (b) amplitud del ciclo anual, (c) fase (meses) del ciclo anual que indica el tiempo en el cual el ciclo es máximo, (d) porcentaje de la varianza explicada para el ciclo anual. Se indican las isopicnas de 25.5 y 26.5 kg m^{-3} en líneas gruesas y blancas, las cuales representan las aproximaciones del límite inferior del núcleo de la CC (SAW) y del núcleo de la CU (ESsW), respetivamente.

Capítulo I. Figura 5. Contornos de temperatura (°C, paneles superiores) y salinidad a lo largo de la línea 100 (paneles inferiores) para los meses de enero, abril, julio y octubre. Los valores fueron estimados del análisis armónico de los datos colectados durante 11 años por el programa IMECOCAL. Se indican las isopicnas de 25.5 y 26.5 kg m^{-3} en

líneas gruesas y blancas, las cuales representan las aproximaciones del límite inferior del núcleo de la CC (SAW) y del núcleo de la CU (ESsW), respetivamente.

Capítulo I. Figura 6. Secciones transversales de velocidad geostrófica (cm s^{-1}) estimados para los meses de enero, abril, julio y octubre a partir del análisis armónico de los datos colectados durante 11 años por el programa IMECOCAL. El nivel de referencia es 400dbar. Los valores negativos (positivos) indican flujos hacia el ecuador (hacia el polo). El intervalo de los contornos es 2 cm s^{-1}.

Capítulo I. Figura 7. Contornos de temperatura (°C) y salinidad para la estación 100.30 y para la estación ENSENADA a partir de los datos colectados desde octubre del 2006 a noviembre del 2008. Se indican las isopicnas de 25.5 y 26.5 kg m^{-3} en líneas gruesas y blancas, las cuales representan las aproximaciones del límite inferior del núcleo de la CC (SAW) y del núcleo de la CU (ESsW), respetivamente. Los puntos blancos indican las profundidades estándares.

Capítulo I. Figura 8. Anomalías mensuales del índice de surgencia para la posición geográfica 30°N, 119°W (líneas y puntos negros) y valores del índice multivariado del ENSO (MEI) (área gris) para el periodo octubre del 2006- noviembre 2008. Los valores de la anmolía del índice de surgencia se obtuvieron de la página web PFEL-NOAA: http://www.pfeg.noaa.gov/products/PFEL/modeled/indices/upwelling/NA/. Los valores del índice MEI de la página web: www.cdc.noaa.gov/people/klaus.wolter/MEI/.

Capítulo I. Figura 9. Promedio de las anomalías de (a) temperatura (°) y (b) salinidad de los primeros 50 m de la columna de agua de los datos colectados en la estación ENSENADA desde octubre del 2006 a noviembre del 2008. Las anomalías fueron calculadas relativas a los promedios climatológicos obtenidos del ajuste anual realizado a los datos hidrográficos de la estación 100.30.

Capítulo I. Figura 10. Contornos de la concentración de (a) oxígeno disuelto (µM) y (b) carbono inorgánico disuelto (µmol kg^{-1}) de los datos colectados en la estación ENSENADA desde octubre del 2006 a noviembre del 2008.

Capítulo I. Figura Suplementaria 1. Promedios estacionales de diagramas T-S de (a) enero, (b) abril, (c) julio y (d) octubre a lo largo de la línea 100, estimados mediante el ajuste armónico realizado a los datos hidrográficos colectados durante 11 años por el programa IMECOCAL. Se indican los límites masas de agua de la región de acuerdo a sus características descritas por Durazo y Baumgartner (2002). Las masas de agua son mostradas en los paneles como sigue: SAW= Agua Subártica, ESsW= Agua Ecuatorial Subsuperficial, PIW= Agua Intermedia del Pacífico. Las líneas punteadas indican la isopicna de 26.5 kg m^{-3}.

Capítulo I. Figura Suplementaria 2. Promedios y desviaciones estándar de los perfiles de (a) temperatura y (b) salinidad de las estaciones 100.30 y ENSENADA. Los valores estadísticos son calculados usando los datos hidrográficos colectados en cruceros coincidentes entre ambas estaciones. Desde octubre del 2006 a noviembre del 2008 las fechas de muestreo en ambas estaciones fueron: 24/oct/06; 23-24/ene/07; 26/abr/07; 25-26/ago/07; 21-23/ene/08; 14-16/abr/08; 2-12/ago/08; 14/oct/08 (solo en la estación 100.30) y 13/nov/08 (solo en la estación ENSENADA).

Capítulo II. Figura 1. Localización de la estación experimental (estación ENSENADA) en las aguas costeras frente a la costa norte de Baja California.

Capítulo II. Figura 2. (A) Índice de Surgencia de Bakun (m^3 s^{-1} por 100 de costa; línea sólida) y su promedio mensual (m^3 s^{-1} por 100 de costa; línea punteada), tomado de NOAA/NMFS/PFEG para los 30°N119°W, durante los seis periodos en que fueron realizados experimentos de dilución en la estación ENSENADA localizada en la costa norte de Baja California, México. Los círculos más grandes y en gris indican el valor del índice de surgencia durante el día en que fue realizado el experimento de dilución. (B) Perfiles de densidad del agua (σ_t; kg m^{-3}) y (C) fluorescencia *in situ* (µg Chl L^{-1}) medida durante cada muestreo en el mismo tiempo en que fue colectada el agua de mar para los experimentos de dilución.

Capítulo II. Figura 3. (A) Forward angle light scattering (FALS) normalizados y (B) contenido de carbono por célula (escala logarítmica) para poblaciones autotróficas y heterotróficas, obtenidos de los 19 experimentos de dilución realizados en la zona

eufótica desde septiembre de 2007 a noviembre de 2008 en la estación ENSENADA localizada frente a la costa norte de Baja California, México. El símbolo ** denota el periodo en que fue registrado un florecimiento algal en la zona de estudio.

Capítulo II. Figura 4. (A) Biomasas iniciales de poblaciones de picoplancton (autotrófico y heterotrófico) (eje-Y izquierdo) y concentraciones iniciales totales de clorofila *a* (eje-Y derecho) y (B) contribución relativa de poblaciones autotróficas (P-Euk, SYN y PRO) al total de biomasa de picofitoplancton obtenidas de los 19 experimentos de dilución realizados en la zona eufótica desde septiembre de 2007 a noviembre de 2008 en la estación ENSENADA localizada frente a la costa norte de Baja California, México. El símbolo ** denota el periodo en que fue registrado un florecimiento algal en la zona de estudio.

Capítulo II. Figura 5. Asociaciones entre la concentración inicial de clorofila *a* total (TChla) y las biomasas iniciales de (A) picoplancton autotrófico (A-Pico) y de (B) picoplancton heterotrófico (H-Bact) obtenidas de los 19 experimentos de dilución realizados en la zona eufótica desde septiembre de 2007 a noviembre de 2008 en la estación ENSENADA localizada frente a la costa norte de Baja California, México. Los paneles de arriba (A) y de abajo (B) muestran las regresiones lineales significativas entre los datos de todos los periodos muestreados, excluyendo los experimentos de abril 2008.

Capítulo II. Figura 6. Tasas de crecimiento (μ) y de pastoreo protista (m) de (A) la comunidad total de fitoplancton (TChla), (B) de las poblaciones de picoautótrofos (A-Pico) y (C) de las bacterias heterotróficas (H-Bact) obtenidas de los 19 experimentos de dilución realizados en la zona eufótica desde septiembre de 2007 a noviembre de 2008 en la estación ENSENADA localizada frente a la costa norte de Baja California, México. El símbolo ** denota el periodo en que fue registrado un florecimiento algal en la zona de estudio.

Capítulo II. Figura 7. Razones entre las tasas de pastoreo protista (m) y de crecimiento (μ) de (A) la comunidad total de fitoplancton (TChl*a*) y (B) las poblaciones de picoplancton (autótrofo y heterótrofo) obtenidas de los 19 experimentos de dilución realizados en la zona eufótica desde septiembre de 2007 a noviembre de 2008 en la

estación ENSENADA localizada frente a la costa norte de Baja California, México. El símbolo ** denota el periodo en que fue registrado un florecimiento algal en la zona de estudio.

Capítulo II. Figura 8. Tasas diarias de (A) producción y (B) pérdidas por pastoreo de protistas sobre poblaciones de picoautótrofos (PicoEukariotes, *Prochlorococcus* y *Synechococcus*), bacterias heterotróficas (H-Bact) y producción primaria por incorporación de C^{14} (14C-PP) (solo en el panel A) obtenidas de los 19 experimentos de dilución realizados en la zona eufótica desde septiembre de 2007 a noviembre de 2008 en la estación ENSENADA localizada frente a la costa norte de Baja California, México. El símbolo ** denota el periodo en que fue registrado un florecimiento algal en la zona de estudio.

Capítulo II. Figura 9. Asociaciones entre la producción primaria medida con el método de c14 y las estimaciones de producción de (A) picoplancton autotrófico (A-Pico) y de (B) picoplancton heterotrófico (H-Bact) obtenidas de los 19 experimentos de dilución realizados en la zona eufótica desde septiembre de 2007 a noviembre de 2008 en la estación ENSENADA localizada frente a la costa norte de Baja California, México. Ambas gráficas muestras las regresiones lineales significativas incluyendo todos los datos. Los paneles de arriba (A) y de abajo (B) muestran las regresiones lineales significativas, excluyendo los experimentos de abril 2008.

Capítulo II. Figura 10. Asociaciones entre la abundancia en escala logarístmica de las poblaciones de A-Pico obtenidas de muestreos a profunidades discretas y las concentraciones de nitrito+nitrato obtenidas de muestras individuales de agua de mar colectadas desde la zona eufótica durante 6 periodo entre septiembre 2007-noviembre 2008 en la estación ENSENADA localizada frente a la costa norte de Baja California, México. Todas las muestras fueron colectadas en el mismo día en que fueron realizados los experimentos de dilución, exceptuando abril de 2008, cuando los datos fueron colectados 5 días después de las incubaciones de dilución.

Capítulo III. Figura 1. Localización de la estación experimental (estación ENSENADA) en las aguas costeras frente a la costa norte de Baja California.

Capítulo III. Figura 2. (A) Índice de Surgencia de Bakun cada seis horas ($m^3 s^{-1}$ por 100 de costa; línea sólida) y (B) su promedio mensual ($m^3 s^{-1}$ por 100 de costa; línea punteada), tomado de NOAA/NMFS/PFEG para los 31.6°N 116.8°W, para el periodo septiembre 2007 a noviembre de 2008, durante el cual fueron realizados experimentos de dilución en la estación ENSENADA localizada en la costa norte de Baja California, México. El panel (A) muestra círculos más grandes y en gris que indican el valor del índice de surgencia durante el día en que fue realizado el experimento de dilución. El panel (B) muestra barras grises claras que indican los seis periodos de tiempo en que fueron realizados los experimentos de dilución.

Capítulo III. Figura 3. Perfiles de (A) densidad del agua (σ_t; kg m^{-3}), (B) fluorescencia *in situ* (µg Chl L^{-1}), (C) nitrito + nitrato y, (D) silicatos medidos durante cada muestreo en el mismo tiempo en que fue colectada el agua de mar para los experimentos de dilución entre septiembre de 2007 y noviembre de 2008 en la estación ENSENADA localizada en la costa norte de Baja California, México. Para los nutrientes (paneles C y D), se la distribución vertical fue solo representada en los primeros 40 m de la columna de agua, en el tiempo en que fueron realizados los experimentos de dilución. Para el caso de abril de 2008, los nutrientes fueron medidos 5 días después de realizados los experimentos de dilución.

Capítulo III. Figura 4. Biomasa de carbono de (A) autótrofos y heterótrofos totales, (B) autótrofos por categorías de tamaño y (C) heterótrofos por categorías de tamaño de las condiciones iniciales de los 19 experimentos de dilución realizados en la zona eufótica desde septiembre de 2007 a noviembre de 2008 en la estación ENSENADA localizada frente a la costa norte de Baja California, México. Se destaca que las células heterótrofas del picoplancton son totalmente compuestas por bacterias heterotróficas.

Capítulo III. Figura 5. Asociaciones entre la razón de las biomasas de carbono de autótrofos y heterótrofos (C-Hetero: C-Auto) y la biomasa de carbono autótrofo (C-Auto), de las condiciones iniciales de los 19 experimentos de dilución realizados en la zona eufótica desde septiembre de 2007 a noviembre de 2008 en la estación ENSENADA localizada frente a la costa norte de Baja California, México. La línea

discontinua indica que la biomasa de carbono heterótrofo es igual a la biomasa de carbono autótrofo (C-Hetero: C-Auto=1).

Capítulo III. Figura 6. Total de la (A) biomasa de carbono autótrofo (TAuto-C) y concentración de clorofila *a* (TChl*a*), (B) asociaciones entre TChl*a* y TAuto-C y, (C) razones carbono a clorofila, de las condiciones iniciales de los 19 experimentos de dilución realizados en la zona eufótica desde septiembre de 2007 a noviembre de 2008 en la estación ENSENADA localizada frente a la costa norte de Baja California, México. El panel superior en (B) muestra la regresión lineal significativa excluyendo los experimentos de abril 2008. La línea discontinua en la figura (C) indica el valor promedio general para todos los periodos muestreados.

Capítulo III. Figura 7. Tasas instantáneas de crecimiento (μ) y de mortalidad por pastoreo (m) de autótrofos para la (A) comunidad total (basadas en concentración de TChl*a*), (B) diatomeas (basadas en concentración de Fucoxantina), (C) *Synechococcus* (basadas en abundancia celular) y, (D) prasinofitas (basadas en abundancia celular de picoeucariontes), de los 19 experimentos de dilución realizados en la zona eufótica desde septiembre de 2007 a noviembre de 2008 en la estación ENSENADA localizada frente a la costa norte de Baja California, México.

Capítulo III. Figura 8. Tasas diarias de producción primaria (PP) y de pérdidas por pastoreo (G) del microzooplancton basadas en los cambios temporales de la concentración total de clorfila a (TChla), de abundancia celular y de pigmentos biomarcadores específicos para (A) la comunidad total de autótrofos, (B) diatomeas y otros eucariontes autótrofos (Otros A-Euks), (C) *Synechococcus*, (D) prasinofitas y, (E) prymnesiofitas y *Prochlorococcus*, de los 19 experimentos de dilución realizados en la zona eufótica desde septiembre de 2007 a noviembre de 2008 en la estación ENSENADA localizada frente a la costa norte de Baja California, México. El panel (A) muestra además, las tasas de producción primaria por incorporación de C^{14} (14C-PP) que fueron medidas simultáneamente en esta estación costera.

Capítulo III. Figura 9. (A) Contribución relativa al total de la biomasa inicial de carbono de los consumidores ordenados por categorías de tamaños: ciliados < 20μm

(Nano_CIL), ciliados > 20µm (Micro_CIL), flagelados (incluyendo dinoflagelados) < 20µm (Nano_Flag) and flagelados > 20 µm (Micro_Flag), además del impacto de pastoreo ejercido por estos organismos al total de carbono de la comunidad autótrofa y, (B) impacto de pastoreo ejercido sobre los principales grupos fitoplanctónicos: diatomeas, *Synechococcus* (SYN) y prasinofitas (Pras), de los 19 experimentos de dilución realizados en la zona eufótica desde septiembre de 2007 a noviembre de 2008 en la estación ENSENADA localizada frente a la costa norte de Baja California, México. La línea discontinua en el panel (B) indica el valor cuando las pérdidas por pastoreo son iguales a la producción primaria diaria (G=PP).

INTRODUCCIÓN

En los ciclos biogeoquímicos del carbono y nitrógeno, los océanos desempeñan un papel importante, ya que se ha estimado que este sistema contiene aproximadamente 38,000 Pg* de carbono, lo cual corresponde al 85% del carbono global, principalmente como carbono inorgánico disuelto (CID) (Sarmiento y Gruber, 2002). De ambos elementos, el carbono ha sido sujeto de estudio de muchos ciclos biogeoquímicos porque el bióxido de carbono (CO_2) en la atmósfera atrapa las radiaciones infrarrojas reflejadas desde la superficie terrestre, ocasionando un "efecto invernadero" sobre la Tierra. Durante el último siglo se ha incrementado este "atrapamiento" de CO_2 a causa de emisiones antropogénicas a la atmósfera, generando un calentamiento global del planeta de alrededor 0.6°C ± 0.2°C (Sarmiento y Gruber, 2002). La importancia del océano en la regulación natural de los niveles de CO_2 atmosférico ha sido reconocida por más de 60 años. Por tanto, resulta esencial un entendimiento comprensivo y cuantitativo de los procesos que regulan el flujo de carbono entre sus principales reservorios del océano superficial (CO_2, carbono orgánico disuelto y carbono orgánico particulado), con el objetivo de predecir las consecuencias que tiene el patente aumento en los niveles de CO_2 y gases invernadero en la atmósfera producto del cambio climático global. En éste contexto, se han hecho algunas estimaciones de flujos y reservorios de este complejo ciclo del carbono, el cual se esquematiza a continuación.

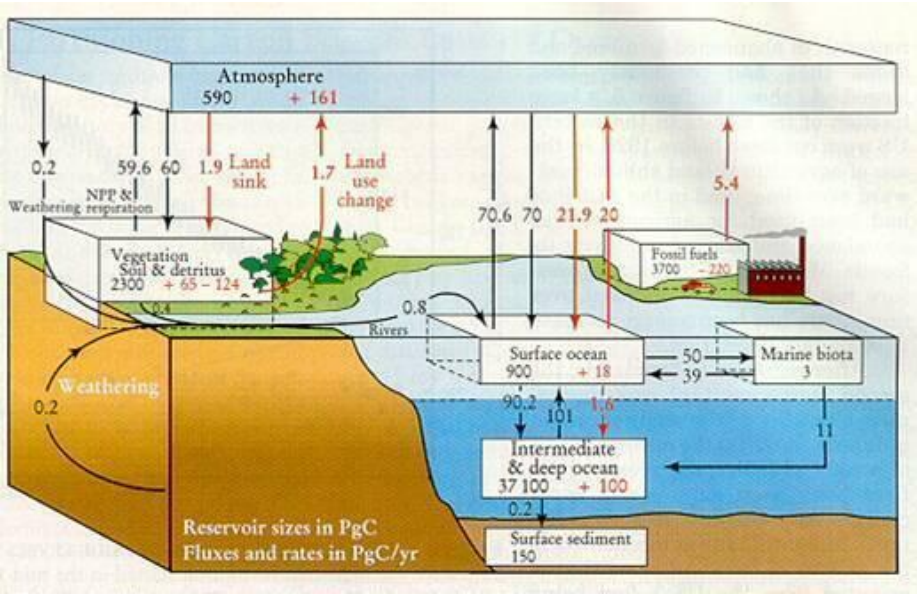

* 1 Petagramo (1Pg)=1x10^{15} gramos 1Gigatonelada (1Gt)=1x10^{9} toneladas (1 billón de toneladas)= 1 Pg

Figura 1. Ciclo Global del Carbono. Las flechas indican los flujos promedio (en Petagramos de carbono por año, Pg C año^{-1}) entre la atmósfera y sus dos principales sumideros, la tierra y el océano, promediados sobre la década de los 80. Los flujos antropogénicos se señalan en rojo; los flujos naturales se indican en negro. El flujo neto entre reservorios es balanceado por procesos naturales pero no por flujos antropogénicos. Dentro de las cajas, los números en negro indican los tamaños pre-industriales de los reservorios y los números en rojo denotan los cambios producto de las actividades humanas desde tiempos pre-industriales. Para el sumidero "tierra", el primer número en rojo es sumidero terrestre inferido cuyo origen es especulativo; el segundo número rojo representa el decrecimiento debido a la deforestación. NPP es producción primaria neta (Figura tomada de Sarmiento y Gruber, 2002).

La transferencia global de carbono hacia los océanos es mediada por dos procesos que contribuyen a almacenar carbono en su interior: la bomba de solubilidad y la bomba biológica (Fig. 2).

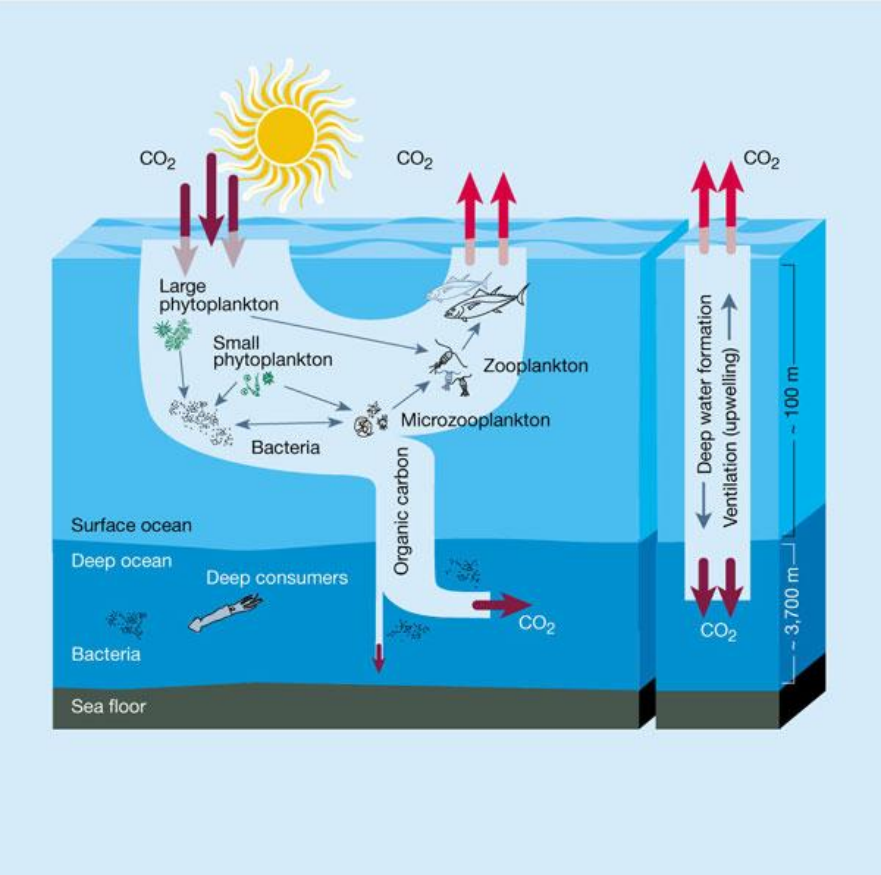

Figure 2. Contribución de carbono al océano mediante la "bomba biológica" (a la izquierda) una compleja estructura mediada por las tramas tróficas pelágicas, y la "bomba de solubilidad" (a la derecha), manejada por los procesos físicos y químicos de los océanos (Figura tomada de Chisholm, 2000).

En la **bomba de solubilidad**, el CO_2 atmosférico (CO_2 gas) se disuelve en las capas superficiales del océano contribuyendo al aporte de CID. Además, eventos como la surgencia de agua profunda desempeñan un papel preponderante en el aporte al océano superficial de aguas ricas en CID, las cuales eventualmente sobresaturan el sistema siendo una fuente de CO_2 hacia la atmósfera. Por tanto, la cuantificación del flujo de carbono entre el océano y atmósfera se basa en mediciones de la presión parcial del CO_2 (pCO_2) entre ambos sistemas, las cuales determinan la dirección entrante o saliente de este flujo. Un entendimiento comprensivo y cuantitativo de los procesos que gobiernan a éste flujo en varios sistemas oceánicos, resulta esencial para predecir las consecuencias del aumento en los niveles de CO_2 y gases invernadero en la atmósfera producto del cambio climático. Al respecto, escasas son las estimaciones realizadas en los sistemas costeros, y el resultado es que actualmente no se conoce si estas regiones son fuentes y/o sumideros netos de gases invernadero. Basado en una extensa revisión bibliográfica sobre las estimaciones anuales del flujo de carbono océano-atmósfera en zonas costeras, se ha reportado de manera general que las áreas con altos valores de índice de surgencia (IS), tales como las localizadas en las costas de California (USA) y de Oman (Mar Arábico), tienden a ser anualmente fuentes de CO_2, en contraste a aquellas regiones con bajos valores de IS que tienden a ser anualmente sumideros de CO_2, tales como los localizados en las costas de Galicia (España) e Isla Vancouver (Canadá). Estas diferencias podrían deberse a que el tiempo de residencia de las masas de agua es muy corto en sistemas de surgencia costera, pero el aporte en nutrientes y CID es lo suficientemente intenso como para evitar la sub-saturación de CO_2 y consumo total de nutrientes (Borges, 2005). Aunado a esta variabilidad anual, una fuerte estacionalidad ha sido reportada en los flujos de carbono desde y hacia la atmósfera debido a los patrones de mezcla. Una moderada estratificación superficial posterior a un aporte de nutrientes y carbono, podría generar altas biomasas fitoplanctónicas que eventualmente producen una rápida y eficiente fijación de CO_2, o inversamente, una baja fijación de CO_2 podría ocurrir en periodos de intensa mezcla, debido a las bajas biomasas de fitoplancton (Torres *et al.,* 2002; Alvarez *et al,* 1999). Esto sugiere que un área costera particular, dependiendo de la época del año y sus procesos físicos asociados, podría ser considerada un sumidero de carbono en algunos periodos, y en otros, una

fuente de carbono, pudiendo estar en balance con la atmósfera a lo largo del año, tal como ha sido reportado para la costa central de California (Pennington *et al.*, 2007).

En **la bomba biológica** se involucran dos procesos: fijación de carbono por fotosíntesis y hundimiento de carbono al océano profundo. En la capa superficial de los océanos, el fitoplancton incorpora los nutrientes y el CO_2 del agua en el proceso de la fotosíntesis para crear materia orgánica (fijación de carbono). Parte de este carbono producido es transferido hacia las tramas tróficas pelágicas, y a su vez una parte de éste puede ser convertido nuevamente a CO_2 en el proceso de la respiración (remineralización del carbono), el cual puede ser eventualmente regresado a la atmósfera. Otra parte del carbono producido, puede ser hundida hacia el fondo del océano en forma particulada (exportación de carbono) o también puede ser mezclado en aguas profundas como carbono orgánico e inorgánico disuelto. El resultado neto, es un transporte de CO_2 desde la atmósfera hacia el océano profundo, donde puede permanecer en promedio unos 1,000 años. De esta manera, inclusive más que la bomba de solubilidad, la bomba biológica mantiene un gradiente en la concentración de CO_2 entre la superficie y las aguas profundas del océano (Chisholm, 2000).

Al respecto, se ha reconocido que las tramas tróficas pelágicas tienen un papel fundamental en la repartición de la producción fitoplanctónica entre los procesos de remineralización a CO_2, transferencia dentro de las comunidades, y exportación hacia el océano profundo en forma particulada y disuelta (Legendre y Rassoulzadegan, 1996; Legendre y Rivkin, 2002; Rivkin y Legendre, 2002). La influencia de las tramas tróficas se basa principalmente en su estructura (tamaño y composición) y en la abundancia relativa de las especies, las cuales modulan la cantidad del carbono fijado en estratos superiores que puede ser "bombeado" hacia el océano interior (Chisholm, 2000). Particularmente, muchos ecosistemas productivos y estacionales, como los sistemas de surgencia costera, han sido comúnmente caracterizados por cortas cadenas tróficas, compuestas generalmente por grandes organismos del fitoplancton (largas cadenas de diatomeas), zooplancton y peces pelágicos (Ryther, 1969). Sin embargo, estudios

recientes han demostrado que muchos de estos sistemas de surgencia costera involucran tramas tróficas multívoras (Legendre and Rassoulzadegan, 1995), donde no solo organismos de la clásica vía trófica herbívora sino también, componentes tróficos microbianos, conforman una estructura trófica compleja que le confieren a éste ecosistema la habilidad de reciclar carbono eficientemente dentro de la zona pelágica (Neuer y Cowles, 1994; Vargas y González, 2004; Böttjer y Morales, 2005; Vargas *et al.*, 2007; Landry *et al.*, 2009; Texeira *et al.*, 2010; Linacre *et al.*, *in prep.*).

Particularmente, la trama trófica pelágica microbiana es una estructura compleja que tiene un papel bastante significativo en la transferencia de materia orgánica (carbono) y energía desde pequeños productores primarios hacia niveles tróficos superiores (Fig. 3). Parte de esta función fundamental es debida al enlace microbiano, un grupo de organismos unicelulares procariontes y eucariontes, tanto autotróficos como heterotróficos, que conforman una componente integral de la trama trófica microbiana. Sus interacciones tróficas (bacterias consumidores de materia orgánica disuelta, flagelados bacterívoros y ciliados consumidores de flagelados) sirven como una vía de regeneración de nutrientes inorgánicos (fosfato y amonio) y como una fuente de materia orgánica hacia la cadena trófica convencional (Azam *et al.*, 1983; Sherr y Sherr, 1988). En esta estructura trófica microbiana, el consumo protista de organismos autótrofos (herbivoría) y/o heterótrofos (bacterivoría) tiene un papel central en la canalización del carbono que es incorporado al océano a través de la producción primaria. Debido al amplio rango de tamaños de los protistas (flagelados < 20 µm, ciliados y dinoflagelados heterotróficos entre 20-200 µm), a sus variados estados tróficos (desde estrictamente fagotróficos a mixótrofos), como también a su amplio rango de presas autotróficas y heterotróficas (desde células picoplanctónicas entre 1-10 µm hasta largas cadenas de diatomeas), éstos organismos se localizan en un lugar trascendental dentro de las cadenas tróficas microbianas, en su función de transferir carbono dentro del océano pelágico (Calbet, 2008; Sherr y Sherr, 1994; 2002; 2007).

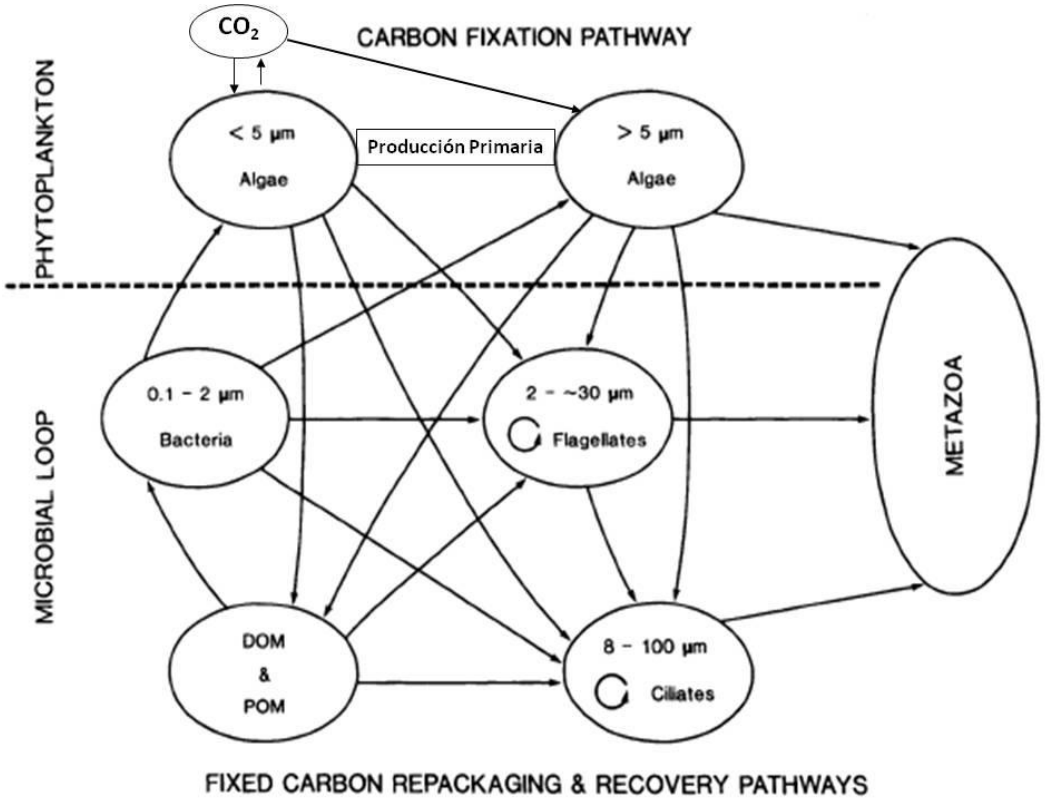

Figura 3. Interacciones tróficas dentro de las tramas tróficas microbianas, donde el enlace microbiano (‘microbial loop”) forma una parte integral de ésta vía trófica. Se muestran en forma separada los componentes del “fitoplancton” y del “enlace microbiano” (bacterias y protistas heterotróficos), destacando varios enlaces directos entre micro-organismos autotróficos y heterotróficos. Entre éstos se incluyen, la ingestión de fitoplancton por flagelados y ciliados, y la ingestión de bacterias por algas mixotróficas. Las líneas curvas dentro de los compartimentos de flagelados y ciliados, indican la interacción predador-presa existente dentro de la amplia gama de tamaños de estos grupos. Se destaca que la producción de algas <5 µm es accesible a los grandes metazoarios solo después de haber sido transferida a través de los protistas componentes de las tramas tróficas microbianas. La vía de de carbono llamada “carbon fixed” es referida a la incorporación de CO_2 por organismos autótrofos, la vía denominada “fixed carbon repackaging” es referida a la incorporación de carbono fijado por productores primarios en la trama trófica hacia sus consumidores heterótrofos y mixótrofos, y la vía llamada “fixed carbon recovery” es transferencia trófica de fuentes de carbono disuelto y particulado por organismos heterótrofos y bacterias (Figura tomada de Sherr y Sherr, 1988).

Con el objeto de cuantificar la vía trófica microbiana, se han realizado sistemáticamente estimaciones de la tasas de crecimiento de fitoplancton y su mortalidad debida al pastoreo por el microzooplancton (definido aquí como consumidores nano y

microplanctónicos <200 µm) en una amplia variedad de hábitats oceánicos (incluyendo los sistemas productivos costeros) utilizando la técnica de dilución (Landry y Hasset, 1982). Así, en promedio se ha estimado que el 67% de la producción diaria de fitoplancton es consumida diariamente por el microzooplancton (Calbet y Landry, 2004), en comparación al menor impacto que generan organismos componentes del mesozooplancton (200-2,000 µm), que en promedio sólo alcanza al 10% de la producción primaria diaria (Calbet, 2001), dejando así una pequeña fracción que es exportada directamente por el hundimiento de las células hacia el océano profundo (Wasmann, 1998).

Por tanto, la dinámica de CO_2 en zonas costeras es un proceso complejo, determinado no solo por la variabilidad anual y/o estacional de procesos físico-químicos que modulan las estimaciones *in situ* de pCO_2 en los océanos, sino además por procesos biológicos, como la producción de materia orgánica relativa a la descomposición de ésta por la respiración biológica, la estructura e interconectividad de las cadenas tróficas pelágicas que influyen en el ciclo de carbono y la transformación biótica de la materia orgánica por diversos procesos (excreción, fragmentación, alimentación, producción de pellets fecales y estructuras orgánicas) dentro de la zona eufótica de estos ecosistemas (Borges, 2005; Legendre y Rivkin, 2005). Aunque no cabe duda del papel importante que desempeñan las cadenas tróficas pelágicas microbianas en los flujos energéticos, es notable la falta de conclusiones más fuertes sobre su efecto en el flujo del carbono en ecosistemas particulares. Por una parte, esto es debido a las limitaciones propias de las metodologías utilizadas para establecer la transferencia de carbono desde un nivel trófico a otro (ejemplo, la técnica de dilución), así como también, por la falta de experimentos *in situ*, los cuales aportarían información valiosa sobre las interacciones microbianas en el flujo de carbono, que no sólo servirán para mejorar modelos ya existentes de flujos de elementos (C, N, Fe) entre el océano y la atmósfera, sino además para crear otros nuevos y más específicos para los distintos tipos de ecosistemas marinos.

JUSTIFICACIÓN

En función a lo anterior, se puede establecer que en sistemas costeros la dinámica del carbono es muy compleja, ya que no sólo depende de factores y procesos físico-químicos que influyen en su flujo hacia y desde el océano, sino también de procesos biológicos, que pueden estar modulando gran parte del ciclo del carbono en éstas regiones. Al respecto, el establecimiento del papel ecológico entre los miembros de una comunidad planctónica, la estimación de la transferencia de carbono entre los productores primarios y sus consumidores, así como la cuantificación de la contribución de los mayores grupos fitoplanctónicos a la producción total de carbono, contribuyen a lograr un mayor entendimiento del ciclo del carbono en las regiones costeras.

OBJETIVOS

Objetivo General

Evaluar el papel de las comunidades de microorganismos planctónicos de la zona eufótica en el flujo de carbono bajo condiciones oceanográficas estacionales de las aguas costeras localizadas en la parte norte de la Península de Baja California, México.

Objetivos Específicos

- Caracterizar temporalmente las condiciones físico-químicas de las aguas costeras localizadas frente a la parte norte de la Península de Baja California, México, con el fin de identificar los procesos más importantes que afectan las variables relacionadas con el ciclo del carbono en ésta zona costera, particularmente en un sitio de monitoreo costero llamado estación ENSENADA.

- Caracterizar la dinámica temporal del flujo del carbono a través de las poblaciones picoplanctónicas autótrofas (cianobacterias y picoeucariontes) y heterótrofas (bacterias) de la zona eufótica, enfocado a su abundancia, biomasa en términos de carbono, crecimiento y producción, como también en su mortalidad debida al pastoreo protista, bajo condiciones oceanográficas contrastantes observadas en un periodo anual en la estación ENSENADA.

- Caracterizar la dinámica temporal de la transferencia de carbono a través de la trama trófica microbiana, mediante estimaciones de producción taxón-específica de carbono fitoplanctónico y de sus pérdidas debida al pastoreo del microzooplancton ejercido sobre el total de la comunidad autotrófica y sobre sus principales grupos fitoplanctónicos, bajo condiciones oceanográficas contrastantes observadas en un periodo anual en la estación ENSENADA.

CAPÍTULO 1: Variabilidad temporal de las características físico-químicas de la columna de agua en un sitio de monitoreo costero: Estación ENSENADA.

Trabajo publicado en la revista Continental Shelf Research: *Linacre et al., (2010). Temporal variability of the physical and chemical water characteristics at a coastal monitoring observatory: Station ENSENADA. Cont. Shelf Res., 30: 1730–1742.*

RESUMEN: Se describe la variabilidad temporal de las condiciones físico-químicas de las aguas costeras frente a Ensenada, Baja California (México). La caracterización se basó en un análisis histórico de 11 años (1998-2008) de registros de temperatura y salinidad medidos cuatrimestralmente por el programa IMECOCAL, en un transecto perpendicular a la costa (Línea 100). Además, fueron descritas las condiciones físico-químicas de una estación de monitoreo costero llamada estación ENSENADA, utilizando una serie continua de 2 años de datos (Octubre 2006-Noviembre 2008) colectados con una mayor resolución temporal. El análisis histórico de la línea 100 mostró una marcada variabilidad estacional en las condiciones termohalinas asociadas a fluctuaciones en el flujo superficial al sur de la Corriente de California, en la Corriente Subsuperficial de California dirigida hacia el polo, como también, en los eventos de surgencia costera cuya magnitud y frecuencia se incrementan hacia primavera-verano. Además, fue observada una variabilidad interanual relacionada a fases cálidas/frías del ENSO, que modifican las características de la columna de agua en esta región costera. Lo más notable de esta variabilidad interanual fue La Niña registrada desde verano 2007 a mediados del 2008. Durante esta fase fría del ENSO, los datos de temperatura, salinidad, oxígeno disuelto, densidad y carbono inorgánico disuelto revelaron la presencia anómala de aguas subsuperficiales en estratos someros de la estación ENSENADA durante la primavera del 2008. Los resultados sugirieron que éste observatorio de monitoreo es sensible a la variabilidad temporal de las condiciones hidrográficas de las aguas costeras sobre la plataforma continental (<50km) frente a Ensenada en la región norte de Baja California. Consecuentemente, la estación ENSENADA podría ser un buen sitio para el monitoreo de alta frecuencia temporal de

las condiciones oceanográficas de ésta región de transición del Sistema de la Corriente de California entre sistemas tropical/subtropical y subártico.

Palabras Claves: Estación ENSENADA; Variabilidad temporal; Sistema de la Corriente de California; El Niño/La Niña; Baja California.

Continental Shelf Research 30 (2010) 1730–1742

Contents lists available at ScienceDirect

Continental Shelf Research

journal homepage: www.elsevier.com/locate/csr

Temporal variability of the physical and chemical water characteristics at a coastal monitoring observatory: Station ENSENADA

L. Linacre [a,*], R. Durazo [b], J.M. Hernández-Ayón [c], F. Delgadillo-Hinojosa [c], G. Cervantes-Díaz [b], J.R. Lara-Lara [d], V. Camacho-Ibar [c], A. Siqueiros-Valencia [c], C. Bazán-Guzmán [d]

[a] Programa de Doctorado en Oceanografía Costera, Facultad de Ciencias Marinas/Instituto de Investigaciones Oceanológicas, Universidad Autónoma de Baja California (UABC), Km 107 Carretera Tijuana-Ensenada, Ensenada CP 22860, Baja California, México
[b] Facultad de Ciencias Marinas, UABC, Km 107 Carretera Tijuana-Ensenada, Ensenada CP 22860, Baja California, México
[c] Instituto de Investigaciones Oceanológicas, UABC, Km 107 Carretera Tijuana-Ensenada, Ensenada CP 22860, Baja California, México
[d] División de Oceanología, Departamento de Oceanografía Biológica, Centro de Investigación Científica y de Educación Superior de Ensenada (CICESE), Km 107 Carretera Tijuana-Ensenada, Ensenada CP 22860, Baja California, México

ARTICLE INFO

Article history:
Received 30 October 2009
Received in revised form
19 May 2010
Accepted 20 July 2010
Available online 24 July 2010

Keywords:
Time series
Station ENSENADA
Temporal variability
California current system
El Niño/La Niña
Baja California

ABSTRACT

The temporal variability of the physical and chemical conditions of coastal waters off Ensenada, Baja California (Mexico) was characterized. A historical analysis was made based on 11 years (1998–2008) of temperature and salinity data records measured quarterly by IMECOCAL, along a transect perpendicular to the coast (CalCOFI line 100). Moreover, the physical and chemical conditions at a coastal monitoring observatory called station ENSENADA were described using a 2-year data series (October 2006–November 2008) obtained with improved temporal resolution. The historical analysis of line 100 showed marked seasonal variability in the thermohaline conditions associated with fluctuations in the flow of the equatorward California Current and the poleward California Undercurrent, as well as with coastal upwelling events whose magnitude and frequency increase towards spring–summer. Interannual variability was also observed, related to warm and/or cold ENSO phases that modify the characteristics of the water column in this coastal region. The most striking characteristics of the interannual variability at station ENSENADA were La Niña conditions recorded from summer 2007 to mid 2008. During this cold ENSO phase, temperature, salinity, dissolved oxygen, density, and dissolved inorganic carbon data revealed the anomalous presence of subsurface water at the surface layers in spring 2008. Results suggest that the coastal observatory is sensitive to the temporal variability of hydrographic conditions on shelf coastal waters (<50 km) off Ensenada in the northern BC region. Consequently, station ENSENADA would be a good location to high-frequency monitors the oceanographic conditions of the transitional region between tropical/subtropical and subarctic systems of the California Current System.

1. Introduction

The California Current System (CCS) is one of the eastern boundary current systems that sustains the most productive ecosystems of the world, mainly due to alongshore winds that generate the upwelling of cold, relatively salty, nutrient-rich waters into the euphotic zone of coastal areas. Much of the knowledge of the CCS off the western coast of the Baja California (BC) peninsula has been obtained through the analysis of hydrographic data collected between 1950 and 1978 by the California Cooperative Oceanic Fisheries Investigations (CalCOFI) program and, since 1997, by the Mexican California Current Investigations (Investigaciones Mexicanas de la Corriente de California, IMECOCAL) program. Additionally, other sporadic studies carried out off the northwestern region of BC have described the hydrographic variability of coastal waters (Barton, 1985; Barton and Argote, 1980; Pérez-Brunius et al., 2006).

In the coastal domain of the CCS off northern BC, two water masses are transported at the surface and subsurface levels. The California Current (CC), a year-round equatorward surface flow, transports Subarctic Water (SAW), characterized by a relative minimum of salinity, high dissolved oxygen content, and a density range from 24.5 to 25.5 kg m^{-3}.The California Undercurrent (CU),

* Corresponding author. Tel.: +52 646 174 4570, +52 646 175 0500x24306; fax: +52 646 174 4103.
E-mail addresses: lorenalinacre@gmail.com, llinacre@uabc.mx (L. Linacre), rdurazo@uabc.edu.mx (R. Durazo), jmartin@uabc.edu.mx (J.M. Hernández-Ayón), fdelgadillo@uabc.edu.mx (F. Delgadillo-Hinojosa), gabita23@gmail.com (G. Cervantes-Díaz), rlara@cicese.mx (J.R. Lara-Lara), vcamacho@uabc.edu.mx (V. Camacho-Ibar), arsiva@uabc.edu.mx (A. Siqueiros-Valencia), cbazan@cicese.mx (C. Bazán-Guzmán).

0278-4343/$ - see front matter © 2010 Elsevier Ltd. All rights reserved.
doi:10.1016/j.csr.2010.07.011

a poleward subsurface (100–400 m) flow that transports Equatorial Subsurface Water (ESsW), characterized by relatively high salinity, high nutrient concentration, and low dissolved oxygen content. Its core of relative maximum salinity is normally confined over the continental slope of the northern and central coast of BC, around the 26.5 kg m^{-3} isopycnal surface (Hickey, 1979; Barton and Argote, 1980; Lynn and Simpson, 1987; Durazo and Baumgartner, 2002; Durazo et al., 2010). A third surface poleward flow has been described within 200 km of the southern California coast as a northward branch of the CC. This is the Inshore Current or California Countercurrent (Lynn and Simpson, 1987). Although the presence of this near surface flow has not been documented off BC at seasonal scales (Lynn and Simpson, 1987; Durazo et al., 2010), surface poleward flows along the continental shelf have been associated with low temperature and small-scale (20–50 km) coastal cyclonic features (Durazo and Baumgartner, 2002; Durazo et al., 2005). Additionally, sustained surface poleward flows have been reported in the continental shelf off Tijuana at 32.5°N (Alvarez et al., 1990), near 30°50′N (Barton, 1985), and at 31.3°N (Alvarez et al., 1984).

Northwesterly winds prevail in the region during most of the year. As a consequence, coastal upwelling events occur year-round off BC. These winds are more intense in spring when the coastal upwelling events are stronger and more frequent (Bakun and Nelson, 1977; Huyer, 1983; Pérez-Brunius et al., 2007; Castro and Martínez, 2010). Additionally, positive wind stress curl near the continental margins in the BC region generates Ekman pumping that brings salty CU waters toward the surface at the coastal regions (Castro and Martínez, 2010).

Climatological analyses of the hydrographic time series have shown that the distribution of properties of CCS water is determined mainly by seasonal to decadal variability (Hickey, 1979; Lynn and Simpson, 1987; Bograd and Lynn, 2003). Seasonal fluctuations have been reported for surface and subsurface flows of the CCS. Off northern BC, the surface equatorward flow intensifies in a coastal jet during spring, while the subsurface poleward flow is practically non-existent in coastal waters or may be located deeper or displaced westward (Bograd and Lynn, 2003; Lynn et al., 2003; Durazo et al., 2010). Towards summer–autumn, the CC is characterized by enhanced mesoscale activity, with gyres and eddies developing along its southward displacement. Likewise, the poleward flow of the CU intensifies during summer–early autumn (Lynn and Simpson, 1987; Soto-Mardones et al., 2004; Jeronimo and Gómez-Valdés, 2007; Durazo et al., 2010). At the interannual time scale, variability observed in the thermohaline conditions of the CCS has been closely linked to remote large-scale forcings with effects in the warming or cooling of local waters during El Niño and La Niña, respectively, mainly due to anomalies in the regional flows and in the intensity of coastal upwelling, as well as changes in water transports modulated by long-term fluctuations in wind patterns (Pérez-Brunius et al., 2006; Durazo, 2009). Particularly at the upper ocean, mixed layer temperature and salinity have demonstrated interannual variability mainly associated with regional (northern and southern BC) differences in the atmosphere–ocean net heat fluxes and with large-scale variability in the sea surface height anomaly, respectively (Gómez-Valdés and Jeronimo, 2009).

Although extensive programs like CalCOFI and IMECOCAL and some other local efforts have generated a comprehensive description of the CCS off BC, they were obtained from data series with low temporal resolution (quarterly surveys) and from a grid of hydrographic stations that poorly described the variability of nearshore waters. These shortcomings together with increasing costs of surveys emphasize the need to establish a coastal site of continuous monitoring to represent the variability of a coastal region in order to generate long-term time-series with higher temporal resolution. The aim of this study is to determine the temporal variability of the physical and chemical properties at a nearshore location, station ENSENADA, with higher frequency sampling, and to demonstrate that this site reflects the main features of the temporal variability (seasonal and interannual) of the coastal waters off Ensenada at northern BC region. The observatory is part of the FLUCAR project (“Carbon sources and sinks in the continental margins of Mexican Pacific waters”) and is a site located at an intense coastal upwelling region within a transition zone of the CCS that is strongly influenced by the tropical and subtropical systems.

The paper is organized as follows: first, the historical analysis of 11 years of temperature and salinity data as well as derived geostrophic flows recorded by the IMECOCAL program along a perpendicular transect off Ensenada (BC) is presented. Then, the seasonal variability is contrasted to the temporal characterization of the physical and chemical conditions based on a 2-year data series obtained at higher temporal resolution at the coastal observatory. Finally, the comparison is assessed to consider whether this coastal observatory could be an ocean environmental sensor that is able to perceive the seasonal and interannual variability in the physical and chemical properties of the water column of the coastal waters off Ensenada in the northern BC region. The continuous monitoring of oceanographic conditions of the northeastern Pacific region will not only provide in a more frequent data set for a dynamic region, but will also serve as a framework for future biogeochemical models in the context of global climate change.

2. Material and methods

2.1. Data collection at IMECOCAL line 100

The IMECOCAL sampling grid (Fig. 1, upper panel) occupies the historical CalCOFI lines off BC (Mexico) and extends from Ensenada (31.8°N) to the Gulf of Ulloa (26.5°N). Line 100 located off Ensenada has seven stations (Fig. 1, lower panel) spaced 37 km apart, from the coast (station 30) to 220 km offshore (station 60). During the period 1998–2008, each station along line 100 was sampled seasonally four times a year, usually in January, April, July, and October (Fig. 2). Hydrographic variables in the entire IMECOCAL sampling grid were measured by casts down to 1000 m depth, bottom depth permitting, using a SBE 9/11 CTD, armed with dual temperature and salinity sensors. Data collection and processing procedures as well as details of the IMECOCAL program can be found at http://imecocal.cicese.mx.

2.2. Data collection at station ENSENADA

The FLUCAR project surveys were conducted at station ENSENADA, located south of Punta Banda in Ensenada, BC (31°40.1′N, 116°41.6′W). This coastal site is located ~8 km eastward of IMECOCAL station 100.30 (Fig.1). Eighteen samplings were conducted at this site between October 2006 and November 2008. Routine activities included CTD/rosette casts down to 100 m, with continuous measurements of pressure, temperature, conductivity, and dissolved oxygen (dO_2) using a SeaBird 19 plus CTD. For the inorganic carbon and nutrient measurements, seawater was collected with 5-L Niskin bottles at 10 depth levels with variable spacing during the cruises depending on the depth of the thermocline and the subsurface maximum of chlorophyll. Seawater (500 mL) from the Niskin bottles was collected in Pyrex bottles to determine dissolved inorganic carbon (DIC, the only carbonate system value reported herein). Samples were

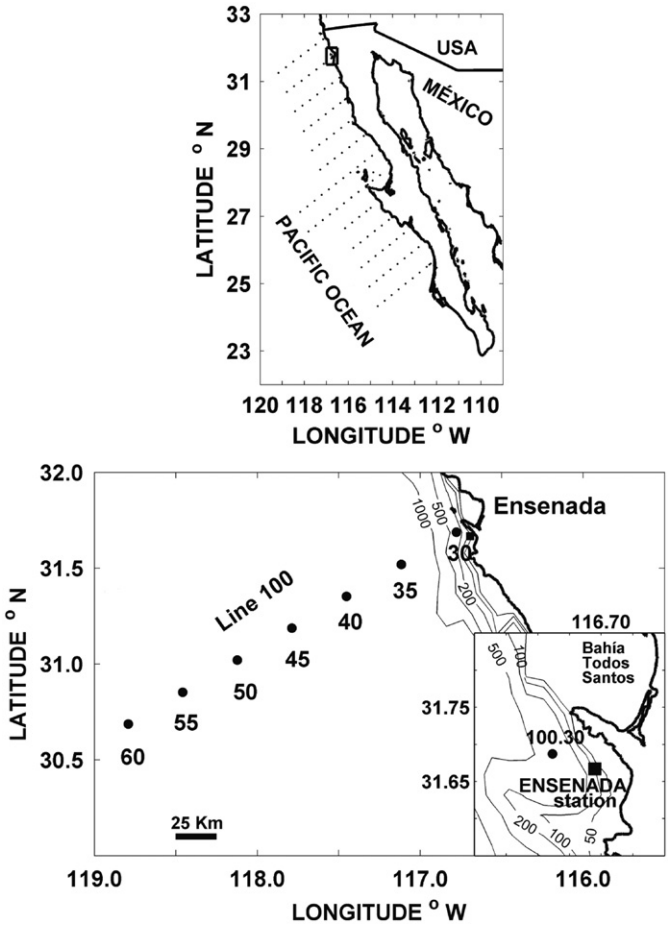

Fig. 1. The IMECOCAL sampling grid (upper panel) and the geographic location of station ENSENADA and the stations of IMECOCAL line 100 (lower panel). Note the proximity of station ENSENADA (8 km) to station 100.30. The 50, 100, 500 and 1000 m isobaths are drawn on the map.

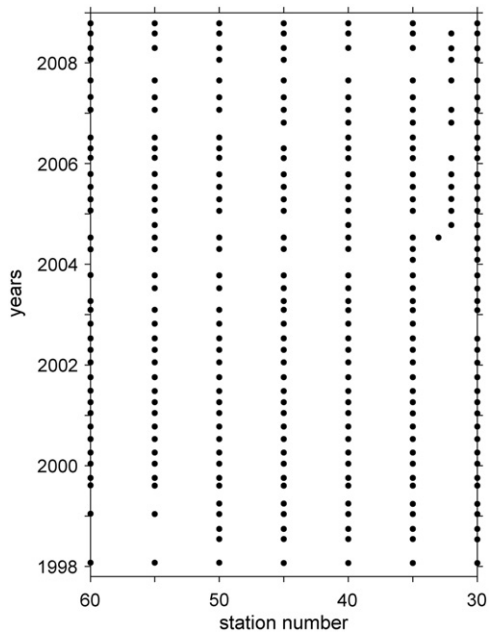

Fig. 2. Station occupation for line 100 used in the harmonic analysis for the period 1998–2008.

immediately poisoned with 100 mL of a saturated HgCl solution to prevent biological alteration, and sealed with Apiezon grease. At the laboratory, DIC was measured by coulometry following the techniques described by DOE (1994). The measuring precision of this procedure was about 1.5 μmol kg^{-1}, whereas the accuracy was approximately 2 μmol kg^{-1}, determined using certified reference material produced by Dr. A. Dickson at Scripps Institution of Oceanography. During each cruise, seawater was also routinely sampled for dO_2 measurements and to calibrate CTD data.

2.3. Data processing

Climatological means of temperature, salinity, and geostrophic velocity were obtained using a harmonic fitting at 12 standard depth levels (0, 10, 20, 30, 50, 75, 100, 125, 150, 200, 250, and 300 m) for all the line 100 stations sampled during the IMECOCAL surveys between 1998 and 2008. The harmonics were calculated following the approach of Lynn (1967) and Chelton (1984), in which the mean seasonal variation is obtained by a least squares regression of the data to annually periodic cosinusoids. The harmonic fitting was restricted to the annual period since the time interval between surveys was 3–4 months. The general form of the harmonic function for the variable $y(t)$ is

$$y(t) = A_0 + A\cos(2\pi\omega t - \varphi)$$

where A_0 is the mean, A and φ are the amplitude and phase of the cosinusoid with frequency ω, and t is the time. The value of A represents half the expected range of variability, while the phase represents the time when the value of $y(t)$ is maximum. Parameters A_0, A, and φ calculated by the fitting were used to obtain estimates of the seasonal means of temperature and salinity for January, April, July, and October.

The variability measured in temperature and salinity vertical distribution pattern at station 100.30 was compared with the hydrographic observations of station ENSENADA obtained over the sampling period (October 2006–November 2008). Chemical data (DIC and dO_2) was also represented for the station ENSENADA during the same sampling period.

Seasonal mean surface and subsurface flow patterns are shown by the cross-section of geostrophic velocity estimations along line 100 for January, April, July, and October. The velocity estimations were computed relative to 400 dbar using the historical hydrographic data of IMECOCAL surveys between 1998 and 2008. The reference level allowed the coastal station (100.30) to be included in the estimates of geostrophic velocity. In order to resolve critical information about slope subsurface currents adjacent to the shelf break, we have included here data from station 100.32, located midway between stations 30 and 35 (Fig. 2).

For the purpose of this work, all data were illustrated by temporal contours between 0 and 300 m depth for the stations of line 100 and between 0 and 95 m depth for the time series of station ENSENADA. Additionally, mean temperature and salinity anomalies of the first 50 m of the water column were calculated for station ENSENADA based on the comparison of the observations done over sampling period October 2006–November 2008 with the seasonal means of temperature and salinity for station 100.30 obtained by the annual fitting to hydrographic data.

Also, to identify interannual variations, monthly upwelling anomalies for 30°N 119°W and bimonthly Multivariate ENSO Indices (MEI, Wolter and Timlin, 1993, 1998) obtained from PFEL-NOAA (http://www.pfeg.noaa.gov/products/PFEL/modeled/indices/upwelling/NA/) and MEI (http://www.esrl.noaa.gov/psd/people/klaus.wolter/MEI/) web pages, respectively, were used for the period sampled at station ENSENADA.

3. Results

3.1. Climatologic analyses of temperature and salinity across line 100

The harmonic fitting parameters resulting from the analysis of line 100 temperature and salinity data are shown in Figs. 3 and 4, respectively. In these figures, density contours of 25.5 and 26.5 kg m^{-3} representing, respectively, the lower limit of CC core (SAW) and the CU core (ESsW) at this latitude (Durazo et al., 2010), are shown. Mean temperature (density) contours in the surface layer (0–100 m, Fig. 3a) show a lifting of the isotherms towards the coast, which indicate that on average the surface flow (CC) is southward, while the downward tilt towards the shore depicted by isolines at larger depths (>150 m) shows that on average the subsurface flow (CU) is poleward. Steeper slopes are located at the nearshore stations over the continental slope (coastward of station 100.35), associated with coastal upwelling, which seems to be a year-round feature over northern BC coastal waters. The climatological mean of salinity (Fig. 4a) shows the raise of the isohalines towards the coast throughout the water column, with the steeper slopes at the nearshore stations. The CC core ($S<33.4$) can be observed at approximately 150 km from station 100.30, centered around 50 m depth. The CU signal ($S>34.2$) is located below 200 m depth at stations close to the coast.

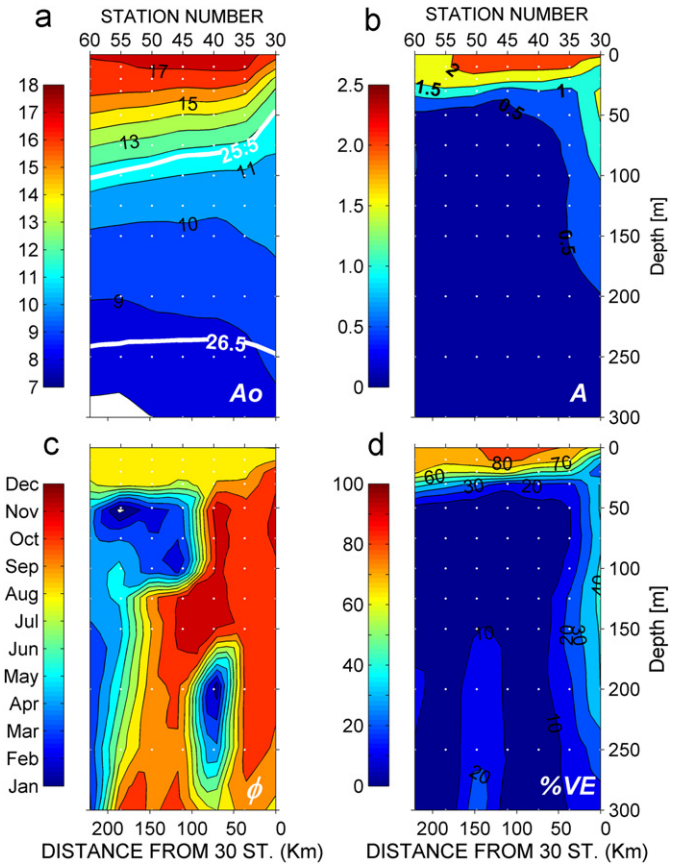

Fig. 3. Climatological temperature (°C) for line 100 generated from 11 years of IMECOCAL data. (a) Mean, (b) amplitude of the annual cycle (°C), (c) phase (months) of the annual cycle that denotes the time in which the cycle is maximum, (d) percentage of explained variance by the annual cycle. The 25.5 and 26.5 kg m^{-3} isopycnal surfaces are indicated by thick white lines, and represent approximations of the lower limit of the CC core (SAW) and the CU core (ESsW), respectively.

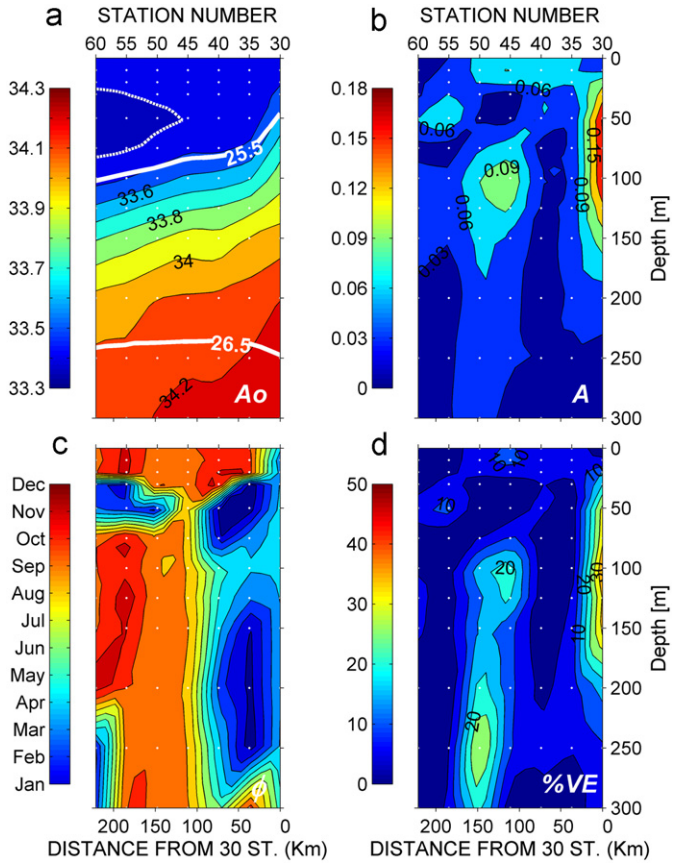

Fig. 4. Climatological salinity contours for line 100 generated from 11 years of IMECOCAL data. (a) Mean, (b) amplitude of the annual cycle, (c) Phase (months) of the annual cycle that denotes the time in which the cycle is maximum, (d) percentage of explained variance by the annual cycle. The 25.5 and 26.5 kg m^{-3} isopycnal surfaces are indicated by thick white lines, and represent approximations of the lower limit of the CC core (SAW) and the CU core (ESsW), respectively.

The seasonal variability, as reflected by the amplitude of the annual signal, is larger than 1.5 °C in the surface layer along the transect and toward nearshore stations (Fig. 3b), associated with the seasonally modulated ocean–atmosphere heat exchange, which warms up/cools down surface waters, and with the seasonal changes of stratification and mixing of the water column due to the variability of the alongshore winds, respectively. Salinity showed larger seasonal amplitude (>0.10) in a coastal band between 25 and 125 m depth, as well as in a central portion of the transect (Fig. 4b), likely related to seasonal changes in the subsurface flows in this region.

The percentage of explained variance by the harmonic fitting to the temperature signal (Fig. 3d) was typically 60% or larger in the surface layer (~0–25 m). In this surface layer, the phase (Fig. 3c) indicates that the maximum (minimum) temperature occurs in August (February), concurring with solar heating and heat storage cycles, and with coastal upwelling events during the spring transition. Towards the coast there is a second relative maxima in the percentage of explained variance (Fig. 3d) in a narrow band (<50 km), coincident with the maximum temperature in October (Fig. 3c) linked with subsurface poleward flows. Conversely, the low percentage of explained variance of the surface layer salinity (Fig. 4d) suggests that the variability is mainly due to non-seasonal fluctuations. Though scant seasonal variability in salinity is observed below the surface, relative maxima in the percentage of explained variance ($>$ 20%, Fig. 4d) coincide approximately with the maximum amplitudes of the

annual harmonic (Fig. 4b). Phase (Fig. 4c) indicates that saltier waters occur in February–April nearshore and in September–October offshore (>150 km). The time of occurrence of the subsurface coastal core in spring (Figs. 4b and c) suggests a lifting of more saline CU waters in response to wind forcing at the surface. The time of occurrence of the offshore maximum in summer–autumn may indicate the presence or increased advection of CU waters in this portion of transect.

3.2. Seasonal estimates of temperature and salinity for line 100

Harmonic fitting parameters were used to estimate temperature and salinity fields along line 100 for the four seasons of the year, represented in this work by the predicted fields for January, April, July, and October (Fig. 5). The temporal evolution of the hydrographic conditions corroborates that most of the variability in temperature is confined to the first 50 m of depth, with the lowest surface values (<15 °C) during January and the highest ($\sim$19 °C) during July. The largest uprising of relatively cold waters ($\sim$12 °C) reaching around 25 m depth near the coast is observed in April (Fig. 5, upper panels), associated with the more intense alongshore winds and offshore Ekman transport during spring. The seasonal trend of the vertical distribution of salinity also reveals a peak lifting of coastal waters and stronger cross-shore gradients during spring, although the raise occurs during most of the year. Also, the approach to the coast of a tongue of relative minimum salinity is observed along the transect during April and July (Fig. 5, lower panels) concurrent with the approach to the coast of the offshore CC core and the intensification and maintenance of an equatorward coastal jet in spring and summer, as will be described below (Fig. 6). By autumn, the temperature and salinity contours as well as the 25.5 isopycnal surface depict a more stratified water column. Therefore, low temperature and less saline waters (SAW), which occupy a greater volume of the surface layer (0–100 m depth) across the transect during this season (Fig. 5, Supplementary Fig. 1) are likely associated with the more meandering flow of the CC while

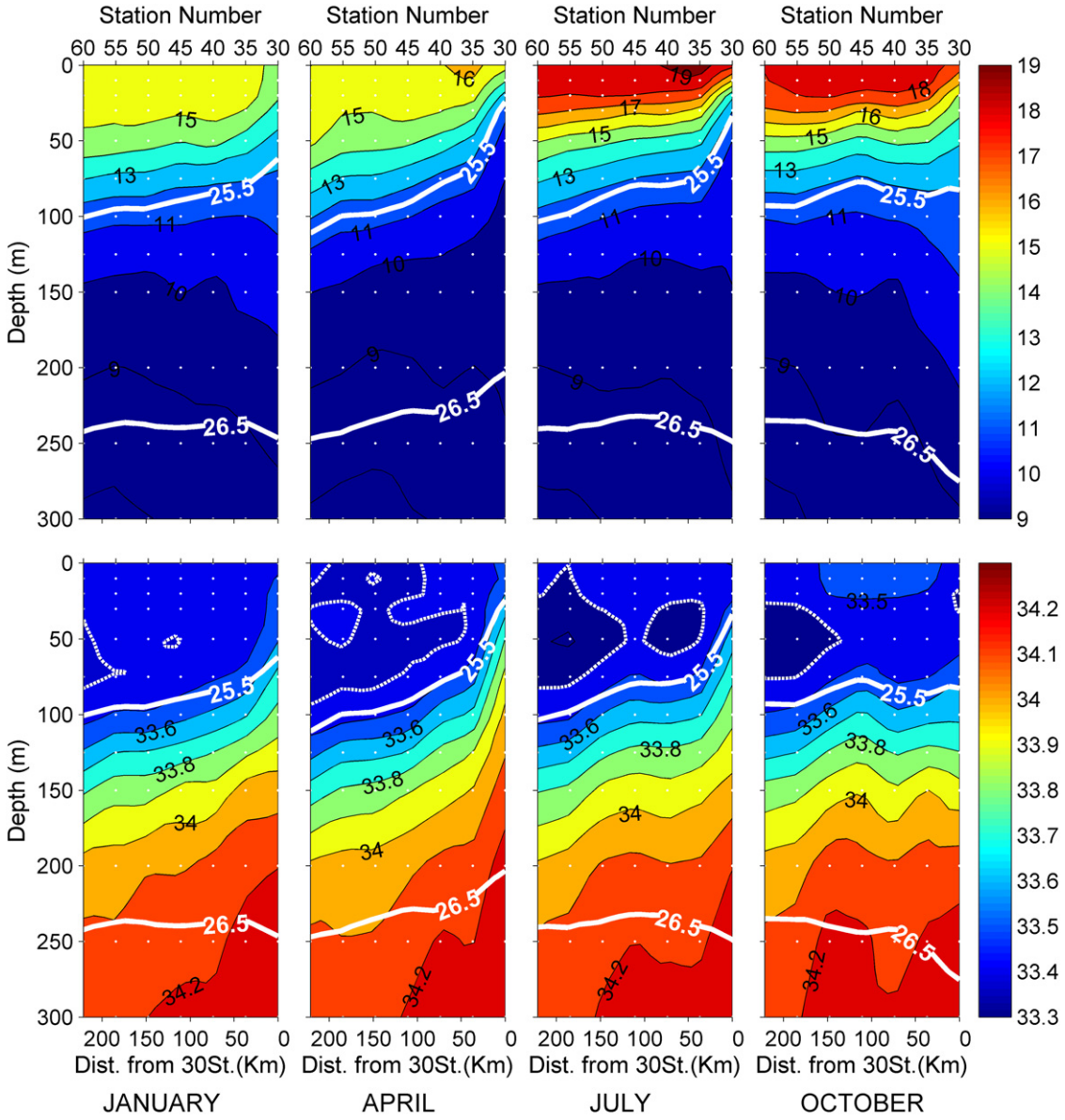

Fig. 5. Temperature (°C, upper panels) and salinity (lower panels) contours for January, April, July, and October across line 100. Values were estimated by harmonic analysis of data collected during 11 years by the IMECOCAL program. The 25.5 and 26.5 kg m^{-3} isopycnal surfaces are indicated by thick white lines and represent approximations of the lower limit of the CC core (SAW) and the CU core (ESsW), respectively.

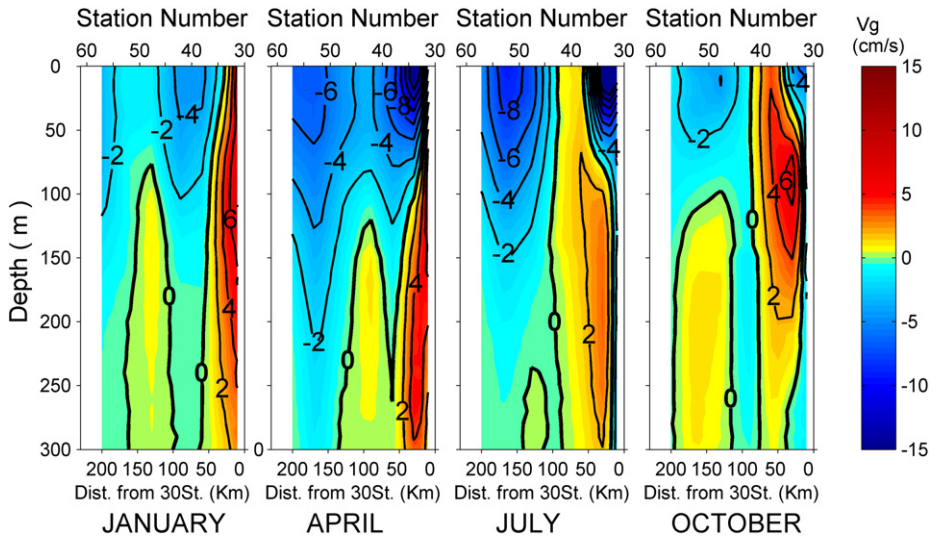

Fig. 6. Cross-sections of geostrophic velocity (cm s^{-1}) for January, April, July, and October across line 100, estimated by harmonic analysis of velocity derived from the hydrographic data collected during 11 years by the IMECOCAL program. The reference level is 400 dbar. Negative (positive) values indicate equatorward (poleward) flows. Contour interval is 2 cm s^{-1}.

passing through northern BC. It is also in this season when near surface (<100 m depth) isolines and the reduced slope of the 25.5 isopycnal surface evidence a slight downwelling coastward, possibly related with the cyclonic recirculation of CC waters originated by the southward displacement of the Southern California Bight (SCB) eddy (Fig. 5). Mostly during July and October, a slight doming of isolines is observed throughout the water column below 100 m depth and between 100 and 150 km offshore (Fig. 5). This doming could be the result of Ekman pumping manifested as the lifting of more saline subsurface waters originated by the cyclonic circulation in the surface of the CC. Also, as will be shown below, the eastern flank of this dome (<50 km) appears to be reinforced by the intensification of the poleward flow of the CU, as is indicated by the maximum slope towards the coast of the 26.5 isopycnal surface.

3.3. Seasonal estimates of geostrophic velocity for line 100

Cross-sections of line 100 geostrophic velocity for January, April, July, and October, estimated using the harmonic analysis coefficients (not shown), are depicted in Fig. 6. As indicated by the mean seasonal slopes of isotherms in the previous section, the mean surface flow (<100 m) depicting the CC is mainly equatorward year-round (negative values), with seasonal variations in its intensity and width across the section (Fig. 6). The equatorward surface flow is divided in two cores, a relatively intense coastal jet that is mainly observed during spring and summer due to the predominance of northwesterly winds favorable to coastal upwelling, and an offshore core associated with the permanent flow of the CC. The coastal jet is also evidenced by the steady lifting of isolines towards the coast during April and July (Fig. 5). Seasonally, the coastal jet is strong (>10 cm s^{-1}) and occupies the upper 80 m of the water column during April and July, associated with the peak of the upwelling season. In October it appears as a weak flow (~1 cm s^{-1}) next to the coast in the upper 25 m. By January the coastal jet has been displaced offshore (around station 100.40) by an inshore poleward flow (positive values, Fig. 6). In April the coastal jet is wider than in July and it is connected with the offshore CC flow. Although weaker, the same connectivity is observed in January. In contrast, the coastal jet is constrained to shore during July (~50 km) and October (~20 km) and is clearly separated from the offshore CC jet by poleward surface flows (Fig. 6). The offshore CC core exhibits seasonal variability and is located around 150 km from station 100.30, coincident with the low-salinity core (Fig. 4a). It is weaker (~2 cm s^{-1}) and further from shore in January, while during April and July it is stronger (>6 cm s^{-1}) and closer to the coast. By October, the offshore CC flow weakens (~3–4 cm s^{-1}) and occupies a large part of the offshore waters at the surface layer (0–100 m depth) of the section (Fig. 6), as is evidenced by the greater volume of low temperature and less saline waters (Fig. 5, Supplementary Fig. 1d). Additionally, the presence of poleward surface flows (positive values) seems to be a quasi-permanent feature year-round. The northward surface flow is located in a coastal band that apparently shows cross-section displacement along the year. It is stronger in January and October (>6 cm s^{-1}), and weaker (<2 cm s^{-1}) in July. In January, it appears as a narrow flow (<50 km) next to the coast. By April, it disappears from the upper layers (<100 m), associated with the intensification of the upwelling winds. In July, this poleward surface current is fully separated from the coast (>50 km offshore) by the strong equatorward coastal jet, while by October, it flows in a broad band of ~100 km from station 100.30, slightly distant of the shore (Fig. 6). This northward surface flow is apparently the result of the shoaling of the more intense subsurface CU, which is possibly reinforced with the mesoscale activity and cyclonic recirculation of the CC, which in turn is modulated by vertical stratification and a positive wind stress curl nearshore (0–500 km) (Fig. 6).

The mean subsurface flow (>100 m depth) is mostly poleward (positive values). A main subsurface core is located against the slope year-round and represents the CU. It also shows seasonal variability in its depth and intensity (Fig. 6). The core of the CU is deeper (>150 m) in April and July, and shallower (~100 m) and more intense (8–10 cm s^{-1}) in January and October. However, the CU is wider (~100 km) in October than in January (<50 km). Except in April, the slope undercurrent apparently appears connected with poleward surface flows (Fig. 6). Offshore, a less intense subsurface poleward flow (~150 km) co-exists with the slope undercurrent throughout the year although it is more clearly noticeable in October and

January. The offshore core has also been observed off Southern California where it has been suggested that may be the result of a bifurcation of the main core of the CU at deep waters.

3.4. Hydrographic variability for stations 100.30 and ENSENADA

In order to determine whether the hydrographic conditions observed in the coastal observatory (station ENSENADA) reflect the main features of the variability of the coastal region off Ensenada, we compare here the temporal distribution of temperature and salinity of the upper water column (0–100 m) recorded at stations 100.30 and ENSENADA during the period from October 2006 to November 2008. Fig. 7 shows the depth–time evolution of properties, including the 25.5 and 26.2 kg m^{-3} density contours. In general, both stations showed a similar vertical distribution of the hydrographic variables, mainly associated with the seasonal warming/cooling cycles of the surface layer modulated by ocean–atmosphere heat exchange during the sampling period, with the upwelling events of relative saltier and cooler subsurface waters mostly during spring months of 2007 and 2008. For each depth, a statistical comparison (*t*-test) of the hydrographic fields for eight concomitant cruises conducted in both stations revealed that arithmetic means computed were not statistically different ($p < 0.05$), i.e., the null hypothesis (H_0: station 100.30 mean = station ENSENADA mean) was not rejected at each depth level from the surface to 100 m depth. The similarity of temperature and salinity mean profiles between both the stations is evidenced in the Supplementary Fig. 2. Mean and standard errors of these hydrographic variables showed similar variability throughout the water column between both stations. Thus no significant difference between station 100.30 and station ENSENADA was found in the vertical distribution of the hydrographic variables.

Except some particular but, statistically non-significant differences between stations 100.30 and ENSENADA, a marked seasonal pattern was found in the near surface (< 10 m) temperature at both locations. In general, this surface pattern was in agreement with the climatologic seasonal estimates of temperature for line 100 (Fig. 5), though the phase was different in each year. The lowest surface values (< 15 °C) were mostly found during spring 2007 and from winter to spring 2008, while the highest (> 17 °C) during autumn 2006 and from summer to autumn 2007 and 2008 (Fig. 7a and b). In the same surface layer, salinity values showed a

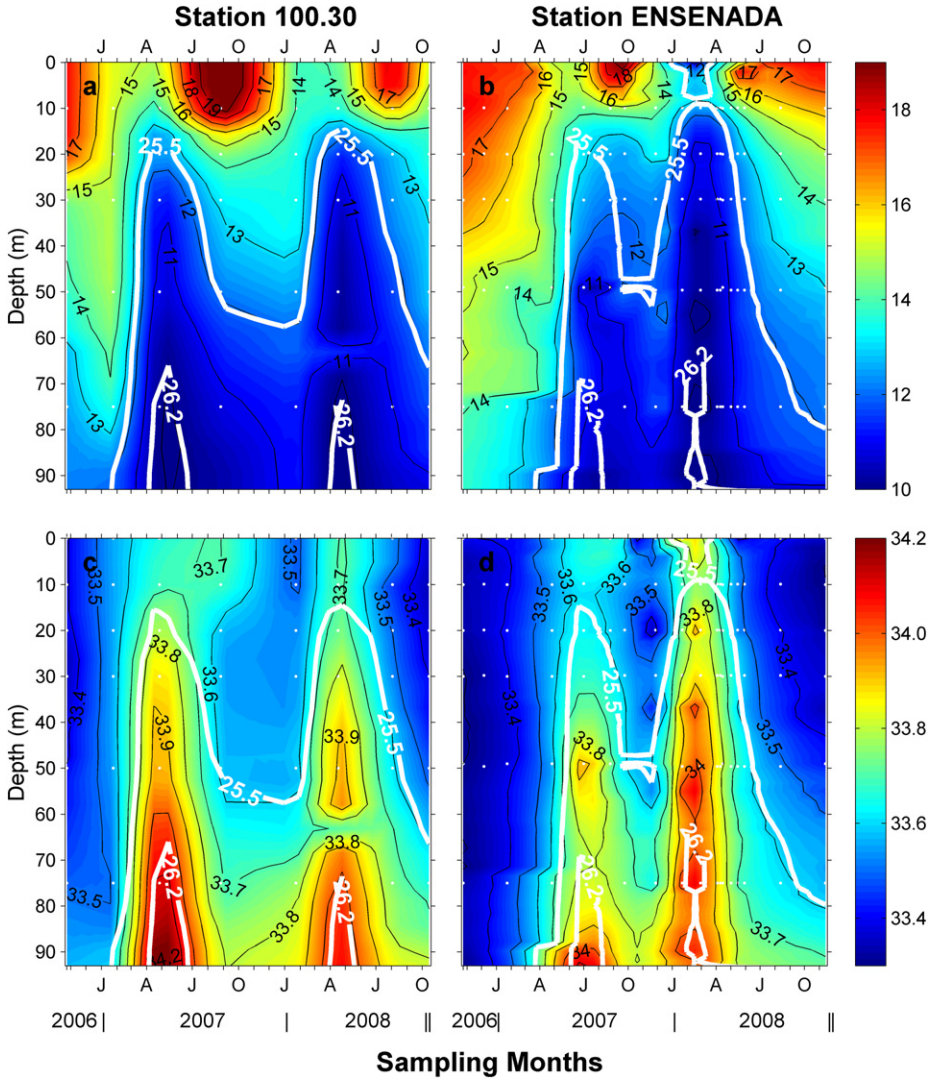

Fig. 7. Temperature (°C) (a, b) and salinity (c, d) contours for station 100.30 and for station ENSENADA of the data collected from October 2006 to November 2008. The 25.5 and 26.2 kg m^{-3} isopycnal surfaces are indicated by thick white lines and represent approximations of the lower limit of the CC core (SAW) and the upper depth limit of the CU (ESsW), respectively. White dots in each plot indicate standard depths.

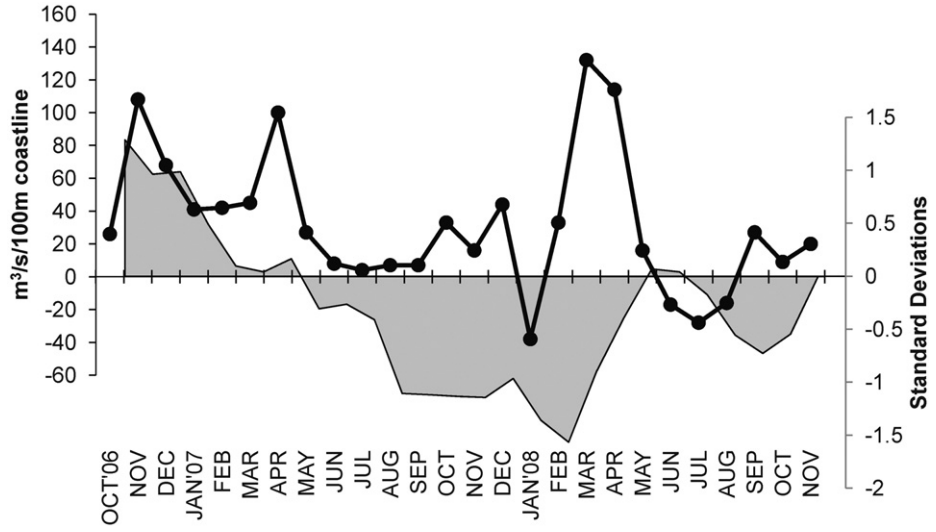

Fig. 8. Monthly upwelling anomalies for 30°N, 119°W (black line-dots) and bimonthly Multivariate ENSO Indices (gray shaded area) for the period October 2006–November 2008. The values of the upwelling index anomaly were obtained from PFEL-NOAA http://www.pfeg.noaa.gov/products/PFEL/modeled/indices/upwelling/NA/, and the MEI index from http://www.cdc.noaa.gov/people/klaus.wolter/MEI/ web pages, respectively.

similar quasi-seasonal pattern (Fig. 7c and d), as was seen in the climatological analyses for line 100 (Fig. 4). Below 10 m depth, a large part of the water column was occupied by cooler (<12 °C) and saltier (>33.8) waters from spring to summer 2007 and also, from winter to spring 2008, likely due to a seasonal lifting of isolines caused by wind-driven vertical pumping at the surface, as was indicated by the appearance of the 26.2 kg m^{-3} isopycnal surface at shallower depths at both stations (Fig. 7c and d). From the sampling period, the upwelling observed during 2008 was more intense than for 2007, as was evidenced by the more saline waters (~33.7) that reached the surface during spring 2008 (Fig. 7c and d). This interannual variation is likely associated with environmental indices related with the intensity of upwelling (Coastal Upwelling Index Anomaly) and the large-scale ocean–atmosphere variability (MEI) (Fig. 8). The surfacing of the relatively salty waters during 2008 was likely associated with an intensification of upwelling events (positive upwelling anomalies) during a cold ENSO phase, i.e. La Niña condition, represented by negative MEI values from summer 2007 to spring 2008 (Fig. 8).

3.5. Temperature and salinity anomalies for station ENSENADA

Harmonic fitting to temperature and salinity data for line 100 showed that their largest fluctuations occur in the first 50 m of the water column (Figs. 3 and 4). Given the fact that temporal variability of properties at station ENSENADA resembles that of station 100.30 (Fig. 7), mean temperature and salinity anomalies of the upper 50 m of the water column were calculated for station ENSENADA (Fig. 9) with respect to the corresponding climatological means obtained for station 100.30 (Figs. 3a and 4a). The temporal evolution showed positive temperature anomalies of ~1 °C at the end of 2006 and beginning of 2007 (Fig. 9a). These anomalies coincided with the higher than normal temperature values recorded above 50 m during winter of 2006 (Fig. 7b) and also at station 100.30 (Fig. 7a). This positive temperature anomaly coincided with the positive MEI values recorded from October 2006 to February 2007 as indicative of the warm ENSO phase, i.e., El Niño condition (Fig. 8). Except the slight positive anomaly observed in August 2007, surface waters were colder than the climatological average from January 2007 to the end of 2008. Maximum negative values were observed between autumn 2007 and spring 2008 (Fig. 9a), which coincided with negative MEI values (La Niña condition) from May–June 2007 to April–May 2008 (Fig. 8). Associated with these large-scale conditions, the region also experienced stronger than normal upwelling during February–April 2008 as was indicated by the upwelling index anomaly for 30°N. Thus, the anomalous conditions observed in spring 2008 were originated by large-scale events that modulated local forcings.

Concomitant with the advection of saltier waters from the south during El Niño and increased upwelling and offshore Ekman transport during La Niña, due to stronger than normal alongshore winds occurring during these cold events, salinity anomalies were positive throughout the sampling period, with larger magnitude during spring of both 2007 and 2008 (Fig. 9b). Maximum values were recorded in spring 2008, and similar to the temperature anomalies, the saltier than normal waters at station ENSENADA were likely caused by an upwelling intensification of subsurface waters under La Niña cold conditions (Fig. 8).

3.6. Distribution of chemical variables for station ENSENADA

The temporal distribution of chemical variables at the coastal station (Fig. 10) showed a similar pattern to that depicted by the thermohaline properties (Fig. 7). Although the highest concentrations of dO_2 depicted a trend occurring at the surface due to the larger ocean–atmosphere exchange, the presence of less saline (Fig. 7d) and well-oxygenated waters (>300 μM) throughout the water column was notable from the end of 2006 to the beginning of 2007 (Fig. 10a). Thus, the prevailing water mass during this period was of subarctic origin (SAW), likely associated with a deeper seasonal thermocline due to El Niño conditions recorded in this period (Fig. 8). Also, the spring seasons of 2007 and 2008 were characterized by a lifting of low dO_2 waters, likely associated with the penetration into the surface layer of waters carried by the CU from the equatorial region. As shown before, this lifting during spring 2008 was very intense, so colder, saltier waters with dO_2 concentrations <150 μM were recorded close to the surface at this coastal observatory (Fig. 10a).

The temporal distribution of DIC throughout the water column showed the highest values associated with deeper waters (Fig. 10b). Worth noting were the low surface values and the lifting of DIC-rich subsurface waters in the spring of both 2007

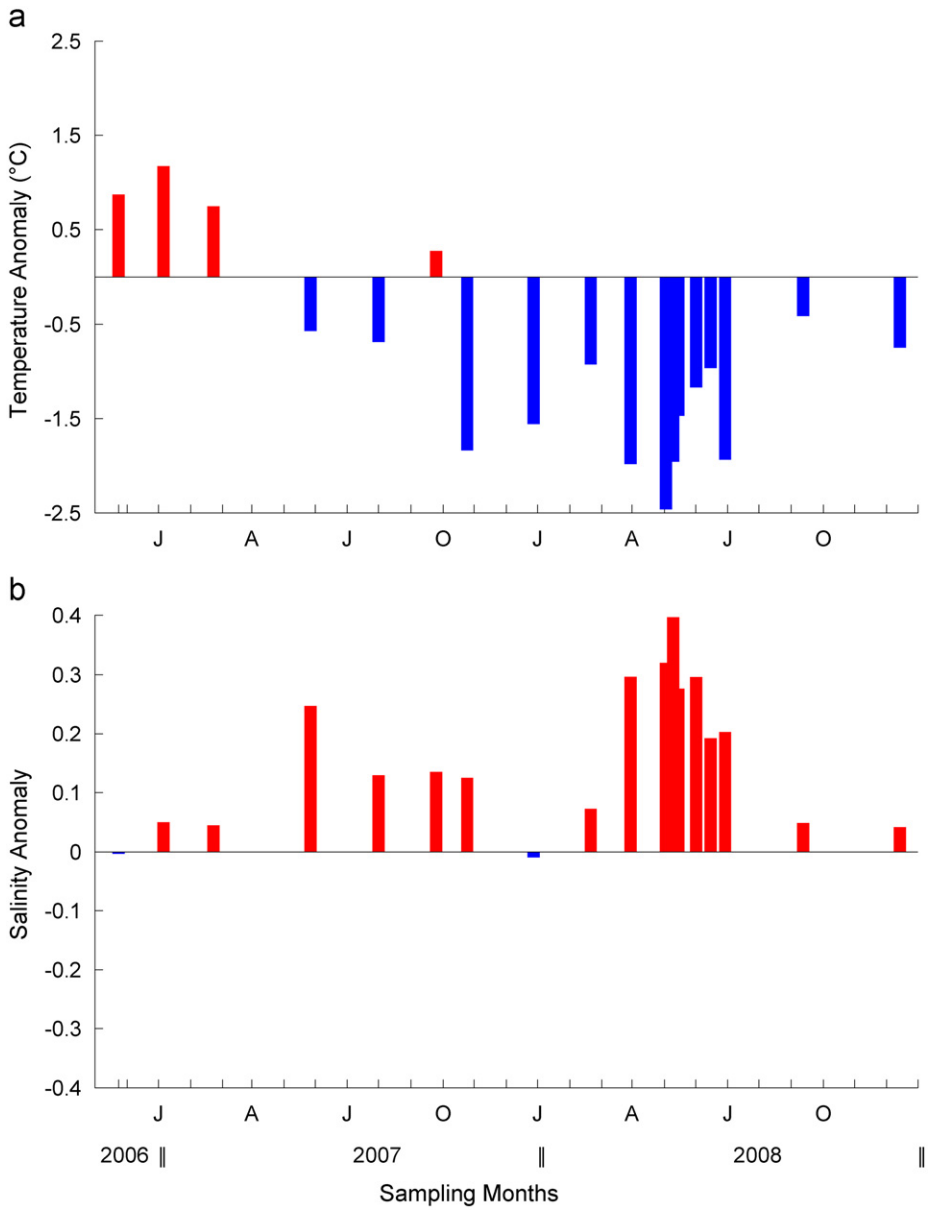

Fig. 9. Mean (a) temperature (°C) and (b) salinity anomalies of the upper 50 m of the water column for the data collected at station ENSENADA from October 2006 to November 2008. Anomalies were computed relative to the climatological means obtained for station 100.30 by the annual fitting to hydrographic data.

and 2008. Concomitant with the behavior of the hydrographic variables, the shoaling of DIC isolines was more pronounced during spring 2008, with maximum values of ~2165 μmol kg^{-1} at a scant 30 m depth. As a macronutrient, DIC presented a similar behavior to that of micronutrients such as nitrate, phosphate, and silicate (data contours not shown). The highest DIC concentrations at shallower depths in April 2008 were associated with the physical characteristics (salty and cold) of the water mass (ESsW) upwelled from subsurface towards surface layers.

4. Discussion

The analysis of the historical hydrographic measurements (1998–2008) at coastal waters off Ensenada presented above illustrates a marked seasonal variability in the physical and chemical conditions. Greatest temperature variability occurred in the surface layer close to the coast (< 100 m, Fig. 3) modulated by seasonal fluctuations in air–sea exchanges, as well as wind variability that controls coastal upwelling, stratification, and surface circulation patterns. The seasonal variability in salinity was found weaker at the surface and stronger toward subsurface layers (Fig. 4), associated with the seasonality of the coastal upwelling and the structure of surface and subsurface flows. Thus, a large part of the variability in the hydrographic conditions off Ensenada is due to the seasonal fluctuations of the strength of the circulation and the variability in the characteristics of water masses feeding into the surface and subsurface flows.

Along the transect analyzed, it was found that the core of the CC that transports equatorward relatively low-salinity water of subarctic origin was located further away from the coast (~200 km) during winter, but closest to shore (~100 km) during spring–summer (Figs. 5 and 6). The proximity to the coast of the mean position of this offshore CC core during spring–summer was also observed in the region of Southern California Bight (SCB) (Bograd and Lynn, 2003), and has been associated with the

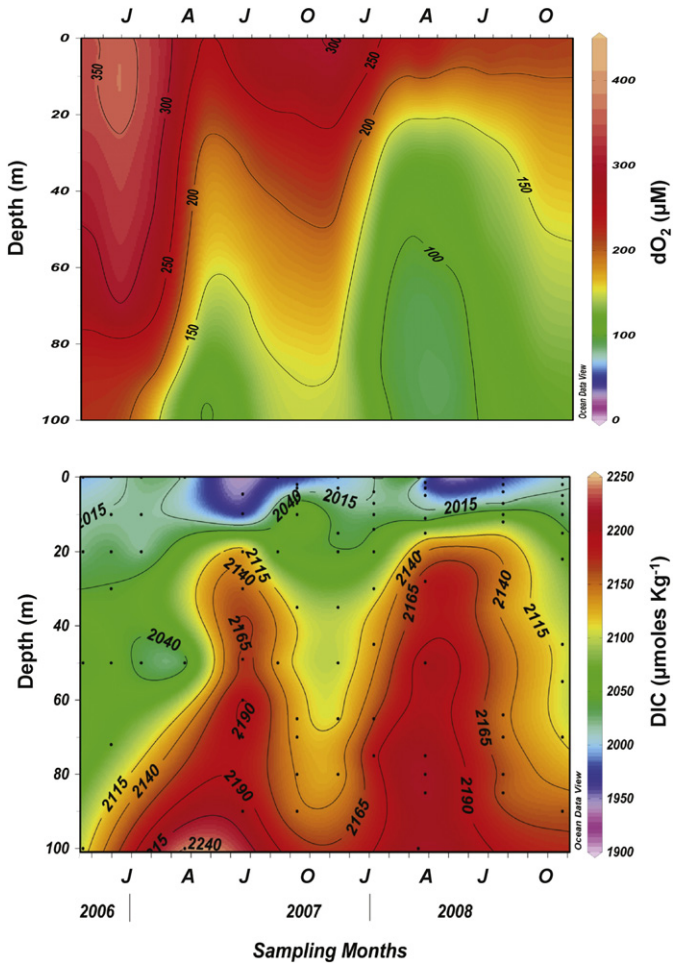

Fig. 10. Contours of concentration of (a) dissolved oxygen (μM) and (b) dissolved inorganic carbon (μmol kg^{-1}) for the data collected at station ENSENADA from October 2006 to November 2008.

springtime development of a coastal equatorward jet (Lynn et al., 2003). The southward flow near to the coast was also recorded in this work, being more intense (>10 cm s^{-1}) during spring and summer (Fig. 6). Since this coastal jet is not associated with the relative minimum of near surface salinity offshore, we suggest that it is made of a mixture of subarctic CC water and more salty subsurface water eroded from the upper CU during strong upwelling events. This finding is supported by the seasonal mean *T* and *S* diagrams for April (Supplementary Fig. 1b) when more saline waters from subsurface layers (ESsW) are evidenced mostly at station 100.30 compared to other stations of the section. This is in agreement with observations conducted further north in the CCS (Hickey, 1979; Lynn and Simpson, 1987; Bograd and Lynn, 2003), although in those regions the coastal jet reverses direction in response to local forcing. The seasonality of the southward coastal flow may be explained in terms of a geostrophic adjustment to coastal upwelling. The alongshore winds are stronger during spring–summer (Pérez-Brunius et al., 2007) and bring to the surface cooler and saltier waters, generating maximum vertical and horizontal gradients of the upper 200 m. This is also seen in the results of the harmonic fitting of salinity (and harmonic fitting of velocity, not shown), which represent a relatively large proportion of the explained variance near the coast with the maximum signal during spring (Fig. 4).

Poleward surface flows were evidenced close to the coast (within the first 100 km from station 100.30) during summer, autumn, and winter (Fig. 6). Previous studies that used current meter moorings in three nominal depths (25, 42 and 60 m) on the continental shelf off Ensenada in the period 1978–1979 (Barton, 1985) demonstrated that flows were northward year-round below 25 m depth, and at all levels only in the period from May to October. Furthermore, Alvarez et al. (1984, 1990) reported surface coastal poleward flows related to weak wind conditions for two coastal sites located at 31.3°N and 32.5°N. Frequently, surface geostrophic flows have been associated with small-scale (20–50 km) cyclonic circulation regions produced by strong upwelling near capes and coastal promontories off BC (Durazo and Baumgartner, 2002; Durazo et al., 2005). More recently, 10 years of ship-borne ADCP measurements analyzed by Gay and Chereskin (2009) demonstrated that coastal poleward surface flows (above 100 m depth) occur inside the SCB slightly separated from the coast by equatorward currents during summer, autumn, and winter. In a regional context, Lynn and Simpson (1987) showed that south of Point Conception (34.5°N), the equatorward CC flows offshore (~500 km) and divides in two branches at the latitude of Ensenada, one that impinges on the coast near Punta Baja (29°N) and another that flows coastward to become the SCB eddy. They demonstrated that the eddy shows a clear seasonal variability in strength and position, with its southernmost location during summer–autumn. These previous findings suggest that July, October, and even January surface poleward coastal flows presented here form part of the eastern limb of the SCB eddy that extends southward over the northern BC region.

The summer, autumn, and winter processes described here seem to be related with wind stress patterns along the coast and the latitudinal displacement of the SCB eddy. As spring transitions to summer–autumn, upwelling winds relax close to the coast, but remain strong further offshore the continental slope, generating a positive wind-stress curl (cyclonic). This positive curl has been associated with the recirculation of CC waters in the SCB region (Di Lorenzo, 2003). Moreover, positive wind stress curl has been reported for northern BC (30°N) by Castro and Martínez (2010), linked to the wind patterns in the SCB region. Such positive wind-stress curl is a physical mechanism that generates Ekman pumping of more saline, poor in dO_2 and nutrient-rich subsurface waters to upper levels, particularly downstream coastal prominences (Bakun and Nelson 1991, Chelton et al., 2004; Rykaczewski and Checkley, 2008). Off Ensenada, evidence of this forcing is seen by the doming structure observed in July and mostly in October (Fig. 5), a feature that extends vertically throughout the water column in the central part of line 100. The seasonality of this "lifting" was made evident in the relatively large explained variance near 200 m depth shown by the harmonic fitting to salinity (Fig. 3d), which has its maximum value around October. Thus, the dome structure observed in our region in July and October is likely due to the pumping of more saline subsurface waters toward upper depth levels (Fig. 5) and would be the subsurface signature of the southward extension of the surface circulation related to the SCB eddy (Fig. 6).

Subsurface flows were identified year-round mainly by the CU flow located over the continental slope and by a weaker secondary core ~150 km offshore (Fig. 6). Their presence in our zone confirms the general feature of the eastern boundary current systems, which has a clear seasonal variability. Hydrographic fields illustrated a downward tilt towards shore of the 26.5 isopycnal surface during most of the year, the approximation of CU core against the slope in our region (Fig. 5). Similarly, the seasonal mean *T–S* diagrams for line 100 (Supplementary Fig. 1) shows the presence of ESsW (transported by the CU) during all year, especially toward the most coastal stations. The poleward subsurface flows were also reflected in the mean seasonal geostrophic velocity contours, being the slope undercurrent stronger (>8–10 cm s^{-1}) and shallower (~100 m) in autumn

and winter compared with summer when it was found to be weak (<2 cm s^{-1}) below 100 m depth. Excepting spring, when the slope undercurrent occurred deeper (below 150 m depth) in a band constrained to the coast, the CU seems to be connected with poleward surface flows the rest of the year. The couplings with northward surface flows have also been recorded for waters off southern California, where the CU was found more intense both in summer and autumn, especially inside the SCB (Gay and Chereskin, 2009). The secondary core has also been documented for Southern California where it has been suggested that the offshore subsurface poleward current results from a bifurcation of the main CU off San Diego, and that such bifurcation converge near Point Conception. Our data indicate that the two cores co-exist off Ensenada. At present, the origin of the secondary offshore subsurface poleward current remains unclear. Subsurface currents along the Baja California peninsula (not shown) suggest a pattern similar to Southern California, with a core south of Punta Eugenia and two cores elsewhere. It has been suggested (Holloway, 1992) that the interaction of mesoscale eddies with bottom topography may have some influence on the generation, width or location of undercurrents near the continental slope. Such subsurface structures are common along the CCS (Garfield et al., 1999; Jeronimo and Gómez-Valdés, 2007). It is thus likely that poleward subsurface flows become well organized before reaching coastal prominences, and that the bifurcation to be generated downcurrent. However, more studies are needed to understand the underlying mechanisms that favor the splitting of the main CU in two branches.

In a regional context, subsurface geostrophic flows (200/500 dbar) off northern BC ($>28^{\circ}$N) are characterized by a cyclonic circulation, a deep signature of the SCB eddy (Durazo, 2009). The position and size of this subsurface cyclonic circulation exhibit seasonal variability, being absent or diffuse during spring and better defined during summer and autumn (Durazo et al., 2010). Since the seasonality of this cyclonic circulation concurs mainly in autumn with the variability of the slope CU flow described here, it is feasible that coastal poleward subsurface flows across line 100 may be identified as the eastern limb of the subsurface cyclonic gyre. Therefore, the seasonal intensification and shoaling of the slope undercurrent, as well as the bifurcation from the main CU core (offshore CU) could be seasonally reinforced by the strengthening and southward extension of the SCB eddy, considered here as a deeper expression of the surface cyclonic recirculation of the CC over northern BC waters.

The higher temporal resolution data set shown for station ENSENADA, located only 8 km eastward of station 100.30 (the closest station to line 100), revealed that this site is capable of perceiving the seasonal variability in the physical and chemical properties of the water column for the coastal region off Ensenada [$<$ 50 km, the local decorrelation scale, Walstad et al., 1991; Denman and Freeland, 1985], and also to some seasonal circulation patterns that have been described above. Consistent with observations for station 100.30, station ENSENADA showed larger surface heating in the summer modulated by seasonal fluctuations in air–sea exchanges, a larger input of cold, saline waters in the surface layer associated with coastal upwelling in spring–summer, and the presence of relatively low-salinity waters in most of the surface layer (<50 m) in autumn–winter (Figs. 7c and 7d). Although station 100.30 is deeper (<500 m) than station ENSENADA ($\sim$100 m), the intensification of poleward flows (CU) during autumn–early winter was practically undetectable at either location. Instead, in spring–summer an equatorward coastal jet characterized by salty waters in comparison to the CC core (Fig. 7b) seems to be more related with the erosion of subsurface waters lifted to shallower depths by vertical Ekman transport produced by the year-round alongshore winds, which are more intense and persistent in spring (Bakun and Nelson, 1977; Huyer, 1983; Pérez-Brunius et al., 2007). Thus, persistent coastal upwelling driven by alongshore winds may be an important physical mechanism for the input of subsurface waters towards the coast in this region, mainly during spring–summer.

Our findings indicate that station ENSENADA is also a site sensitive to interannual signals (Fig. 7c and d) as was reflected by the mean positive temperature anomalies ($\sim$1 $^{\circ}$C; Fig. 9a) recorded during El Niño conditions (Goericke et al., 2007; Durazo, 2009) from late 2006 to the beginning of 2007. This warming was also observed in the positive MEI values recorded by the end of 2006 (Fig. 8). Although positive salinity anomalies were also recorded at station ENSENADA, the values were low (<0.1) in comparison with those recorded in subsequent months (Fig. 9b). This may be because the poleward surface advection of waters of tropical and subtropical origin that has been associated with this type of events off BC (Durazo and Baumgartner, 2002) occurred as a tongue of relatively more saline water that only extended to latitudes close to 29°N (Goericke et al., 2007; Durazo, 2009). Towards early 2007, El Niño conditions quickly disappeared in the CCS giving way to La Niña, which continued until early summer 2008 (McClatchie et al., 2008; Durazo, 2009), as it was indicated by the Oceanic NINO Index reported by the NOAA Climate Prediction Center (http://www.cpc.noaa.gov/) for the period December 2007–January/February 2008, as well as by the negative values of MEI Index from May/June 2007 to April/May 2008 (Fig. 8). During this same period, the Pacific Decadal Oscillation (PDO) Index was negative for the North Pacific due to negative anomalies in sea surface temperature, with colder than usual temperatures in the CC and the Gulf of Alaska (McClatchie et al., 2008). Further, the upwelling favorable winds were more intense than normal off the coasts of central California and BC in spring 2007 and 2008 (Goericke et al., 2007; McClatchie et al., 2008). The upwelling index anomalies data reported by NOAA for 30°N reported high index values in the spring of both 2007 and 2008, with maximum positive anomalies (>100 m^3 s^{-1} per 100 m of coastline) in March and April 2008 (Fig. 8). This concurs with the notable lifting of cold, more saline subsurface waters, poor in dO_2 and rich in nutrients, observed at station ENSENADA from February to June 2008 (Figs. 7c and d and 10). As a consequence, the interannual variability observed in the thermohaline conditions at this coastal location may be linked to ENSO events with effects in the warming (El Niño) or cooling (La Niña) of local waters that generated anomalies in the regional flows and in the intensity of coastal upwelling. At these interannual timescales, the upper mixed layer also exhibits variability in temperature and salinity for the waters along the BC Peninsula, associated mainly with regional (northern and southern BC) differences in the atmosphere–ocean net heat fluxes and with large-scale variability in the sea surface height anomaly, respectively (Gómez-Valdés and Jeronimo, 2009). Thus, it is likely that at longer timescales the signal of large-scale (PDO) variability would be also detected in a shallow coastal region as station ENSENADA.

Changes in hydrographic properties are very important for marine ecosystems. In particular, seasonal and long-term variations in the physical and chemical water properties can cause alterations in the structure of the water column, such as in mixed layer and thermocline depths, and the strength of vertical stratification. Therefore, fluctuations of properties in the water column can generate changes in the input of inorganic nutrients to the euphotic zone, with the consequent impact on primary and secondary production (Lavaniegos and Ohman, 2003; Gaxiola-Castro et al., 2008). In the long-term, these changes could become evident at station ENSENADA that is modulated by seasonal and interannual variability. Particularly during spring 2008, the

fluctuations in the hydrographic variables were associated with the intensified upwelling of subsurface waters that were poor in dO_2, but rich in DIC and nutrients, into the euphotic zone (Fig. 10). Enhanced advection of low-pH subsurface waters, rich in DIC and subsaturated in aragonite, onto the continental shelf, can seriously affect marine organisms that form calcareous shells and skeletons. In fact, recent results have shown that upwelling plays an important role in the transport of waters affected by the acidification of the ocean over the continental shelf of North America (Feely et al., 2008). Likewise, an increased input of poor dO_2 waters into surface layers caused by seasonal upwelling can result in severe ecological impacts on the ecosystem, especially in areas where the continental shelf is close to hypoxic conditions. For example, in coastal waters off southern California, a decrease in dO_2 as well as an increase in the hypoxic limit ($\sim$60 μmol/kg) above 90 m depth have been recorded in the surface layer at 100 m depth over a period of 23 years, mainly along the continental shelf and break (Bograd et al., 2008). An expansion in the water column of the oxygen minimum layer could lead to cascading effects on benthic and pelagic ecosystems, including habitat compression and community reorganization (Bograd et al., 2008; Chan et al., 2008). Thus, monitoring the oceanographic conditions at a coastal station in the northeastern Pacific not only provides a more frequent data set for this dynamic region, but also generates an environmental framework to evaluate the variability in the coastal waters at different timescales (seasonal, interannual, decadal) of this part of the CCS, as well as to define a baseline for future biogeochemical models in the context of global climate change.

5. Conclusions

The results of the historical analysis of hydrographic data gathered at coastal waters off Ensenada, BC, revealed a marked seasonal variability in the physical and chemical conditions of the northern BC region. It was found that temperature variability occurs mainly in nearshore surface layers (<100 m), while salinity variability increases towards subsurface layers. The variability described in both parameters is modulated by seasonal fluctuations in air–sea exchanges and also by wind patterns (alongshore and cyclonic wind-stress curl) that control coastal upwelling, stratification of the water column, and surface (CC) and subsurface (CU) seasonal circulation patterns. During spring–summer, the main physical process that modifies the nearshore hydrographic conditions is coastal upwelling driven by strong alongshore winds, which results in the presence of relatively more saline, cooler, poor in dO_2 and nutrient-rich subsurface waters and the intensification of an equatorward surface coastal jet. It was also found that a large part of the variability during summer–autumn and winter represents the main features of the seasonality of circulation patterns off southern California and northern BC, namely: (1) the southward extension of the SCB eddy with an intense mesoscale activity, (2) the surface poleward flows in a narrow coastal band (<100 km) and below this, the subsurface poleward flows of the CU, both linked to the CC cyclonic recirculation and the permanent northern subsurface cyclonic eddy, (3) the offshore bifurcation of the main CU core located against the slope, (4) the upward intrusion of more saline subsurface waters by Ekman pumping (positive wind-stress curl), and (5) the intensification of the slope undercurrent.

Particularly, the seasonal variability observed at station ENSENADA, a coastal monitoring observatory, was similar to that described for station 100.30, and reflects adequately the seasonal variability of the coastal waters (<50 km) off Ensenada, BC. In addition to this seasonal variability, the coastal site reflected the interannual variability associated with warm and/or cold basin-wide events that modified the water column structure in this coastal region. This was evidenced in station ENSENADA by the negative temperature (~ -1.5 °C) and positive salinity ($\sim$0.3) anomalies recorded in spring 2008, when subsurface waters of equatorial origin poor in dO_2 and rich in DIC were found at 30 m depth due to the intensification of coastal upwelling events at this time of year. This coincided with high positive anomalies of the upwelling index (>100 m^3 s^{-1} per 100 m of coastline) reported by NOAA in March and April 2008 at 30°N, and with an increase in wind intensity off central California and BC in spring 2008, all related to the La Niña event indicated by the MEI index from the summer 2007 to mid 2008. Thus, station ENSENADA would be a good site to monitor the oceanographic conditions of coastal waters of the northern BC region, an area that not only is located within a transition zone of the CCS strongly influenced by subarctic waters from the north, and tropical and subtropical systems from the south, but also is part of a major eastern boundary current system where upwelling controls the structure of the water column and ecosystems.

Acknowledgments

The IMECOCAL program has been mainly funded by CONACYT (projects G0041T, G35326T, 017PÑ-1297, C02-42569, 47044, 48367, and 23947), SEMARNAT-CONACYT (23804), and UC-MEXUS (CN07-125), as well as by UABC (323 and 341). The FLUCAR project was supported by CONACYT (SEP-2004-C01-45813/A-1) and the project entitled "Studies of parameters of the CO_2 system in coastal Pacific waters" by CONACYT (25339). We thank the crew of the R/V *Francisco de Ulloa* for the time and effort dedicated during all the cruises, as well as the crew of the skiff boat *GENUS* for their initiative and collaboration. Special thanks to the CICESE and UABC students, technicians, and researchers whose work was crucial for the success of the IMECOCAL and FLUCAR programs. We are also grateful to the two anonymous reviewers for their valuable comments that greatly improve this work.

Appendix A. Supplementary material

Supplementary data associated with this article can be found in the online version at doi:10.1016/j.csr.2010.07.011.

References

Alvarez, L.G., Durazo, R., Pérez, J., Navarro, L.F., Hernández, R., 1984. Observaciones de corrientes costeras superficiales mediante trazadores Lagrangeanos II. Eréndira, Baja California, 1979–1981. Unpublished Report, Departamento de Oceanografía Física, Centro de Investigación Científica y de Educación Superior de Ensenada, Ensenada, México (in Spanish).

Alvarez, L.G., Godínez, V.M., Lavín, M.F., 1990. Near-shore dispersion off Tijuana, Baja California. Ciencias Marinas 16, 87–109.

Bakun, A., Nelson, C.S., 1977. Climatology of upwelling related processes off Baja California. California Cooperative Oceanic Fisheries Investigation Reports 19, 107–127.

Bakun, A., Nelson, C.S., 1991. The seasonal cycle of wind-stress curl in subtropical eastern boundary current regions. Journal of Physical Oceanography 21, 1815–1834.

Barton, E.D., 1985. Low-frequency variability of currents and temperatures on the Pacific continental shelf off northern Baja California, 1978 to 1979. Continental Shelf Research 4, 425–443.

Barton, E.D., Argote, M.L., 1980. Hydrographic variability in an upwelling area off Northern Baja California in June, 1976. Journal of Marine Research 38, 631–649.

Bograd, S.J., Lynn, R.J., 2003. Long-term variability in the southern California Current System. Deep Sea Research Part II 50, 2355–2370.

Bograd, S.J., Castro, C.G., DiLorenzo, E., Palacios, D., Bailey, H., Gilly, W., Chavez, F.P., 2008. Oxygen declines and the shoaling of the hypoxic boundary in the California current. Geophysical Research Letters 35, L12607. doi:10.1029/2008GL034185.

Castro, R., Martínez, A., 2010. Variabilidad espacial y temporal del campo de viento frente a la península de Baja California. In: Durazo, R., Gaxiola, G. (Eds.), Dinámica del Ecosistema Pelágico frente a Baja California, 1997-2007: Diez Años de Investigaciones Mexicanas de la Corriente de California. Instituto Nacional de Ecología (INE)/ Centro de Investigación Científica y de Educación Superior (CICESE), México (in Spanish).

Chan, F., Barth, J.A., Lubchenco, J., Kirincich, A., Weeks, H., Peterson, W.T., Menge, B.A., 2008. Emergence of anoxia in the California current large marine ecosystem. Science 319, 920.

Chelton, D.B., 1984. Seasonal variability of alongshore geostrophic velocity off central California. Journal of Geophysical Research 89 (C3), 3473–3486.

Chelton, D.B., Schlax, M.G., Freilich, M.H., Milliff, R.F., 2004. Satellite measurements reveal persistent small-scale features in ocean winds. Science 303, 978–983.

Denman, K.L., Freeland, H.J., 1985. Correlation scales, objective mapping, and a statistical test of geostrophy over the continental shelf. Journal of Marine Research 43, 517–539.

Di Lorenzo, E., 2003. Seasonal dynamics of the surface circulation in the Southern California current system. Deep Sea Research Part II 50, 2371–2388.

DOE, 1994. Handbook of methods for the analysis of the various parameters of the carbon dioxide system in sea water. In: Dickson, A.G., Goyet, C. (Eds.), Version 2. ORNL/CDIAC-74.

Durazo, R., Baumgartner, T., 2002. Evolution of oceanographic conditions off Baja California: 1997–1999. Progress in Oceanography 54, 7–31.

Durazo, R., Gaxiola-Castro, G., Lavaniegos, B., Castro-Valdez, R., Gomez-Valdes, J., Mascarenhas Jr., A.S., 2005. Oceanographic conditions west of baja California, 2002–2003: a weak El Niño and subartic water enhancement. Ciencias Marinas 31, 537–552.

Durazo, R., 2009. Climate and upper ocean variability off Baja California, Mexico: 1997–2008. Progress in Oceanography, doi:10.1016/j.pocean.2009.07.043.

Durazo, R., Ramírez, A.M., Miranda, L.E., Soto-Mardones, L.A., 2010. Climatología hidrográfica de la Corriente de California frente a Baja California. In: Durazo, R., Gaxiola, G. (Eds.), Dinámica del Ecosistema Pelágico frente a Baja California, 1997–2007: Diez Años de Investigaciones Mexicanas de la Corriente de California. Instituto Nacional de Ecología (INE)/ Centro de Investigación Científica y de Educación Superior (CICESE), México (in Spanish).

Feely, R.A., Sabine, C.L., Hernandez-Ayón, J.M., Ianson, D., Hales, B., 2008. Evidence for upwelling of corrosive "acidified" water onto the continental shelf. Science 320, 1490. doi:10.1126/science.1155676.

Gay, P.S., Chereskin, T.K., 2009. Mean structure and seasonal variability of the poleward undercurrent off southern California. Journal of Geophysical Research 114, C02007. doi:10.1029/2008JC004886.

Gaxiola-Castro, G., Durazo, R., Lavaniegos, B., De la Cruz-Orozco, M.E., Millán-Nuñez, E., Soto-Mardones, L., Cepeda-Morales, J., 2008. Pelagic ecosystem response to interannual variability off Baja California. Ciencias Marinas 34, 263–270.

Goericke, R., Venrick, E., Koslow, T., Sydeman, W.J., Schwing, F.B., Bograd, S.J., Peterson, W.T., Emmett, R., Lara-Lara, J.R., Gaxiola-Castro, G., Gómez-Valdés, J., Hyrenbach, K.D., Bradley, R.W., Wiese, M.J., Harvey, J.T., Collins, C., Lo, N.C.H., 2007. The state of the California current, 2006–2007: regional and local processes dominate. California Cooperative Oceanic Fisheries Investigation Reports 48, 33–66.

Garfield, N., Collins, C.A., Paquette, R.G., Carter, E., 1999. Lagrangian exploration of the California Undercurrent, 1992–95. Journal Physical Oceanography 29, 560–583.

Gómez-Valdés, J., Jeronimo, G., 2009. Upper mixed layer temperature and salinity variability in the tropical boundary of the California current, 1997–2007. Journal of Geophysical Research 114, C03012. doi:10.1029/2008JC004793.

Hickey, B.M., 1979. The California current system, hypotheses and facts. Progress in Oceanography 8, 191–279.

Holloway, G., 1992. Representing topographic stress for large-scale ocean models. Journal Physical Oceanography 22, 1033–1046.

Huyer, A., 1983. Coastal upwelling in the California current system. Progress in Oceanography 12, 259–284.

Jeronimo, G., Gómez-Valdés, J., 2007. A subsurface warm-eddy off northern Baja California in July 2004. Geophysical Research Letter 34, L06610. doi:10.1029/2006GL028851.

Lavaniegos, B.E., Ohman, M.D., 2003. Long-term changes in pelagic tunicates of the California current. Deep Sea Research 50, 2473–2498.

Lynn, R., 1967. Seasonal variation of temperature and salinity at 10 meters in the California current. California Cooperative Oceanic Fisheries Investigation Reports 11, 157–186.

Lynn, R., Simpson, J.J., 1987. The California current system: the seasonal variability of its physical characteristics. Journal of Geophysical Research 92, 12947–12966.

Lynn, R., Bograd, S., Chereskin, T., Huyer, A., 2003. Seasonal renewal of the California current: the spring transition off California. Journal of Geophysical Research 108 (C8), 3279. doi:10.1029/2003JC001787.

McClatchie, S., Goericke, R., Koslow, J.A., Schwing, F.B., Bograd, S.J., Charter, R., Watson, W., Lo, N., Hill, K., Gottschalk, J., L'Heureux, M., Xue, Y., Peterson, W.T., Emmett, R., Collins, C., Gaxiola-Castro, G., Durazo, R., Kahru, M., Mitchell, B.G., Hyrenbach, K.D., Sydeman, W.J., Bradley, R.W., Warzybok, P., Bjorkstedt, E., 2008. The state of the California current, 2007–2008: La Niña conditions and their effects on the ecosystem. California Cooperative Oceanic Fisheries Investigation Reports 49, 39–76.

Pérez-Brunius, P., López, A., Pineda, J., 2006. Hydrographic conditions near the coast of northwestern Baja California: 1997–2004. Continental Shelf Research 26, 885–901.

Pérez-Brunius, P., López, M., Parés-Sierra, A., Pineda, J., 2007. Comparison of upwelling indices off Baja California derived from three different wind data sources. California Cooperative Oceanic Fisheries Investigation Reports 48, 204–214.

Rykaczewski, R.R., Checkley, D.M., 2008. Influence of ocean winds on the pelagic ecosystem in upwelling regions. PNAS, doi:10.1073pnas.0711777105.

Soto-Mardones, L., Pares-Sierra, A., Garcia, J., Durazo, R., Hormazabal, S., 2004. Analysis of the mesoscale structure in the IMECOCAL region (off Baja California) from hydrographic, ADCP and altimetry data. Deep Sea Research Part II 51, 785–798.

Walstad, L.J., Allen, J.S., Kosro, P.M., Huyer, A., 1991. Dynamics of coastal transition zone through data assimilation studies. Journal of Geophysical Research 96, 14959–14977.

Wolter, K., Timlin, M.S., 1993. Monitoring ENSO in COADS with a seasonally adjusted principal component index. In: Proceedings of the of the 17th Climate Diagnostics Workshop, Norman, OK, NOAA/NMC/CAC, NSSL, Oklahoma Clim. Survey, CIMMS and the School of Meteor., University of Oklahoma. pp. 52–57.

Wolter, K., Timlin, M.S., 1998. Measuring the strength of ENSO events—how does 1997/98 rank? Weather 53 315–324.

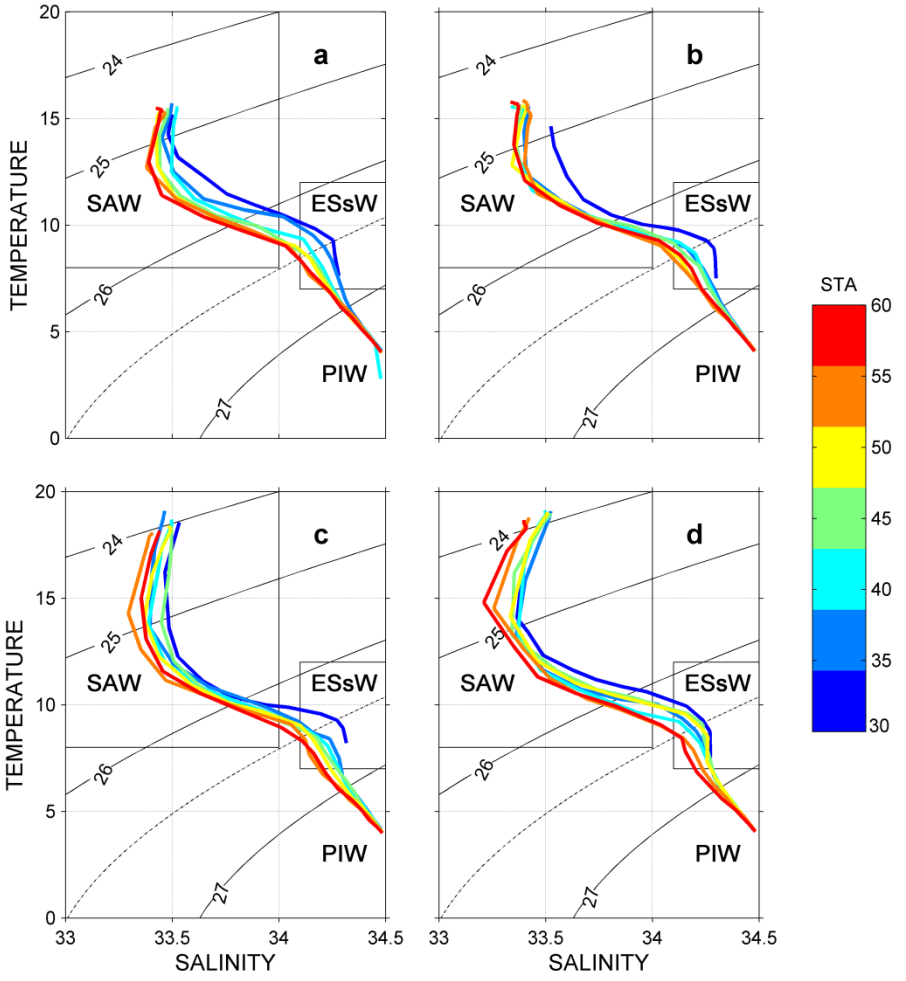

Figura Suplementaria 1. Promedios estacionales de diagramas T-S de (a) enero, (b) abril, (c) julio y (d) octubre a lo largo de la línea 100, estimados mediante el ajuste armónico realizado a los datos hidrográficos colectados durante 11 años por el programa IMECOCAL. Se indican los límites masas de agua de la región de acuerdo a sus características descritas por Durazo y Baumgartner (2002). Las masas de agua son mostradas en los paneles como sigue: SAW= Agua Subártica, ESsW= Agua Ecuatorial Subsuperficial, PIW= Agua Intermedia del Pacífico. Las líneas punteadas indican la isopicna de 26.5 kg m^{-3}.

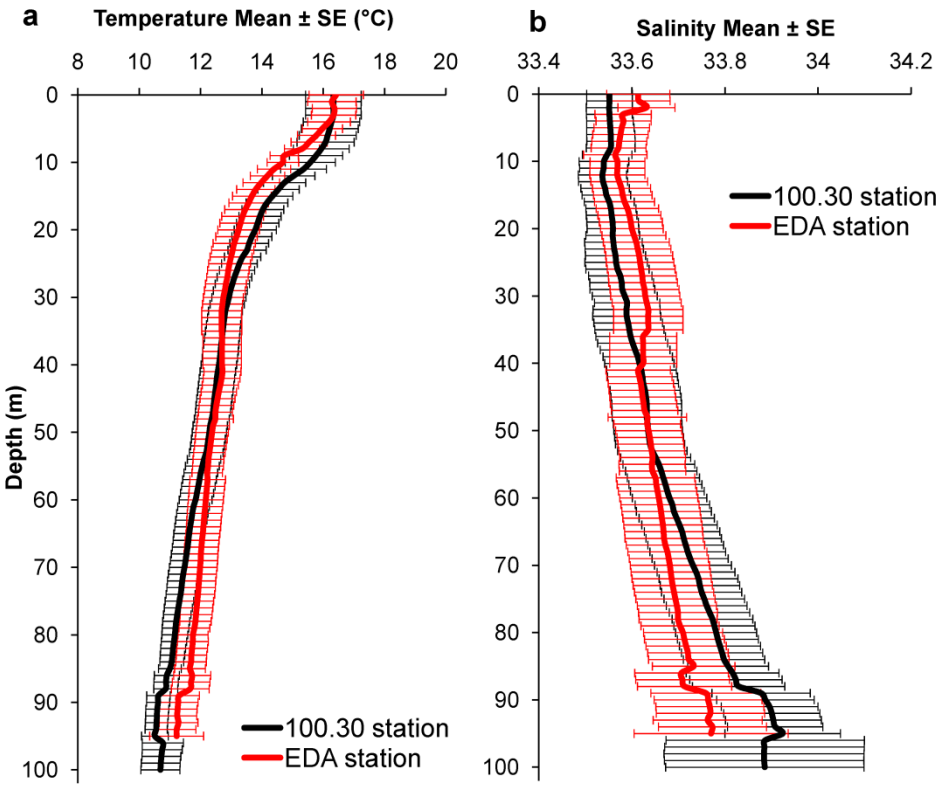

Figura Suplementaria 2. Promedios y desviaciones estándar de los perfiles de (a) temperatura y (b) salinidad de las estaciones 100.30 y ENSENADA. Los valores estadísticos son calculados usando los datos hidrográficos colectados en cruceros coincidentes entre ambas estaciones. Desde octubre del 2006 a noviembre del 2008 las fechas de muestreo en ambas estaciones fueron: 24/oct/06; 23-24/ene/07; 26/abr/07; 25-26/ago/07; 21-23/ene/08; 14-16/abr/08; 2-12/ago/08; 14/oct/08 (solo en la estación 100.30) y 13/nov/08 (solo en la estación ENSENADA).

CAPÍTULO 2: Dinámica del flujo del carbono a través de las poblaciones picoplanctónicas autótrofas (cianobacterias y picoeucariontes) y heterótrofas (bacterias) de la zona eufótica, bajo condiciones oceanográficas contrastantes en la estación ENSENADA.

Trabajo publicado en la revista Journal of Plankton Research: *Linacre et al., (2010). Picoplankton dynamics during contrasting seasonal oceanographic conditions at a coastal upwelling station off Northern Baja California, México. J. Plankton Res., 32(4): 539-557.*

RESUMEN: Durante seis cruceros (septiembre 2007-noviembre 2008) fue investigada la dinámica ecológica del picoplancton en el sistema de surgencia costera localizado al norte de Baja California. Poblaciones de *Prochlorococcus*, *Synechococcus*, picoeucariontes y bacterias heterotróficas fueron estimadas mediante citometría de flujo (FCM). En cada fecha de muestreo, se realizaron incubaciones *in situ* de 24 horas a tres o cuatro niveles de profundidad, utilizando la técnica de dilución abreviada a 3 tratamientos y experimentos de C^{14} para determinar las tasas de crecimiento, pastoreo y producción de las poblaciones picoplanctónicas (FCM) y de la comunidad fitoplanctónica (TChl*a*). Globalmente, el picoplancton comprendió una componente activa e importante de la comunidad, con valores de biomasa (2.3-69.8 µgC L^{-1}) y tasas de producción (0.8-68.4 µgC L^{-1} $día^{-1}$) que variaron positivamente con la Chl *a* y con la producción comunitaria estimada con la técnica de C^{14}. La excepción a éste patrón fue encontrada durante un intenso florecimiento algal bajo condiciones de surgencia intensificadas por el evento de La Niña en abril del 2008, durante el cual las biomasas y producciones estimadas del picofitoplancton tuvieron sus valores más bajos de todo el periodo, sugiriendo que los productores primarias más pequeños fueron reemplazados por células más grandes. Así, para la mayoría de las circunstancias ambientales registradas durante nuestro estudio, los resultados sustentan la reciente hipótesis de "rising tide" que indica un crecimiento de todas las clases de tamaño fitoplanctónicas ante condiciones ambientales favorables (nutrientes), incluyendo al picofitoplancton. Sin embargo, ante las condiciones ambientales extremas de surgencia observadas en nuestra zona de estudio, el picofitoplancton declinó abruptamente a pesar del aparente

incremento (en promedio) de las tasas de crecimiento de este grupo. Son necesarios estudios futuros para proveer un entendimiento más mecanístico de los factores físicos (advección fuera de costa), fisiológicos (absorción de nutrientes y control de la temperatura) y ecológicos (tramas tróficas) que afectan a la respuesta no-lineal del picofitoplancton ante el forzamiento y riqueza ambiental.

Palabras Claves: dinámica del picoplancton; método de dilución; tasas de crecimiento; tasas de pastoreo; sistema de surgencia costera.

JOURNAL OF PLANKTON RESEARCH | VOLUME 32 | NUMBER 4 | PAGES 539–557 | 2010

Picoplankton dynamics during contrasting seasonal oceanographic conditions at a coastal upwelling station off Northern Baja California, México

LORENA P. LINACRE[1]*, MICHAEL R. LANDRY[2], J. RUBÉN LARA-LARA[3], J. MARTÍN HERNÁNDEZ-AYÓN[4] AND CARMEN BAZÁN-GUZMÁN[3]

[1]PROGRAMA DE DOCTORADO EN OCEANOGRAFÍA COSTERA, FACULTAD DE CIENCIAS MARINAS/INSTITUTO DE INVESTIGACIONES OCEANOLÓGICAS, UNIVERSIDAD AUTÓNOMA DE BAJA CALIFORNIA (UABC), ENSENADA, BAJA CALIFORNIA, MEXICO, [2]INTEGRATIVE OCEANOGRAPHY DIVISION, SCRIPPS INSTITUTION OF OCEANOGRAPHY, LA JOLLA, CA, USA, [3]DEPARTAMENTO DE OCEANOGRAFÍA BIOLÓGICA, CENTRO DE INVESTIGACIÓN CIENTÍFICA Y DE EDUCACIÓN SUPERIOR DE ENSENADA, ENSENADA, BAJA CALIFORNIA, MEXICO AND [4]INSTITUTO DE INVESTIGACIONES OCEANOLÓGICAS, UABC, ENSENADA, BAJA CALIFORNIA, MEXICO

*CORRESPONDING AUTHOR: llinacre@uabc.mx; lorenalinacre@gmail.com

Received October 15, 2009; accepted in principle December 18, 2009; accepted for publication December 23, 2009

Corresponding editor: William K.W. Li

The ecological dynamics of picoplankton were investigated at a coastal upwelling system of northern Baja California during six cruises (September 2007–November 2008). Populations of *Prochlorococcus*, *Synechococcus*, PicoEukaryotes and heterotrophic bacteria were assessed by flow cytometry (FCM). On each sampling date, we used an abbreviated three-treatment dilution technique and ^{14}C-uptake experiments to determine population (FCM) and community (TChl *a*) rates of growth, grazing and production from 24-h *in situ* incubations at three to four euphotic depths. Overall, picoplankton comprised an active and important component of the community, with biomass values (2.3–69.8 μg C L^{-1}) and production rates (0.8–68.4μg C L^{-1} day^{-1}) that varied positively with Chl *a* and community ^{14}C-production. The exception was an intense algal bloom (>25 μg Chl *a* L^{-1}) during La Niña-intensified upwelling conditions in April 2008, during which biomass and production estimates of picophytoplankton were at their lowest levels, suggesting that the smallest primary producers were being replaced by larger cells. Thus, for most of the environmental circumstances encountered during our study, our results supported the recent "rising tide" hypothesis that improved growth (nutrient) conditions benefit all size classes, including picophytoplankton. Under extreme conditions of upwelling, however, the picophytoplankton declined abruptly, despite seemingly strong (average) growth rates. Future studies need to provide a better mechanistic understanding of the physical (advection), physiological (nutrient uptake and temperature) and ecological (food web) factors that result in this dramatic nonlinearity in picophytoplankton response to system forcing and richness.

KEYWORDS: picoplankton dynamics; dilution method; growth rate; grazing rate; coastal upwelling system

doi:10.1093/plankt/fbp148, available online at www.plankt.oxfordjournals.org. Advance Access publication January 27, 2010

INTRODUCTION

The coastal region off western Baja California (WBC) is the southern limit of the California Current System (CCS). The hydrography of WBC is characterized by an alongshore near-surface equatorward flow carrying relatively cool and fresh water from the subarctic, a subsurface poleward current flowing along the edge of the continental slope, and coastal upwelling episodes driven by northerly winds during most of the year. At the seasonal scale, subarctic waters dominate during the peak of the upwelling season in spring and summer, while tropical and subtropical influences are commonly observed during later summer and fall (Lynn and Simpson, 1987; Durazo *et al.*, in press).

Physical and chemical characteristics of the coastal waters from a monitoring observatory off Ensenada, México (ENSENADA station), display the seasonal and interannual characteristics derived from 11 years of recent oceanographic measurements in the northern region off WBC (Linacre *et al.*, in preparation), ranging from strong seasonal upwelling that produces dense algal blooms in the euphotic layer to periods of strong stratification and oligotrophy. Seasonal climatological means from ENSENADA station demonstrate that this coastal site is representative of a broader area (Linacre *et al.*, in preparation). Consequently, it is a convenient site for the study of plankton community and production responses to strongly variable conditions throughout this dynamic coastal ecosystem.

Classical and microbial pathways are a useful dichotomy for distinguishing among the alternate fates of primary production carbon in marine ecosystems (Calbet and Landry, 2004). In highly productive coastal upwelling areas, it has long been assumed that carbon production via chain-forming diatoms is either efficiently transferred to higher trophic levels through the classical food web (Ryther, 1969) or exported from the euphotic zone as fecal pellets, detritus or by sedimentation of "marine snow" aggregates (Turner, 2002). However, there is increasing evidence that the microbial components of food webs are an ubiquitous and important feature of not only oligotrophic but also eutrophic systems, including seasonally variable coastal upwelling areas (Cuevas *et al.*, 2004; Worden *et al.*, 2004; Vargas *et al.*, 2007). Most productive and seasonal systems involve multivorous food webs, where both classical and microbial trophic components play significant roles (Legendre and Rassoulzadegan, 1995). It has also been recently noted that the onset of favorable growth conditions for diatom-dominated blooms does not necessarily lead, as often assumed, to the successional replacement of the smaller cells that dominate during less productive times (Barber and Hiscock, 2006). The picophytoplankton assemblage can respond positively in growth rates and biomass to improved growth conditions, although its biomass increase is often modest compared with larger phytoplankton, which escape control by protistan grazers via the "loophole" blooming mechanism (Irigoien *et al.*, 2005; Barber and Hiscock, 2006).

Heterotrophic protists (here defined as nano- to micro-sized grazers <200 μm) play an important role in pelagic food webs, where they are a major source of mortality for small and large primary producers, as well as heterotrophic bacteria (Sherr and Sherr, 2002). Globally, grazing impact by protists has been estimated to consume two-thirds of phytoplankton daily growth (production), with moderate variations among marine habitats and regions (Calbet and Landry, 2004). In coastal environments, protistan grazing accounts for ~60% of daily primary production on average, although this value appears to vary dynamically with seasonality and the state of the phytoplankton bloom and bust cycles (Neuer and Cowles, 1994; Böttjer and Morales, 2005; McManus *et al.*, 2007). Similar to protistan consumption of autotrophs, strong grazing pressure is exerted on heterotrophic bacteria mainly by nanoflagellates. Removal of >100% of daily bacterial production has been reported in the coastal upwelling areas of the Humboldt Current System, mostly during non-upwelling seasons (Cuevas *et al.*, 2004; Vargas *et al.*, 2007). Since bacterial growth is ultimately supported by autotrophic sources of DOC, even when the seasons of production and utilization are temporally separate, a significant fraction of annual primary production is channeled through bacteria to heterotrophic nanoflagellates, reflecting the importance of microbial food webs in carbon cycling in coastal upwelling systems (Cuevas *et al.*, 2004; Vargas *et al.*, 2007).

The aim of the present study was to assess the temporal dynamics of phytoplankton and bacteria in the coastal upwelling system off northern WBC, focusing on abundance, biomass, growth, grazing mortality and production of autotrophic and heterotrophic picoplankton populations under contrasting seasonal oceanographic conditions.

METHOD

In situ dilution experiments

Experimental studies of phytoplankton growth and protistan grazing were conducted at the ENSENADA station (31°40.105′N, 116 °41.596′W) at the northern

region off WBC (Fig. 1), as part of the FLUCAR (*Carbon Sources and Sinks in the Continental Margins of the Mexican Pacific Waters*) project. During the period from 24 September 2007 to 11 November 2008, six sets of experiments were incubated *in situ* for 24 h at a fixed coastal station, following the experimental approach of Landry *et al.* (Landry *et al.*, 2008). Routine station activities included CTD/rosette casts to 100 m depth with continuous measurements of pressure, temperature, conductivity, dissolved oxygen, chlorophyll fluorescence and PAR light, as well as seawater collection with 5-L Niskin bottles for flow cytometric (FCM) and nutrient analyses ($NO_3^- + NO_2^-$, $Si(OH)_4$ and PO_4^{3-}) at 10 depths which were variable among cruises. Nutrient analyses were performed with a Skalar SAN^{plus} segmented-flow nutrient analyzer; $NO_3^- + NO_2^-$ determination was based on a modification of the Armstrong *et al.* (Armstrong *et al.*, 1967) procedure. Seawater for the experiments was also collected with 5-L Niskin bottles at variable depths among cruises within the euphotic zone (from 56 to 0.3% of average PAR light from the first meter, $\%I_o$). Based on the *in situ* fluorescence profiles, the collection depths were at the deep chlorophyll maximum (DCM) and one level above and one level below the DCM. For each set of experiments, the treatments were prepared in clear polycarbonate bottles (2.0 L) with 100 (undiluted), 30 and 10% of whole seawater (diluted with 0.1-μm filtered seawater) at each depth. All dilution treatments were done by filtering directly from the Niskin bottles using a peristaltic pump, silicone tubing and an in-line Suporcap filter capsule that had previously been acid washed (10% trace-metal grade HCl followed by distilled water and seawater rinses). Each bottle was sub-sampled for FCM analysis to confirm initial concentrations and volume dilutions. The bottles were tightly capped, then placed into net bags and secured with snap hooks to a weighted line hanging from surface floats and attached to a fixed buoy at the depths of initial sample collection. All experiments were started in the early morning and deployed prior to sunrise; the total elapsed time from Niskin sampling to array deployment was about 2.0 h.

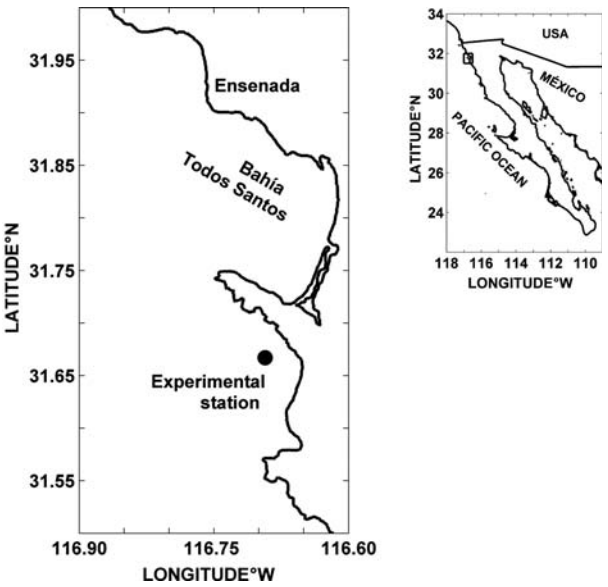

Fig. 1. Location of experimental station in the coastal waters off WBC, México.

Pigment and picoplankton analyses

Samples were taken for chlorophyll *a* (Chl *a*) and FCM analyses at the start and end of each experiment to determine initial abundances and dilution concentrations and to compute growth and grazing loss rates in the dilution incubations. Triplicate samples (250 ml) for Chl *a* analyses were filtered onto 25-mm Gelman GF/F filters, analyzed by the fluorometric non-acidification method (Welshmeyer, 1994). For this, we used a Turner Designs Trilogy fluorometer previously calibrated with pure Chl *a*.

For enumeration of picophytoplankton and heterotrophic bacteria, 2-mL samples were collected, preserved (0.5% paraformaldehyde, final concentration), flash frozen and stored in liquid nitrogen until analysis on the flow cytometer. Samples were thawed in batches, then stained with Hoechst 34 442 (1 μg mL^{-1}, final concentration) (Monger and Landry, 1993). For this analysis, a Beckman–Coulter Altra cytometer was used (operated by the SOEST Flow Cytometry Facility, www.soest.hawaii.edu/sfcf), with an Harvard Apparatus syringe pump for quantitative volume sampling and two argon ion lasers for UV (200 mW) and 488 nm (1 W) excitation. Scatter (side and forward) and fluorescence signals were collected using filters as appropriate, including those for Hoechst-bound DNA, phycoerythrin and chlorophyll. Fluorescence signals were normalized to 0.5 and 1.0 μm yellow–green (YG) polystyrene beads (Polysciences Inc., Warrington, PA, USA). Sample list-mode files were analyzed using FlowJo software (Treestar, Inc., www.flowjo.com). Cell abundances were converted to biomass using carbon per cell conversion factors, computed based on literature values used in coastal waters of the CCS. Estimates of carbon content were made using mean cell estimates of 20, 39, 82 and 1000 fg C cell^{-1} as a starting point for heterotrophic bacteria (H-Bact), *Prochlorococcus* spp. (PRO), *Synechococcus* spp. (SYN) and PicoEukaryotes (P-Euk), respectively (Lee and Fuhrman, 1987; Worden *et al.*, 2004; Sherr *et al.*, 2005). Cell size variability around these values was

then determined using bead-normalized Forward Angle Light Scattering (FALS) as a relative measure of biovolume (BV) and carbon content, assuming constant cell carbon density (C:BV) for each population category. Thus, using the scaling factor $FALS^{0.55}$ (Binder *et al.*, 1996; Landry *et al.*, 2003), the carbon content for each category was determined for each cruise and depth (sample = i) from the taxon-specific mean cell carbon from the literature and the FALS ratio = $(FALS_i/FALS_{mean})^{0.55}$.

Growth and grazing estimates

Instantaneous rates of phytoplankton growth (μ) and mortality loss (m) to protistan grazers were estimated from dilution incubations according to Landry and Hassett (Landry and Hassett, 1982), using an abbreviated three-treatment dilution protocol. Initial pigment concentrations and FCM population abundances (C_o) were determined for each dilution treatment from measured concentrations in the unfiltered seawater and the proportion of unfiltered (D_i) seawater in the treatment. Final concentrations (C_t) were measured in each bottle at the end of the 24-h incubations (t). Daily net rates of change (day^{-1}) were determined as $k_i = \ln(C_t/C_o)/t$. The typical linear relationship between k_i and D_i allowed estimation of m and μ daily rates from the slope and intercept of the trendline, respectively. Although the responses were linear in most of the experiments, estimates of k_i from the most diluted treatment (10%) were lower than the 30% treatment, on a few occasions in these analyses, typically toward the base of the euphotic zone where the net rates and the population concentrations were both low and difficult to measure, and perhaps a feeding threshold response occurred (Frost, 1972). In these cases, μ and m rates were estimated following the two-treatment dilution approach of Landry *et al.* (Landry *et al.*, 2008, 2009), using two equations: $m = (k_d - k)/(1 - 0.30)$ and $\mu = k + m$, where k_d and k are the daily net rates of change in the 30% and undiluted treatments, respectively. The lack of nutrient-added treatments in the experimental design may mean that the computed rates are underestimates. However, a systematic bias was not observed in comparing the results from three-bottle *in situ* experiments to several full dilution experiments with nutrient treatments (data not shown) that were done in the laboratory during the same period of this work.

Mortality rate estimates were assumed to be unaffected by changes in phytoplankton physiological condition during the experimental incubations. However, growth rate estimates could be affected by physiological adjustments. We attempted to correct for such effects using FCM measurements of red fluorescence to account for cellular changes in Chl *a* from each group of photosynthetic picophytoplankton (PRO, SYN and P-Euk). For each category, FCM analyses provided initial (i) and final (f) estimates of bead-normalized Chl *a* red fluorescence per cell (F1), from which a "weighted mean normalized red fluorescence" (WF1) was used to compute daily instantaneous rates of change for the 24-h (t) incubations as $\ln(WF1_f/WF1_i)/t$. These computations were made for each initial and final whole seawater samples and applied to μ based on measured Chl *a* changes, as a correction factor for pigment photoadaptation. Thus, the corrected growth rate was calculated as, μ-$[\ln(WF1_f/WF1_i)/t]$ (Landry *et al.*, 2003).

Experimental values of μ and m were combined with biomass estimates to compute rates of production and grazing for populations of autotrophic and heterotrophic picoplankton according to Calbet and Landry (Calbet and Landry, 2004). Production estimates (PP, $\mu g\ C\ L^{-1}\ day^{-1}$) were calculated as, $PP = \mu^*(C_o\ [e^{(\mu - m)t} - 1]/(\mu - m)t)$, where C_o is expressed in carbon term ($\mu g\ C\ L^{-1}$). Similarly, the biomass consumption of protistan grazers (G, $\mu g\ C\ L^{-1}\ day^{-1}$) was computed as, $G = m * (C_o\ [e^{(\mu - m)t} - 1]/(\mu - m)t)$. Finally, the ratios of grazing to growth (m:μ) were estimated as a measure of protistan grazing impact on the production of the phytoplankton community (based on Chl *a*) and the individual populations of picoplankton.

^{14}C-Uptake primary production

As a basis of comparison to population production estimates from dilution experiments, we also measured primary productivity by the standard ^{14}C-bicarbonate-uptake technique (Steemann Nielsen, 1952). Seawater samples collected on the same hydrocast as dilution experiments were screened through a 150-μm net to exclude macrozooplankton, and inoculated with ~5 μCi $NaH^{14}CO_3$ in 250-mL polycarbonate bottles. Replicated light and dark bottles were placed into net bags on the array line together with dilution bottles and deployed at the initial collection depth for 24 h. After incubation, the labeled particulate matter was filtered onto 0.45-μm pore Millipore HA filters. To purge $NaH^{14}CO_3$ that was not fixed by photosynthesis, filters were placed in 20-mL scintillation vials with 0.5 mL of 10% HCl for 3 h. Scintillation cocktail (10 mL Ecolite) was added to each vial, and the radioactivity was determined with a Beckman LS-6500 scintillation counter. Primary production rates were calculated from these radioactivity counts according to Parsons *et al.* (Parsons *et al.*, 1984), subtracting the carbon uptake of the dark bottles.

RESULTS

Environmental conditions

Seasonal and interannual variability in the physical and chemical conditions at ENSENADA station are described in detail by Linacre *et al.* (Linacre *et al.*, in preparation). However, a brief description of the oceanographic conditions during the sampling for the dilution experiments is given in Table I and Fig. 2. The upwelling is a semi-permanent feature in northern coastal waters off WBC; however, it is stronger and more frequent during spring and summer seasons (Lynn and Simpson, 1987; Durazo *et al.*, in press). Figure 2A shows the daily Upwelling Indices at 30°N 119°W (solid line) and the monthly means (dashed line) for the sampling period at ENSENADA station. The index for each incubation day is highlighted in enlarged gray circles. Except for a few notable days in January 2008, the values over the sampling periods were neutral to positive in this region, ranging from 0 to 250 $m^3 s^{-1}$ per 100 m of coastline. The upwelling indices for individual incubation days were variable, but were close to monthly means. The highest index value occurred during the April 2008 experiments (154 $m^3 s^{-1}$ per 100 m of coastline), while the lowest values were found during November 2007 and January 2008 (15 $m^3 s^{-1}$ per 100 m of coastline).

The vertical distributions of seawater density (σ_t, kg m^{-3}) and *in situ* fluorescence (μg Chl L^{-1}) for each cruise are shown in Fig. 2B and C, respectively. The summer periods (September 2007 and August 2008) displayed a strong and marked pycnocline around 10 m, while the colder periods (November 2007–08, January 2008 and April 2008) showed a more homogeneous water column. The density values for all periods oscillated between 24.5 and 25.5 kg m^{-3} throughout 0–100 m of depth, except for April 2008, when anomalously high values (>25.7 kg m^{-3}) associated the cold and salty upwelled water reached to the surface (Fig. 2B). In this particular case, the normal seasonal intensification of upwelling was enhanced by La Niña conditions observed during winter to spring 2008 in the northern region off WBC (McClatchie *et al.*, 2008; Durazo, 2009) and indicated by the Oceanic NINO Index reported by the NOAA Climate Prediction Center (http://www.cpc.noaa.gov/) for the period from December 2007 to January/February 2008, as well as by the Multivariate ENSO Index (Wolter and Timlin, 1998)

Table I: Initial environmental conditions for in situ dilution experiments conducted at ENSENADA station located in the northern region off WBC, México

Cruise	Depth (m)	Light (%I_o)	Temp (°C)	Dissolved nutrients[a]			Total phyto	Picoautrotrophs (cell $L^{-1} \times 10^6$)			Heterotrophic Bacteria (cell $L^{-1} \times 10^8$)
				NO_3^- (μM)	PO_4^{3-} (μM)	$Si(OH)_4$ (μM)	TChl *a* (μg L^{-1})	PRO	SYN	P-Euk	
September 2007	2	56	15.4	0.3	0.2	2.3	4.7	15	187	53	30
September 2007	7	23	14.6	5.5	0.6	9.1	5.2	18	160	45	23
September 2007	10	15	13.2	7.2	0.7	6.1	2.4	21	49	15	12
September 2007	35	1	11.9	11.0	0.9	10.7	1.1	2	11	11	11
November 2007	10	13	15.2	4.2	0.9	6.5	1.3	18	71	21	11
November 2007	20	6	14.0	4.4	0.9	6.1	1.5	32	46	16	7
November 2007	30	2	12.8	6.0	1.0	6.0	1.1	46	35	9	6
January 2008	5	25	13.8	0.6	0.5	4.0	2.7	33	223	38	26
January 2008	20	2	13.2	7.7	1.6	7.7	4.5	12	140	43	18
January 2008	30	0.3	12.9	12.6	1.6	13.0	1.9	5	42	15	11
April 2008[b]	5	22	11.6	–	–	–	25.1	0	3	7	11
April 2008[b]	10	8	11.3	–	–	–	13.2	0	3	4	7
April 2008[b]	15	3	10.5	–	–	–	9.4	0	4	5	8
August 2008	5	36	16.3	0.3	0.5	5.4	4.4	99	120	14	16
August 2008	10	17	14.4	8.7	0.7	7.7	2.6	36	80	11	10
August 2008	20	4	12.3	17.0	1.3	11.5	1.1	7	12	3	6
November 2008	5	47	16.0	0.1	0.7	5.1	2.9	88	105	8	16
November 2008	12	14	15.0	1.8	0.8	6.2	3.2	56	80	10	11
November 2008	30	1	13.9	6.6	1.1	8.0	1.0	11	6	2	5

Nutrients and light conditions were measured at midday CTD-cast. Temperature and initial concentrations of chlorophyll *a* and picoplankton abundance were measured in pre-dawn CTD cast during the collection of seawater for *in situ* dilution experiments. Groups of picoautotrophs distinguished by flow cytometry were *Prochlorococcus* spp. (PRO), *Synechococcus* spp. (SYN) and PicoEukaryotes (P-Euk). Because of high winds, station operations were abandoned in April 2008 before the hydrographic cast for nutrient sampling.

[a]Values were acquired from samples analyzed by Dr Víctor Camacho-Ibar from IIO-UABC.

[b]An algal bloom condition was recorded during this season.

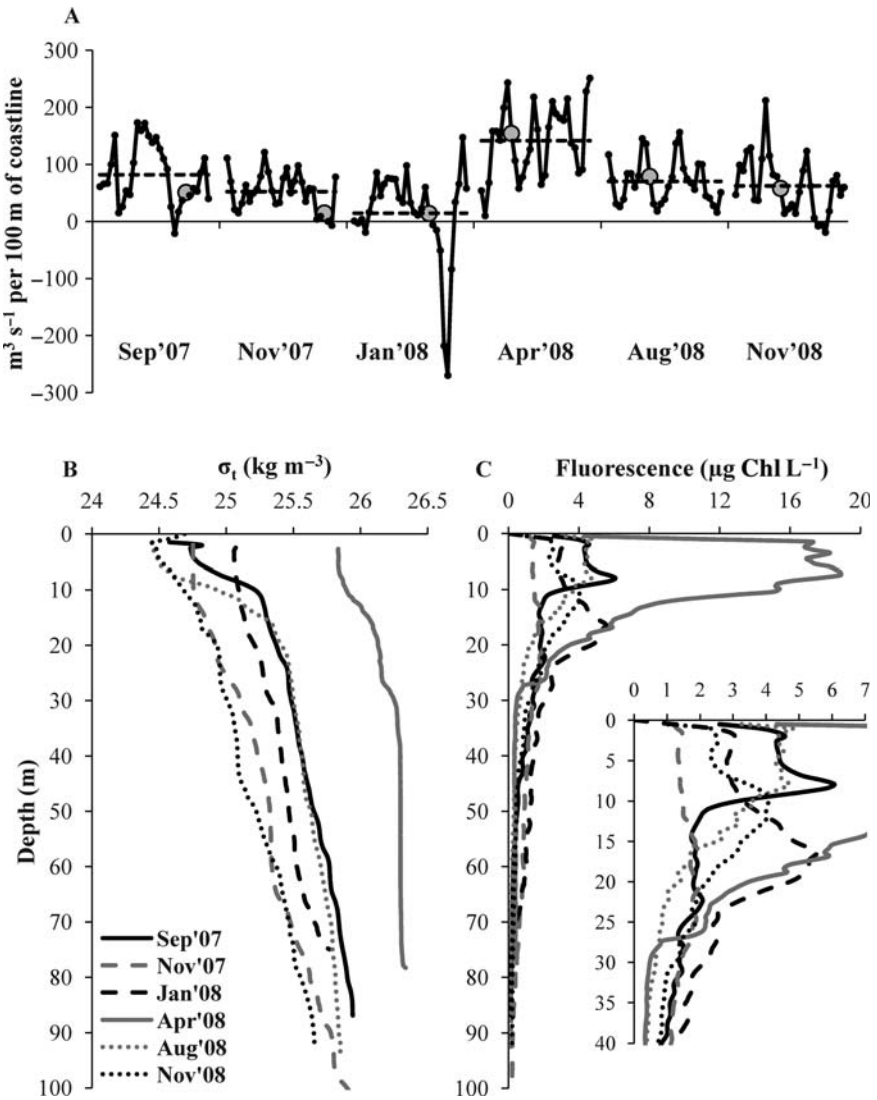

Fig. 2. (**A**) Bakun upwelling index ($m^3\ s^{-1}$ per 100 m of coastline; solid line) and monthly mean ($m^3\ s^{-1}$ per 100 m of coastline; dashed line) from NOAA/NMFS/PFEG for 30°N 119°W, during the six periods when the dilution experiments were done at ENSENADA station in the northern region off WBC, México. The gray and enlarged circles indicate the index value for the day when incubation dilutions were done. (**B**) Profiles of water density (σ_t; kg m^{-3}) and (**C**) *in situ* fluorescence (µg Chl L^{-1}), measured at the time of the seawater collection for the dilution experiments during each cruise.

(http://www.cdc.noaa.gov/people/klaus.wolter/MEI/). At ENSENADA station, this cold event in April 2008 was evident in anomalously high salinity (>33.9), low temperature (<12°C) and consequently high density values (>25.7 kg m^{-3}) throughout the water column (Table I, Fig. 2B), as well as euphotic zone waters depleted in dissolved oxygen (dO_2 <200 µmol L^{-1}) but rich in dissolved inorganic carbon (DIC >2140 µmol kg^{-1}) (Linacre *et al.*, in preparation).

In situ fluorescence profiles showed highest values in the first 30 m of the water column during all periods (Fig. 2C), where the Chl *a* concentrations were typically in the range of 1–5 µg L^{-1} (Table I) and the DCM was in general above 15 m of depth, except for January 2008, when the DCM was notably deeper (~20 m; Fig. 2C). The lowest fluorescence values in the water-column occurred in November 2007, and they appeared close to Chl *a* concentrations measured at the depths sampled for the dilution experiment done in this season (Table I, Fig. 2C). Conversely, in April 2008, an algal bloom with surface Chl *a* concentrations of >25 µg L^{-1} (Table I) and a dense layer of cells was evident in the upper 20 m (~20 µg Chl L^{-1}; Fig. 2C). The depth of the euphotic zone, defined here by 0.1% surface light penetration (%I_o relative to the average measurement for the first meter), varied from 37 m in

January 2008 to 63 m in November 2007. Despite this variability, the euphotic zone was always deeper than the base of pycnocline, allowing upwelled water with high nutrients to penetrate into euphotic depths during all cruises (Table I).

Taxon-specific carbon content and biomass

Population variability of normalized FALS, a proxy of cell size, and the estimated carbon contents of picoplankton cells are shown in Fig. 3. P-Euk exhibited the most size variability associated with light level (depth) on a given cruise, which is understandable since this category is composed of different taxa, compared at least to the genus-level grouping of photosynthetic bacteria. We also use the "pico" size category non-rigorously for P-Euk since our FCM measurements likely include some cells that are larger than the formal 2-μm diameter cut-off. Perhaps due to compositional changes, the patterns of variability were not consistent for P-Euk, which sometimes increased (September 2007, November 2007 and January 2008) and sometimes decreased in size (April 2008, August 2008, November 2008) with depth, as opposed to the typical slight increase in size with depth of the photosynthetic bacteria. Overall, H-Bact showed very little size differences among depths within cruises, but there was a general shift from larger to smaller sizes over the study period and especially between January 2008 and April 2008 (Fig. 3). Seasonally, larger SYN and P-Euk cells (but relatively small H-Bact) were found during April 2008, coincident with the algal bloom episode at ENSENADA station during that time (Table I). PRO was too scarce to enumerate in the samples collected during this major coastal bloom.

Estimates of picoplankton carbon biomass ranged from 2 to 60 μg C L^{-1} for picoautotrophs (A-Pico combined PRO, SYN and P-Euk) and from 9 to

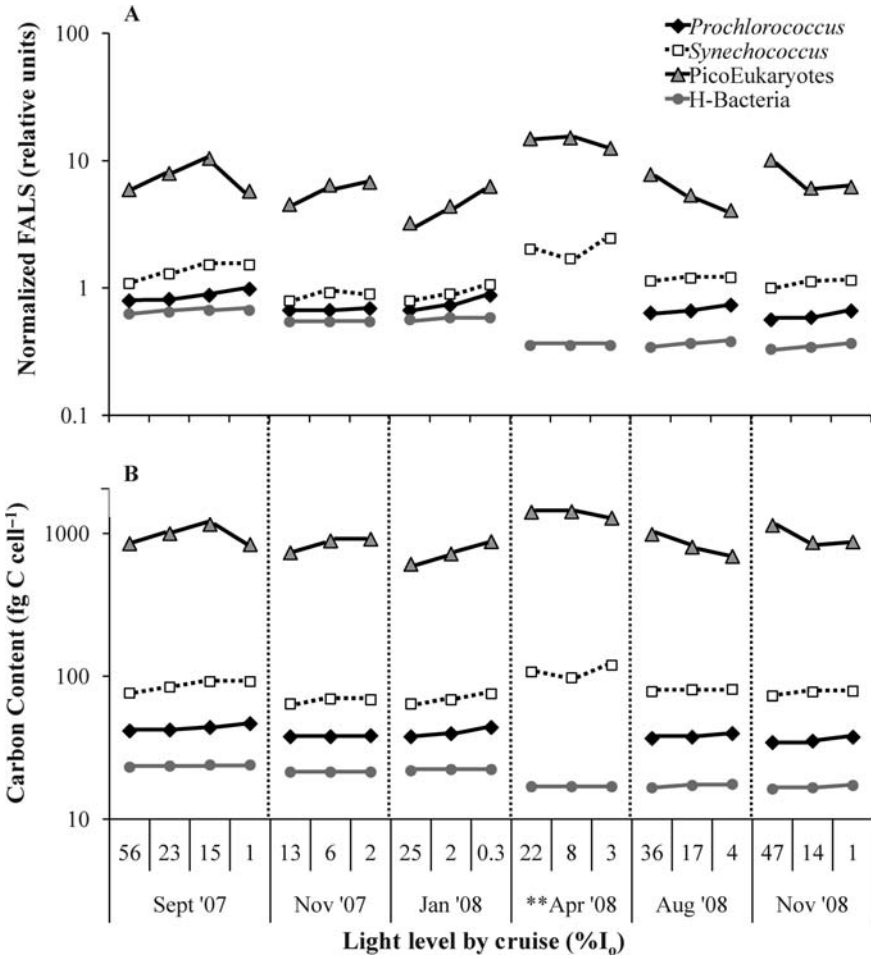

Fig. 3. Initial (**A**) bead-normalized forward angle light scattering (FALS) and (**B**) carbon content per cell (log scale) for autotrophic and heterotrophic populations, from 19 dilution experiments conducted in the euphotic zone from September 2007 to November 2008 at ENSENADA station in the northern region off WBC, México. The ** symbol denotes that a major algal bloom occurred during this cruise.

70 μg C L^{-1} for H-Bact (Fig. 4). Biomass of picoautotrophs and heterotrophs were strongly correlated ($R^2 = 0.89$, $P < 0.0001$), with both showing highest values during September 2007 and secondary peaks in January 2008. The lowest values were registered during April 2008, when A-Pico was represented mainly by P-Euk (Fig. 4B). Depth distributions of picoplankton typically showed the highest abundance and biomass at near-surface light levels and the lowest at the deepest light levels (Fig. 4, Table I). Among populations of autotrophic picoplankton, SYN had the highest abundances on most sampling dates (Table I). However, SYN only contributed an overall average of 25% of the total A-Pico carbon biomass, compared with 70% for the larger P-Euk. PRO is both the smallest A-Pico cell and occurs in relatively low abundance at this coastal site relative to the open ocean. PRO therefore comprised a minor portion of A-Pico biomass (5%) throughout the year, and was notably absent during the upwelling bloom in April 2008 (Table I, Fig. 4B).

Concentrations of total chlorophyll *a* (TChl *a*) in the euphotic zone, a proxy for relative biomass of the total phytoplankton community, were relatively high throughout the study period, varying from ~1 to 25 μg Chl *a* L^{-1}. As previously noted, strong upwelling and La Niña conditions produced extraordinary bloom levels of TChl *a* in April 2008 (Table I). Biomass of P-Euk and photosynthetic bacteria, in particular, was at their lowest levels, in absolute and relative terms, during this bloom, which therefore mostly involved larger phytoplankton (Fig. 4B). In contrast, A-Pico components were at their highest values during the more modest secondary peak of TChl *a* in September 2007. The lowest TChl *a* values were observed throughout the euphotic

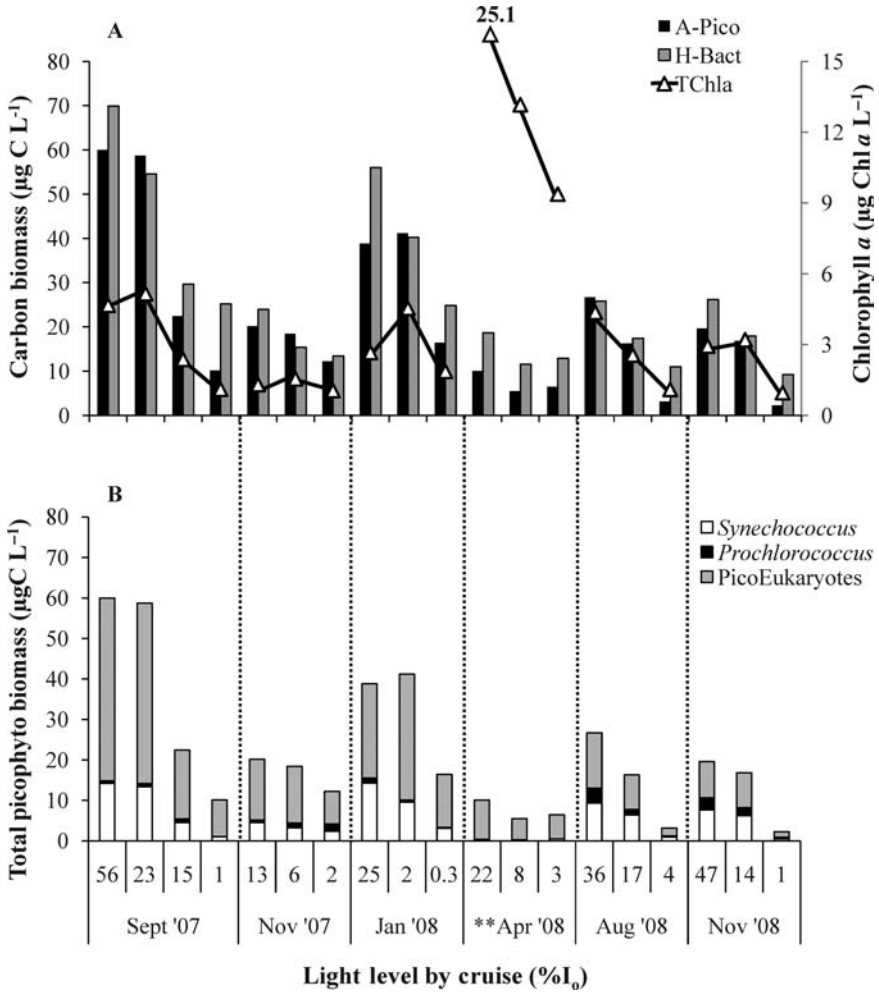

Fig. 4. (**A**) Initial biomasses of picoplankton (autotrophic and heterotrophic) populations (left *Y*-axis) and initial total concentration of chlorophyll *a* (right *Y*-axis), and (**B**) contribution of autotrophic populations (PicoEukaryotes, *Prochlorococcus* and *Synechococcus*) to total picophytoplankton biomass, from 19 dilution experiments conducted in the euphotic zone from September 2007 to November 2008 at ENSENADA station in the northern region off WBC, México. The ** symbol denotes that a major algal bloom occurred during this cruise.

zone in November 2007 and at the deepest light levels in August 2008–November 2008 (Table I, Fig. 4A).

For most of the sampling times, a positive relationship between picoplankton populations and the phytoplankton community was found, except for April 2008, when the lowest biomass levels of picoplankton populations were measured (Fig. 5). Excluding the April 2008 data, A-Pico biomass ($R^2 = 0.73$, $P < 0.0001$) and H-Bact biomass ($R^2 = 0.52$, $P = 0.0017$) were both positively and significantly correlated with TChl *a* (Fig. 5A and B).

Experimental rate estimates

Community- and population-level estimates of growth (μ) and grazing mortality (m) rates were computed, respectively, from the measured net changes in TChl *a* and cell abundances of picoplankton (A-Pico and H-Bact) (Fig. 6). TChl *a* estimates of μ ranged seasonally from 0.06 to 2.06 day^{-1}, and m varied from 0.05 to 1.09 day^{-1} (Fig. 6A). Picoplankton growth rates ranged from 0.14 to 2.02 day^{-1} and 0.19 to 1.71 day^{-1} for A-Pico and H-Bact, respectively. Protistan grazing rates on picoplankton varied between 0.21–1.37 and 0.09–1.53 day^{-1} for A-Pico and H-Bact, respectively (Fig. 6B and C).

Among all cruises and light levels, TChl *a*-based estimates of μ and m were highly correlated ($R^2 = 0.67$, $P < 0.0001$). Seasonally, the highest community rates (>1 day^{-1}) were found during experiments conducted in September 2007 and April 2008, when TChl *a* was also high. However, growth rates were lower during the massive bloom in April 2008, compared with the

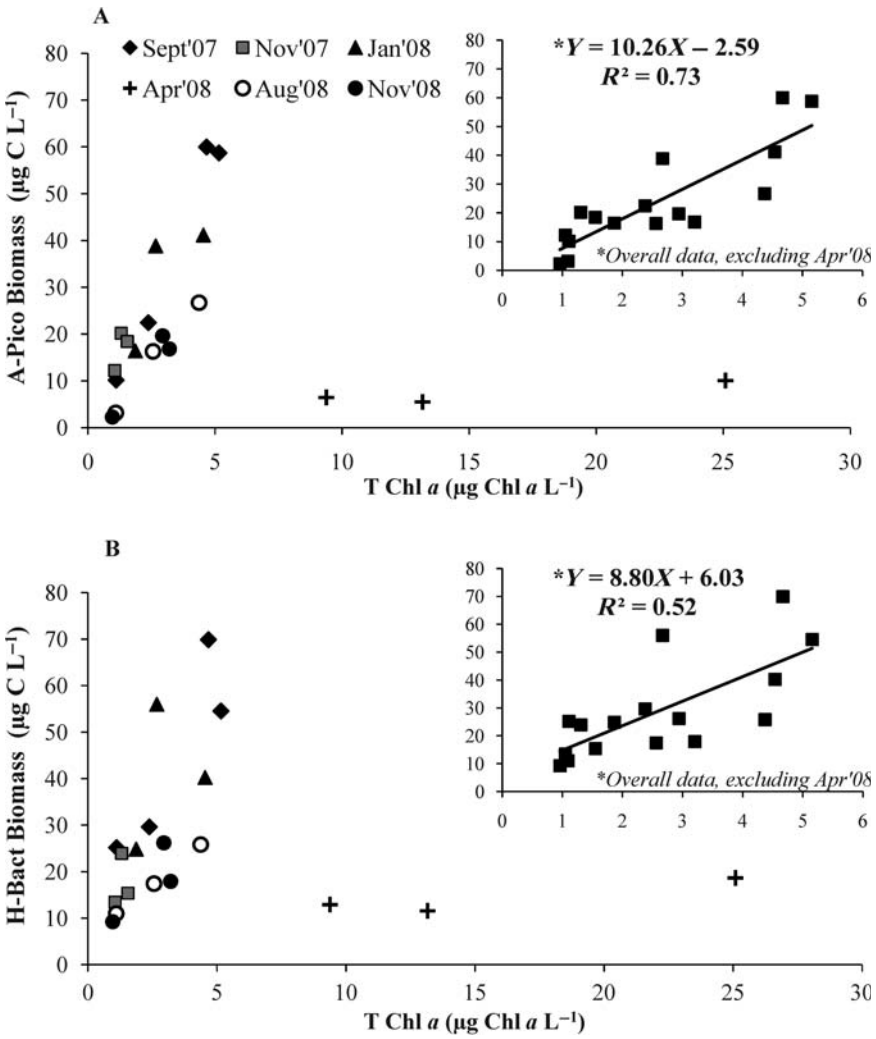

Fig. 5. Scatter plots between initial total concentration of chlorophyll *a* (TChl *a*) and initial biomasses of (**A**) autotrophic picoplankton (A-Pico) and of, (**B**) heterotrophic picoplankton (H-Bact), from data of 19 dilution experiments conducted in the euphotic zone from September 2007 to November 2008 at ENSENADA station in the northern region off WBC, México. The top (A) and bottom (B) panels show significant linear regressions from overall data, excluding April 2008 experiments.

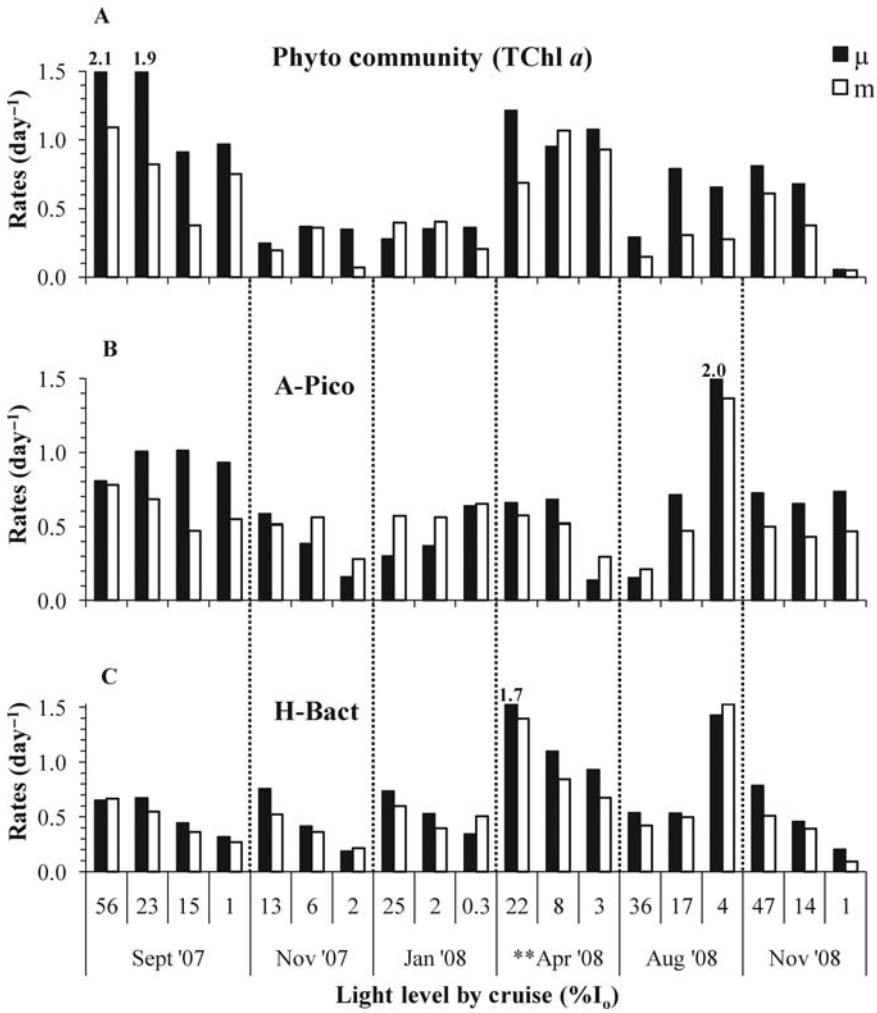

Fig. 6. Growth (μ) and protistan grazing (*m*) rates of (**A**) total phytoplankton community (TChl *a*), (**B**) picoautotrophic populations (A-Pico) and (**C**) heterotrophic bacteria (H-Bact), from 19 dilution experiments conducted in the euphotic zone from September 2007 to November 2008 at ENSENADA station in the northern region off WBC, México. The ** symbol denotes that a major algal bloom occurred during this cruise.

almost 2X higher estimates of September 2007. The lowest community rates were measured seasonally during autumn (November 2007) and winter (January 2008) experiments. Nonetheless, substantially higher community growth rate and TChl *a* were found at surface light levels in November 2008 compared with November 2007, despite 40X higher surface nitrate concentrations in November 2007 (Fig. 6A, Table I).

Cell-based μ and *m* rates of the picoautotrophs, calculated as the "weighted mean" from population-specific rate assessments of PRO, SYN and P-Euk, generally followed the trends for TChl *a* community rates, although the range was suppressed, especially in the higher values of the upper mixed-layer μ for A-Pico ($0.7-1.0\ day^{-1}$) during experiments conducted in September 2007 and April 2008 (Fig. 6B). On half of the experimental dates (January 2008, August 2008 and November 2008), A-Pico rates at the lowest light levels greatly exceeded the rates inferred from TChl *a* changes. For August 2008, in particular, exceptionally high cell growth and grazing rates for A-Pico populations were found at the pycnocline base, at 4% I_o light level (Figs 6B and 2B, Table I). Grazing losses exceeded growth rates during autumn (November 2007) and winter (January 2008) experiments when growth rates in the upper light levels were lowest (Fig. 6B). Growth and grazing mortality rates for A-Pico were significantly correlated ($R^2 = 0.73$, $P < 0.0001$) throughout the year at different light levels.

Similar to TChl *a* data, the relationship between *m* and μ rates for H-Bact cells was significant and strong ($R^2 = 0.86$, $P < 0.0001$). H-Bact rate estimates, however, were typically low compared with A-Pico or TChl *a*-based rates, except during the April 2008

phytoplankton bloom (Fig. 6C). We generally found high rates for H-Bact in the upper mixed-layer and low rates in deeper incubations, except during August 2008, when coincident with A-Pico, high growth and grazing rates were observed at the 4% light level (Fig. 6C).

Grazing impact assessments

Grazing mortality (m) rates for TChl *a* and picoplankton populations often equaled or exceeded 50% of μ, indicating a substantial removal of autotrophic and heterotrophic planktonic cells by protists at this coastal station throughout the year (Fig. 7). The m:μ ratios for TChl *a* showed higher predatory pressure during autumn-winter seasons (November 2007–08 and January 2008) and at light levels $<10\%$ I_o during the April 2008 bloom. Grazing impact on the phytoplankton community was lower in late summer (September 2007 and August 2008) than the seasonal average. Overall, m:μ averaged ($\pm$SD) 0.66 ± 0.20 for TChl *a* ($n = 19$; these and other m:μ data were arctangent transformed, averaged, then tangent back-converted, as in Calbet and Landry, 2004). This result indicates that protistan grazers consumed about two-thirds of total phytoplankton cell production in this coastal area (Fig. 7A).

A-Pico cells were even more strongly impacted by nano/micrograzers than the phytoplankton community as a whole (Fig. 7B). The weighted average impact of protistan grazers on A-Pico cells was 0.94 ± 0.22. The highest A-Pico m:μ ratios (>1.5) were mainly observed during autumn-winter experiments (November 2007–January 2008) and at the base of the euphotic zone, close to the bottom of the algal bloom, in April 2008

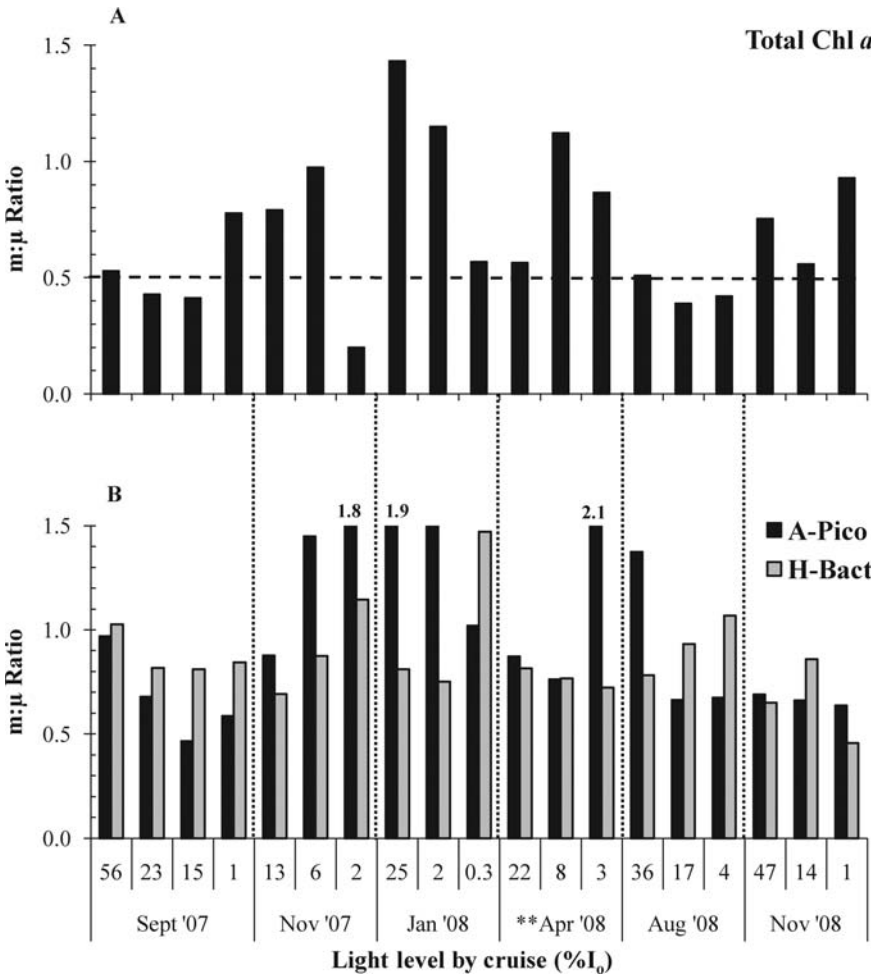

Fig. 7. Ratio of protistan grazing (m) to growth (μ) rates of (**A**) total phytoplankton community (TChl *a*) and (**B**) picoplankton (autotrophic and heterotrophic), from 19 dilution experiments conducted in the euphotic zone from September 2007 to November 2008 at ENSENADA station in the northern region off WBC, México. The ** symbol denotes that a major algal bloom occurred during this cruise. Dashed horizontal line on top panel indicates grazing equivalent to half of phytoplankton growth.

(Figs 7B and 2C). In order of population-specific percentage losses of A-Pico production to protistan consumers, PRO ($>100 \pm 25\%$) was highest, followed by P-Euk ($96 \pm 25\%$) and SYN ($93 \pm 23\%$). Similarly, the m:μ ratios for H-Bact oscillated around an average value of 0.84 ± 0.11 and was distributed more uniformly with time and depth (Fig. 7B).

^{14}C-uptake primary production and biomass production-loss estimates

Throughout the euphotic zone, the measured rates of ^{14}C-uptake primary production were variable among seasons and light levels, ranging from 0.24 to 217 μg C L^{-1} day^{-1}. Highest productivity rates were found during September 2007 and April 2008 within the mixed layer and above $\sim$10% I_o. The lowest values were registered during the November cruises (2007–08) and at the deepest light levels close to 1% I_o (Fig. 8A). During the high production period of September 2007, A-Pico exhibited their highest rates of biomass production and grazing losses. That was not the case, however, for the high production period of April 2008, when A-Pico populations, represented basically by P-Euk, had their lowest production and grazing loss estimates (Fig. 8).

Among A-Pico populations, P-Euk contributed the most to production estimates throughout the study, with population-specific rates ranging from 1.13 to

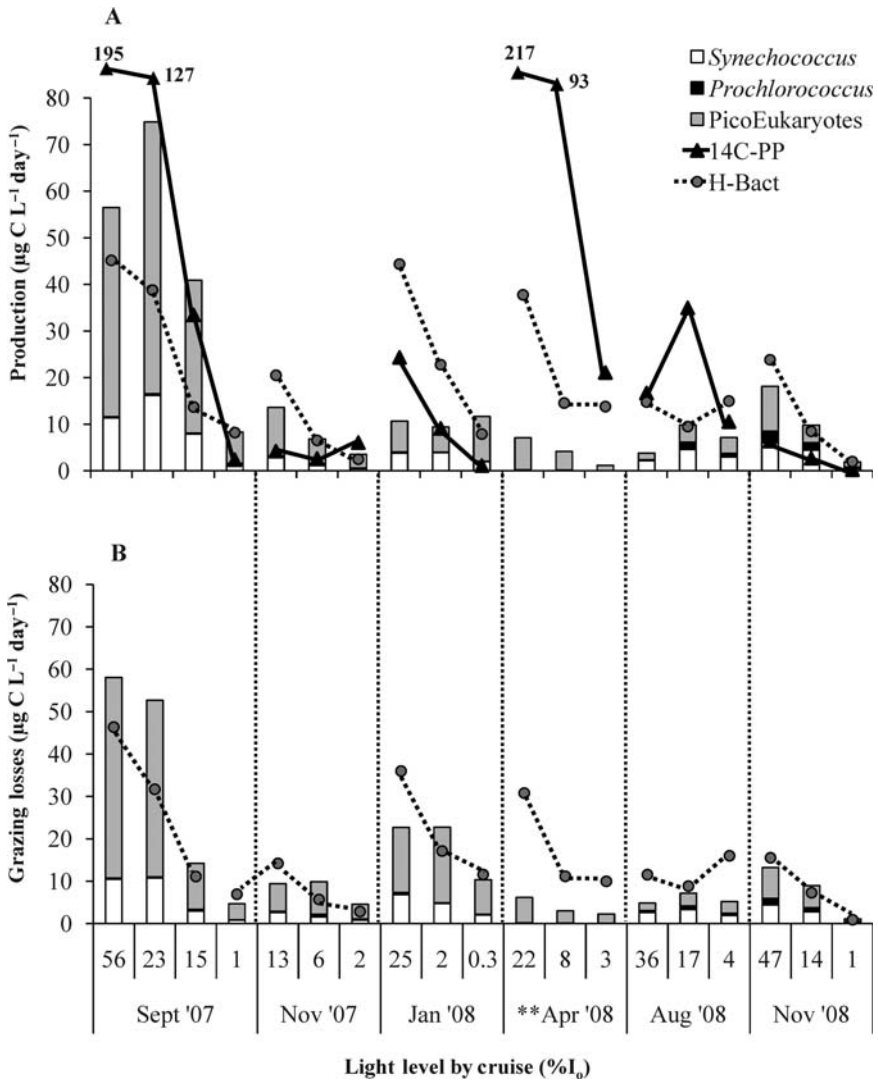

Fig. 8. Daily rates of (**A**) production and (**B**) grazing losses by protists of picoautotrophic populations (PicoEukaryotes, *Prochlorococcus* and *Synechococcus*), heterotrophic bacteria (H-Bact) and ^{14}C-uptake primary production (only panel **A**), from 19 dilution experiments conducted in the euphotic zone from September 2007 to November 2008 at ENSENADA station in the northern region off WBC, México. The ** symbol denotes that a major algal bloom occurred during this cruise.

58.3 μg C L^{-1} day^{-1} (Fig. 8A). In comparison, production estimates varied between 0.02–16.2 μg C L^{-1} day^{-1} and 0.08–2.5 μg C L^{-1} day^{-1} for SYN and PRO, respectively. Higher production values of A-Pico were found at the surface light levels and lower towards the base of euphotic layer, as was the general tendency for ^{14}C-uptake rates. The notable exception was in January 2008, when the production estimates were relatively similar among all experiments and even slightly higher at the lowest light level. On several occasions (mainly November 2007–08 cruises), estimates of A-Pico cell biomass production exceeded contemporaneous estimates of community production by ^{14}C-uptake. The strongest discrepancy was at the lowest light level (0.3% I_o) in January 2008, when ^{14}C-uptake was 10X lower than estimated A-Pico production (Fig. 8A). Secondary production estimates for H-Bact varied between 2.0 and 45.2 μg C L^{-1} day^{-1} and displayed their higher values during September 2007, January 2008 and April 2008 at the highest light levels (Fig. 8A).

In order of A-Pico biomass losses to protistan grazing, P-Euk rates were highest (0.58–47.3 μg C L^{-1} day^{-1}), followed by SYN (0.07–10.7 μg C L^{-1} day^{-1}) and PRO (0.09–1.58 μg C L^{-1} day^{-1}). Grazing losses of H-Bact ranged from 0.91 to 46.3 μg C L^{-1} day^{-1} (Fig. 8B). The highest consumption rates of picoplankton were found in September 2007 in the upper mixed-layer.

Overall, A-Pico production estimates and ^{14}C-primary production were slightly correlated with a low significance ($R^2 = 0.26$, $P = 0.0261$; Fig. 9A), but this positive relationship was much stronger when the April 2008 data were excluded ($R^2 = 0.74$, $P < 0.0001$; Fig. 9A, inset). The slope of the linear regression indicated that A-Pico production rate typically increased as 13% of the ^{14}C-uptake rate. However, this production rate increased as 29% of the community production when the April 2008 bloom data were excluded from the regression analysis (Fig. 9A). H-Bact production was also significantly correlated with ^{14}C-primary production ($R^2 = 0.49$, $P = 0.0008$; Fig. 9B) for all experiments at the ENSENADA station, and increased only slightly when the April 2008 data were excluded ($R^2 = 0.51$, $P = 0.0020$; Fig. 9B, inset). The slopes of both relationships (including and excluding April 2008 data) indicated that H-Bact production rate increased as 14–19% of the ^{14}C-uptake rate (Fig. 9B).

Picoautotroph populations and nutrients in the euphotic layer

Over all cruises and euphotic sampling depths, the log-scale abundance of A-Pico was negatively correlated with nitrate + nitrite concentration ($R^2 = 0.45$, $P < 0.0001$, Fig. 10). Lower abundances of A-Pico when nutrients are high could reflect recently upwelled water in the euphotic layer; conversely, high abundance of picophytoplankton is also naturally associated with stratified, nutrient-poor waters.

DISCUSSION

The present data were not collected at sufficient temporal resolution to define the seasonal dynamics of phytoplankton in the northern region off WBC. They do, however, provide six contrasted temporal "snapshots" that capture the system at differing states of productivity. The most productive conditions encountered during our study (September 2007 and April 2008) were associated with high nutrient delivery into the euphotic zone from episodic upwelling. Such events occur stronger and more frequently during spring and summer months in the coastal eastern boundary ecosystem off northern Baja California (Lynn and Simpson, 1987; Durazo *et al.*, in press). Particularly during September 2007 and April 2008, upwelling indices showed strong increases during or a few days before the dilution incubations were conducted (Fig. 2A). Although September 2007 and April 2008 were marked by comparable high levels of ^{14}C production in the upper 10 m of the water column, September 2007 results are more coherent with other times sampled, while the situation in April 2008 stands out as extraordinary in terms of TChl *a* accumulation and community structure. The normal seasonality of phytoplankton was intensified during this period by La Niña conditions (McClatchie *et al.*, 2008; Durazo, 2009), which have the effect of bringing the pycnocline and nutricline closer to the ocean surface and more easily entrained into the upper euphotic zone by upwelling favorable winds. The very cold sea surface temperature during our sampling in April 2008 was indicative of a massive influx of nutrients from deeper waters, which had subsequently been incorporated into phytoplankton. Although the circumstances leading up to the bloom were not observed, increased offshore transport of surface water is implied by the strong upwelling-favorable winds in the week prior to our sampling in April 2008 (Fig. 2A). Physically, this could have had the effect of moving the community that had established itself in upper euphotic zone at this site further offshore. Thus, advective transport may have contributed to changes observed in community composition, in addition to *in situ* biological responses to the altered hydrography (Li, 2002). Turbulence and the upward displacement of water associated with upwelling would also help increase the residence time of large primary producers in the euphotic layer against their tendency to sink (Rodríguez *et al.*, 2001).

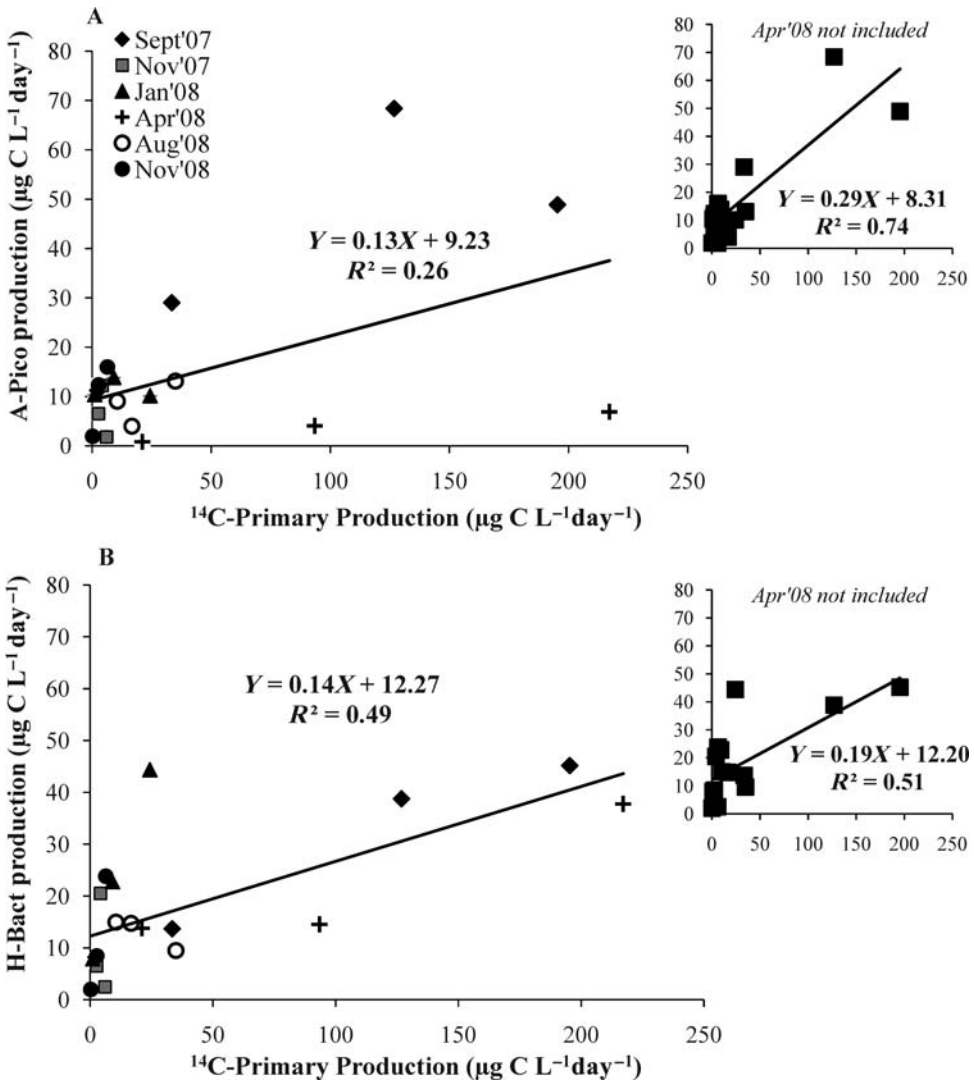

Fig. 9. Scatter plots between ^{14}C-uptake primary production and production estimates of (**A**) autotrophic picoplankton (A-Pico) and (**B**) heterotrophic picoplankton (H-Bact), from data of 19 dilution experiments conducted in the euphotic zone from September 2007 to November 2008 at ENSENADA station in the northern region off WBC, México. Top (A) and bottom (B) panels show significant linear regressions from overall data. Top (A) and bottom (B) inset panels show the significant linear regressions excluding the April 2008 experiments.

The phytoplankton community structure at ENSENADA station may, therefore, be shaped in part by the direct effects of physical processes (advection and turbulence), as well as their indirect effects on nutrient availability and biological interactions. From spring to late summer in the coastal waters off Oregon, an upwelling front physically separates high abundances of coccoid cyanobacteria and small eukaryotic phototrophs seaward of the front from low abundances on the coastal side (Sherr *et al.*, 2005). We do not know if a similar type of hydrographic barrier may have been set up off of ENSENADA station in April 2008, but it is a possibility.

The factors that regulate size structure of phytoplankton under different trophic conditions are still under debate (Agawin *et al.*, 2000; Sherr *et al.*, 2005; Echevarría *et al.*, 2009). Conventional thinking is represented by Li (Li, 2002), who found inverse relationships between picoplankton cell number and biomass relative to total chlorophyll values from a series of cruises crossing biogeographical provinces in the North Atlantic. On a smaller scale, Sherr *et al.* (Sherr *et al.*, 2005) also obtained a negative relationship between integrated abundance of P-Euk cells and Chl *a* for samples collected from a cross-shelf transect of stations in the Oregon coastal upwelling ecosystem. More recently, a negative trend of reduced picoplankton cells under eutrophic conditions has also been reported from three coastal systems south of the Iberian Peninsula

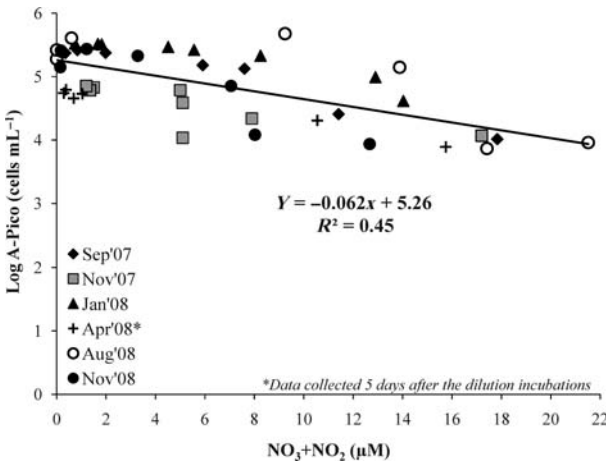

Fig. 10. Scatter plot between log-scale abundance of A-Pico populations from discrete depths and nitrate + nitrite concentrations for individual water samples collected within euphotic layer in six periods during September 2007–November 2008 at ENSENADA station in the northern region off WBC, México. All the samples were collected in the same day of incubation dilutions, excepting April 2008, when the data were sampled 5 days after dilution incubations.

(Echevarría *et al.*, 2009). In contrast, during seasonal studies in the Arabian Sea, the highest biomass levels of P-Euk occurred coincident with the highest biomass of diatoms and total phytoplankton at coastal upwelling stations during the SW Monsoon (Garrison *et al.*, 2000), though that was not the case for photosynthetic bacteria, especially *Prochlorococcus*. Recent work in the equatorial Pacific upwelling system, however, has shown that *Prochlorococcus* varies positively with TChl *a* and can dominate the phytoplankton community response to open-ocean upwelling (Selph *et al.*, in preparation). In as far as Barber and Hiscock (Barber and Hiscock, 2006) have developed their rising tide hypothesis largely based on observations of phytoplankton response to iron fertilization experiments in the equatorial Pacific, there may be cause to think that picophytoplankton responses to perturbations in tropical/subtropical systems may differ from those in more temperate and highly seasonal environments. The warmer systems, for example, tend to maintain a strong interactive network of producers and consumers throughout the year and may promote more tightly coupled trophic responses at all levels that help regulate the explosive growth potential of bloom taxa.

At our study location, which has strong tropical/subtropical influences, increases in TChl *a* were generally paralleled by increases in picoplankton biomass (Fig. 5A, inset). Thus, over a productive range, but excluding extreme environmental conditions, our results are consistent with the rising tide hypothesis (Barber and Hiscock, 2006). Although picophytoplankton carbon grew with total phytoplankton, the rate of A-Pico increase was slower. If we assume a carbon conversion factor of 30 μg C per μg TChl *a* (Eppley, 1968) to compute total phytoplankton carbon for comparison with A-Pico biomass, the resulting regression gives a slope of 0.34 (data not shown). This less than 1:1 relationship indicates in our case, as well as in previous observations (Agawin *et al.*, 2000; Li, 2002; Sherr *et al.*, 2005; Echevarría *et al.*, 2009), that the relative contribution of picoautotrophs to total phytoplankton biomass decreases significantly under more productive conditions. The positive relationship between A-Pico production estimates and ^{14}C-primary production at our coastal station, also had a <1.0 positive slope (Fig. 9A, inset), even when the most productive period of April 2008 was considered (Fig. 9A). Thus, in the majority of our temporal "snapshots", favorable environmental conditions tended to lift all phytoplankton together, although small cells increased slower than large cells.

Mechanistically, smaller cells are better adapted to low-nutrient conditions due to larger surface to BV ratios (Chisholm, 1992), while large cells may have physiological advantages, such as better internal nutrient storage or more effective nutrient uptake, under high nutrient conditions (Echevarría *et al.*, 2009). Our finding of an overall negative relationship between the log-abundance of A-Pico cells and euphotic zone nitrate + nitrite concentrations (Fig. 10) suggests that small cells were not able to grow well at the expense of high nutrient concentrations in recently upwelled water, which can, however, support a large biomass accumulation of large-sized diatoms, and oppositely, the highest abundances of A-Pico cells were able to grow efficiently at nitrate + nitrite concentrations <2 μM (Fig. 10). Similar results were found in other ecosystems such as the coastal waters off Oregon (Sherr *et al.*, 2005), and even, in contrasting trophic environments (Agawin *et al.*, 2000; Echevarría *et al.*, 2009). However, nutrient availability *per se* could be not the direct cause of A-Pico diminished abundance or relative performance with increasing trophic state; temperature for example has a strong impact on *Prochlorococcus*, which disappeared when colder waters were present during April 2008 (Table I), and generally lack the functional capability to utilize nitrate (Moore *et al.*, 2002; Martiny *et al.*, 2009).

April 2008 was the most productive sampling period at our coastal station, generating a strong bloom of phytoplankton and providing an interesting counterpoint to the rising tide hypothesis (Barber and Hiscock, 2006). During this period, we found evidence of reasonably good growth conditions for picophytoplankton; instantaneous growth rates were about equal to seasonally averaged levels (Fig. 6B), and a significant correlation

was found between A-Pico production estimates and contemporaneous estimates of community production by ^{14}C-uptake (Fig. 9A). However, the low biomass of A-Pico (Fig. 4A), mainly represented by P-Euk, and the strong mortality impact of protistan grazers (the highest m:μ ratio of all cruises was found at the base of pycnocline; Fig. 7B) point to the possibility that, while large phytoplankton cells were still growing and accumulating in absence of high losses by consumers, the small cells were already top-down controlled (A-Pico production and grazing losses showed similar and low estimates; Fig. 8). Thus, the greatly reduced production of A-Pico during the April 2008 bloom (Fig. 8A) was determined principally by the decline in biomass, which could be related at some point to inadequate growth to accumulate, or even maintain, picophytoplankton standing stock during the bloom. As noted previously, however, advective losses of surface waters away from the upwelling station may also have contributed to this dramatic decline, greatly exacerbating the appearance of a rapid replacement of small by large cells. In effect, the virtual collapse of A-Pico during April 2008 bloom appears to be consistent with the conventional view of a successional replacement of small phytoplankters by the larger responders to bloom-favorable growth conditions, but the mechanisms in our system (biological versus physical) are not clear. At the very least, the rising tide hypothesis needs to be carefully examined in tropical/subtropical systems for circumstances that are more typical of highly seasonal temperate environments, where growth-favorable nutrient conditions are strongly associated with colder waters and uncoupled food webs.

Another possible explanation for the low abundances (biomass) of picoautotrophs during April 2008 is the elevated concentration of trace metals (particularly cadmium) in the upwelled waters. As noted off Oregon, for example, cadmium may be differentially toxic to small versus large phytoplankton, especially to coccoid cyanobacteria, for which only $\sim$0.1 nM can greatly affects growth rate (Sherr *et al.*, 2005). During 2008 at a coastal site off Punta Banda, Ensenada, cadmium concentrations averaged 0.27 nM ($\pm$0.03) and increased ($>$0.3 nM) in surface waters from winter to spring (F. Delgadillo, Ensenada, BC, personal communication). From these results, it is possible that during the initial and peak phase of the April 2008 bloom, a high input of trace metals to surface layers favored the predominance of larger phytoplankton to the detriment of the smaller cells. High abundances of large diatoms and autotrophic dinoflagellates were clearly evident during April 2008 via epifluorescence microscopy. Consequently, the outcome is consistent with what we might expect for a classic spring bloom, where large primary producers with high growth rate potential, like chain-forming diatoms, can effectively decouple from grazing losses (the "loophole" mechanism; Irigoien *et al.*, 2005) and dominate the phytoplankton community response.

Except for the April 2008 bloom, picoplankton comprised an important component of the community under all other conditions sampled at the ENSENADA coastal station. A-Pico carbon biomass almost always exceeded 20 μg C L^{-1} in the upper euphotic zone, and was typically comparable to the biomass of H-Bact (Fig. 4). Small eukaryotes dominated A-Pico biomass, especially at elevated concentrations of TChl *a*. Although small-sized phytoplankton are typically thought to be characteristic of oligotrophic open-ocean systems, high abundance of autotrophic bacteria and P-Euk have also been observed in other upwelling ecosystems of the CCS (Worden *et al.*, 2004; Sherr *et al.*, 2005). However, this fraction was higher in our uppermost experimental incubations of $<$10–12 m depth and relatively high light, where A-Pico typically accounted for half or more of the corresponding estimates from ^{14}C-PP incubated under the same *in situ* conditions and 24-h time interval (Fig. 8A). Especially in near-surface incubations during November 2007 and November 2008, A-Pico production estimates exceeded ^{14}C by double (Fig. 8A). Some of this difference reflects the fact that while our estimates measure the total production of new A-Pico cells over the incubation period, which may be closer to a gross production rate, a good deal of the ^{14}C uptake during the incubation can be lost to cycling before the net total particulate label remaining is measured. It is also possible, however, that our mean carbon content assumed as a starting point for estimations of biomass and production of P-Euk for cells size on average $\sim$2.1-μm diameter (1000 fg C cell^{-1}, from Sherr *et al.*, 2005) might be too high for this system. If that is the case, then the biomass and production estimates would also be systematically high. Because of the diversity in types of cells that comprise the P-Euk category and the vagaries of size inferences from FCM, independent assessment of mean P-Euk carbon content is therefore very important for future analyses of production size structure in plankton communities.

Carbon content alone cannot account, however, for the relative production rates many times higher than the contemporaneous ^{14}C results at the light levels closer or lower than 1% I_o, as were showed in September 2007, January 2008 and November 2008 (Fig. 8A). The inverse pattern with depth of the growth rates (Fig. 6B) and the production estimates (Fig. 8A) for January 2008 suggest, for example, that an error

(switch) was made in incubating the bottles at the correct depth of collection or in sub-sampling the bottles for FCM analyses. Either of these possibilities would have left unmistakable signs in the FCM results, which were carefully examined to diagnose the problem. The key signal is the bead-normalized red fluorescence per cell, which rigorously defines the depth order of the samples collected (deeper cells have substantially higher chlorophyll content) and would show marked changes if low-light adapted cells had been inadvertently incubated at a near-surface light (the January conditions were bright sunlight). We found no evidence of a sub-sampling or incubation problem in the raw cytograms, the cell counts or the Chl *a*-content inferences for these experiments. The relatively high growth rates measured at low light, not only in this particular experiment, but also in September 2007, August 2008 ($\mu = 2$ day^{-1}) and November 2008 (Fig. 6B), beg the question of whether A-Pico populations may be able to use alternate carbon sources for growth (i.e. mixotrophy of dissolved organics or particulate prey) under low light or benefit in some other way from the physical–chemical conditions at the base of the euphotic zone.

During the study period, more than half of phytoplankton community production was typically lost daily to protistan grazers in the coastal waters off WBC (Fig. 7A). On average, nano/micrograzer consumption was equivalent to 66% of the phytoplankton community growth, suggesting a close coupling between daily production and consumption of phytoplankton in this region, as has been previously reported for other coastal systems (Strom *et al.*, 2001; McManus *et al.*, 2007). Also, this assessment based on TChl *a* agrees with global estimates of percent primary production grazed by microzooplankton in temperate (61–69%) and coastal systems (57–60%) (Calbet and Landry, 2004). The seasonal variability of the grazing impact measured in this study is similar to mixed-layer results from other upwelling regions with contrasting trophic conditions along the year (Neuer and Cowles, 1994; Böttjer and Morales, 2005; McManus *et al.*, 2007). We also found heavy predatory pressure on picoplankton populations for most of the year (Fig. 7B). Overall, the consumption of A-Pico averaged 94% of their daily production. Grazing vulnerability of A-Pico also varied slightly among populations (PRO > 100%, P-Euk = 96% and SYN = 93%) and was likely associated with their relative biomass and presence during the year (PRO < SYN and P-Euk). This pattern has been reported previously in coastal waters of the Southern California Bight, where carbon consumed:produced ratios ranged seasonally from 23 to >100% per day among A-Pico populations, with highest ratios for PRO relative to P-Euk and SYN populations, as well as total absence of PRO cells during spring months (Worden *et al.*, 2004), as was described in our work. Similarly, high percentages of A-Pico production grazed per day have been reported for the western South China Sea, with highest mean values for PRO (83 ± 57%) and lowest for SYN (61 ± 25%), although population growth rates <0.2 day^{-1} were excluded from these computations (Chen *et al.*, 2009). Furthermore, strong grazing impact accounted for 84% of the daily production of H-Bact on average, indicating that the top-down processes play an important role in regulating bacterial biomass at the ENSENADA station. In fact, the predatory pressure was similar to other coastal upwelling regions, as was reported for the Humboldt Current system, where >100% of H-Bact biomass was daily removed mainly by heterotrophic nanoflagellates, mostly during the non-upwelling seasons (Cuevas *et al.*, 2004; Vargas *et al.*, 2007). Based on measured rates and stocks, our estimates of bacterial production (BP) were significantly correlated with primary production (Fig. 9B), but BP values were many times higher than ^{14}C-uptake rates during the less productive autumn-winter periods of the sampling (Fig. 8A), when protistan grazing on A-Pico populations was strongest (m:μ values >1.5) (Fig. 7B). This may reflect a more tightly coupled dependency of BP on DOC production from grazing processes during such times, or the utilization of previously fixed, excess DOC that is stored and returned to the system by the upwelling circulation.

Highly productive upwelling systems are commonly characterized as having short food chains composed of large-sized phytoplankton, zooplankton and pelagic fish (Ryther, 1969). However, the temporal snapshots of plankton dynamics described here for the coastal upwelling system of WBC show an active and generally significant component associated with the growth, production and grazing turnover of picophytoplankton populations. For most of the year, the high production contributions of A-Pico and H-Bact compared with ^{14}C-uptake measurements and the strong grazing impacts on A-Pico and H-Bact populations indicated that a significant fraction of production was channeled through the microbial food web. The situation observed in April 2008 was exceptional, however, in terms of TChl *a* accumulation and community structure associated with intensified spring upwelling under La Niña conditions. While picophytoplankton as a group varied positively with the rest of the community in response to less extreme variations in growth conditions, the "rising tide" hypothesis therefore appears to apply under most conditions in our coastal upwelling area. However,

under extreme conditions, as in April 2008, the dynamics of the picoplankton could be modulated by physical forcing (low standing stocks due to increased offshore advection of small cells in surface waters) and/or by a metabolic response (no evidence of A-Pico biomass accumulation in cold and rich-nutrient upwelled water) that lead to a replacement of small cells by the larger phytoplankters in this coastal upwelling station. Given the significance of microbial trophic pathways in coastal upwelling systems, further studies are needed to understand at a mechanistic level what gives rise to these unexpected dynamics.

ACKNOWLEDGEMENTS

We gratefully acknowledge all students, technicians and scientists whose efforts facilitated and contributed to our results, as well as, the captain and crew of R/V *Francisco de Ulloa* and the boat *GENUS* for their help during the hard work at the sea. We are also grateful to Dr Karen Selph (SOEST, Hawaii) for her valuable help and suggestions in the processing of FCM data, and to Dr Víctor Camacho-Ibar (IIO-UABC) for the nutrient analysis. We are also grateful with two anonymous referees who made helpful comments on a previous version of this manuscript.

FUNDING

This study was supported by FLUCAR project from CONACyT grants SEP-2004-C01-45813/A-1 and 25339. M.L. was supported by the California Current Ecosystem Program (CCE-LTER; NSF OCE 04-17616).

REFERENCES

Agawin, N. S. R., Duarte, C. M. and Agustí, S. (2000) Nutrient and temperature control of the contributions of picoplankton to phytoplankton biomass and production. *Limnol. Oceanogr.*, **45**, 591–600.

Armstrong, F. A., Stearns, C. R. and Strickland, J. D. (1967) The measurement of upwelling and subsequent biological processes by means of the Technicon AutoAnalyzer and associated equipment. *Deep-Sea Res.*, **14**, 381–389.

Barber, R. T. and Hiscock, M. R. (2006) A rising tide lifts all phytoplankton: Growth response of other phytoplankton taxa in diatom-dominated blooms. *Global Biogeochem. Cycles*, **20**, GB4S03. doi: 10.1029/2006GB002726.

Binder, B., Chisholm, S., Olson, R. *et al.* (1996) Dynamics of picophytoplankton,ultraphytoplankton and bacteria in the central equatorial Pacific. *Deep-Sea Res. II*, **43**, 907–931.

Böttjer, D. and Morales, C. E. (2005) Microzooplankton grazing in a coastal embayment off Concepción, Chile, (~36°S) during non-upwelling conditions. *J. Plankton Res.*, **27**, 383–391.

Calbet, A. and Landry, M. (2004) Phytoplankton growth, microzooplankton grazing, and carbon cycling in marine systems. *Limnol. Oceanogr.*, **49**, 51–57.

Cuevas, L. A., Daneri, G., Jacob, B. *et al.* (2004) Microbial abundance and activity in the seasonal upwelling area off Concepción (~36°S), central Chile: a comparison of upwelling and non-upwelling conditions. *Deep-Sea Res. II*, **51**, 2427–2440.

Chen, B., Liu, H., Landry, M. R. *et al.* (2009) Close coupling between phytoplankton growth and microzooplankton grazing in the western South China Sea. *Limnol. Oceanogr.*, **54**, 1084–1097.

Chisholm, S. W. (1992) Phytoplankton size. In Falkowski, P. G. and Woodhead, A. D., (eds), *Primary Productivity and Biogeochemical Cycles in the Sea.* Plenum Press, New York, pp. 213–237.

Durazo, R. (2009) Climate and upper ocean variability off Baja California, Mexico: 1997–2008. *Prog. Oceanogr.*, **83**, 361–368.

Durazo, R., Ramírez, A. M., Miranda, L. E. *et al.* Climatología hidrográfica de la Corriente de California frente a Baja California. In Durazo, R. and Gaxiola, G. (eds), *Dinámica del Ecosistema Pelágico frente a Baja California, 1997–2007.* Published by Instituto Nacional de Ecología (INE)/ Centro de Investigación Científica y de Educación Superior (CICESE), México, 20 pp. (in press).

Echevarría, F., Zabala, L., Corzo, A. *et al.* (2009) Spatial distribution of autotrophic picoplankton in relation to physical forcings: the Gulf of Cádiz, Strait of Gibraltar and Alborán Sea case study. *J. Plankton Res.*, **31**, 1339–1351.

Eppley, R. W. (1968) An incubation method for estimating the carbon content of phytoplankton in natural samples. *Limnol. Oceanogr.*, **13**, 574–582.

Frost, B. W. (1972) Effect on size and concentration of food particles on feeding behavior of the marine planktonic copepod *Calanus pacificus*. *Limnol. Oceanogr.*, **17**, 805–815.

Garrison, D. L., Gowing, M. M., Huges, M. P. *et al.* (2000) Microbial food web structure in the Arabian Sea: A US JGOFS study. *Deep-Sea Res. II*, **47**, 1387–1422.

Irigoien, X., Flynn, K. J. and Harris, R. P. (2005) Phytoplankton blooms: a 'loophole' in microzooplankton grazing impact? *J. Plankton Res.*, **27**, 313–321.

Landry, M. R. and Hassett, R. P. (1982) Estimating the grazing impact of marine micro-zooplankton. *Mar. Biol.*, **67**, 283–288.

Landry, M. E., Brown, S. L., Neveux, J. *et al.* (2003) Phytoplankton growth and microzooplankton grazing in high-nutrient, low-chlorophyll waters of the equatorial Pacific: Community and taxon-specific rate assessments from pigment and flow cytometric analyses. *J. Geophys. Res.*, **108**, 8142. doi: 10.1029/2000JC000744.

Landry, M. R., Brown, S. L., Rii, Y. M. *et al.* (2008) Depth-stratified phytoplankton dynamics in Cyclone *Opal*, a subtropical mesoscale eddy. *Deep-Sea Res. II*, **55**, 1348–1359.

Landry, M. R., Ohman, M. D., Goericke, R. *et al.* (2009) Lagrangian studies of phytoplankton growth and grazing relationships in a coastal upwelling ecosystem off Southern California. *Prog. Oceanogr.*, **83**, 208–216.

Lee, S. and Fuhrman, J. A. (1987) Relationships between biovolume and biomass of naturally derived marine bacterioplankton. *Appl. Environ. Microbiol.*, **53**, 1298–1303.

Legendre, L. and Rassoulzadegan, F. (1995) Plankton and nutrient dynamics in marine waters. *Ophelia*, **41**, 153–172.

Li, W. K. W. (2002) Macroecological patterns of phytoplankton in the Northwestern Atlantic Ocean. *Nature*, **419**, 154–157.

Lynn, R. J. and Simpson, J. J. (1987) The California current system: the seasonal variability of its physical characteristics. *J. Geophys. Res.*, **92**, 12947–12966.

Martiny, A. C., Kathuria, S. and Berube, P. M. (2009) Widespread metabolic potential for nitrite and nitrate assimilation among *Prochlorococcus* ecotypes. *Proc. Natl Acad. Sci. USA*, **106**, 10787–10792.

McClatchie, S., Goericke, R., Koslow, J. A. *et al.* (2008) The state of the California Current, 2007–2008: La Niña conditions and their effects on the ecosystem. *CalCOFI Rep.*, **49**, 39–76.

McManus, G. B., Costas, B. A., Dam, H. G. *et al.* (2007) Microzooplankton grazing of phytoplankton in a tropical upwelling region. *Hydrobiology*, **575**, 69–81.

Monger, B. C. and Landry, M. R. (1993) Flow cytometric analysis of marine bacteria with Hoechst 33342. *Appl. Environ. Microbiol.*, **59**, 905–911.

Moore, L. R., Post, A. F., Rocap, G. *et al.* (2002) Utilization of different nireogen sources by the marine cyanobacteria *Prochlorococcus* and *Synechococcus*. *Limnol. Oceanogr.*, **47**, 989–996.

Neuer, S. and Cowles, T. J. (1994) Protist herbivory in the Oregon upwelling system. *Mar. Ecol. Prog. Ser.*, **113**, 147–162.

Parsons, T. R., Maita, Y. and Lalli, C. M. (1984) *A Manual of Chemical and Biological Methods for Seawater Analysis*. Pergamon Press, Oxford, 173 pp.

Rodríguez, J., Tintoré, J., Allen, J. *et al.* (2001) Mesoscale vertical motion and the size structure of phytoplankton in the ocean. *Nature*, **410**, 360–363.

Ryther, J. H. (1969) Photosynthesis and fish production in the sea. *Science*, **166**, 72–76.

Sherr, E. B. and Sherr, B. F. (2002) Significance of predation by protists in aquatic microbial food webs. *Antonie van Leeuwenhoek*, **81**, 293–308.

Sherr, E. B., Sherr, B. F. and Wheeler, P. A. (2005) Distribution of coccoid cyanobacteria and small eukaryotic phytoplankton in the upwelling ecosystem off the Oregon coast during 2001 and 2002. *Deep-Sea Res. II*, **52**, 317–330.

Steemann Nielsen, E. (1952) The use of radio-active carbon (^{14}C) for measuring organic production in the sea. *J. Cons. Int. Mer.*, **18**, 117–140.

Strom, S. L., Brainard, M. A., Holmes, J. L. *et al.* (2001) Phytoplankton blooms are strongly impacted by microzooplankton grazing in coastal North Pacific waters. *Mar. Biol.*, **138**, 355–368.

Turner, J. T. (2002) Zooplankton fecal pellets, marine snow and sinking phytoplankton blooms. *Aquat. Microb. Ecol.*, **27**, 57–102.

Vargas, C. A., Martínez, R. A., Cuevas, L. A. *et al.* (2007) The relative importance of microbial and classical food webs in a highly productive coastal upwelling area. *Limnol. Oceanogr.*, **52**, 1495–1510.

Welshmeyer, N. (1994) Fluorometric analysis of chlorophyll *a* in the presence of the chlorophyll *b* and pheopigments. *Limnol. Oceanogr.*, **39**, 1985–1992.

Worden, A. Z., Nolan, J. K. and Palenik, B. (2004) Assessing the dynamics and ecology of marine picophytoplankton: the importance of the eukaryotic component. *Limnol. Oceanogr.*, **49**, 168–179.

Wolter, K. and Timlin, M. S. (1998) Measuring the strength of ENSO events—how does 1997/98 rank? *Weather*, **53**, 315–324.

CAPÍTULO 3: Dinámica taxón-específica del fitoplancton y transferencia de carbono a través de la red trófica microbiana bajo condiciones oceanográficas contrastantes en la estación ENSENADA.

Trabajo en preparación: *Linacre et al., (2011). Taxon-specific phytoplankton dynamics and carbon transfer through the microbial food web in a coastal upwelling system off northern Baja California, México.*

RESUMEN: Durante seis cruceros (septiembre 2007-noviembre 2008) fue investigada la dinámica temporal del flujo de carbono a través de la trama trófica microbiana en el sistema de surgencia costera localizado al norte de Baja California. En la estación ENSENADA, un punto costero localizado en estas aguas, se realizaron estimaciones de biomasa de carbono de los principales grupos funcionales autótrofos (desde células picoplanctónicas hasta microplanctónicas) y de sus consumidores nano/microzooplanctónicos basado en análisis de citometría de flujo, HPLC y microscopía de epifluorescencia. En cada fecha de muestreo, se realizaron incubaciones *in situ* de 24 horas a tres o cuatro niveles de profundidad, utilizando la técnica de dilución abreviada a 3 tratamientos, para determinar las tasas taxón-específicas de crecimiento y pastoreo del fitoplancton. Asimismo, en base a las estimaciones de biomasa de carbono y a las tasas de crecimiento y pastoreo instantáneas medidas experimentalmente se determinaron las tasas taxón-específicas diarias de producción de carbono y su pérdida por el pastoreo del nano/microzooplancton. La mayoría del año este sistema costero estuvo dominado por componentes heterótrofos, excepto en periodos de intensos y frecuentes eventos de surgencia costera, los cuales modifican el sistema hacia la autotrofía debido al mejoramiento en las condiciones ambientales (nutrientes) que favorecen el crecimiento del fitoplancton dentro de la zona eufótica. La producción primaria (PP) comunitaria atribuida a células autótrofas tanto pequeñas (mayormente *Synechococcus* y Prasinofitas) como grandes (mayormente diatomeas y dinoflagelados autótrofos) fue significativamente impactada (91 ± 31% de la PP) por el pastoreo del nanozooplancton (2-20 µm) y microzooplancton (20-200 µm), a través de un amplio rango de condiciones de luz (desde 56% al 0.3% de la luz superficial) y nutrientes (desde 0 a >10 µM) observados en la estación ENSENADA. Nuestros resultados sugieren que la

trama trófica microbiana (incluyendo a las grandes células fitoplanctónicas como presas de consumidores) es una compleja estructura trófica y una significante componente que recicla eficientemente el carbono dentro de las capas superficiales de este sistema de surgencia costera del noroeste de Baja California.

Palabras Claves: método de dilución; flujo de carbono; tasas de crecimiento de fitoplancton; tasas de pastoreo de fitoplancton; estación ENSENADA.

Taxon-specific phytoplankton dynamics and carbon transfer through the microbial food web in a coastal upwelling system off northern Baja California, México.

Lorena P. Linacre, *et al.*, *en preparación*. Primer borrador

Abstract

We investigated the temporal dynamics of carbon flow through the microbial food web a coastal upwelling system (ENSENADA station) of northern Baja California during six cruises (September 2007 – November 2008). Carbon biomass assessments for major autotrophic functional groups (from pico- to micro-sized cells) and their nano/microzooplankton grazers were based on analyses by flow cytometry, HPLC pigments and epifluorescence microscopy. On each sampling date, experimental taxon-specific phytoplankton growth and microzooplankton grazing rates were determined by 24-h *in situ* incubations at 3-4 euphotic depths using an abbreviated 3-treatment dilution technique. The products of carbon biomass and instantaneous rate determinations were used to estimate daily rates of taxon-specific production and losses to microzooplankton grazing. For most of the year, microbial heterotrophic biomass at this coastal site exceeded autotrophic biomass. The exception was a period of very strong upwelling (April 2008), which favored large phytoplankton and high autotrophic production, leading to a system shift toward the autotroph dominance. Community primary production attributed both to small (mostly *Synechococcus* and prasinophytes) and large (mostly diatoms and autotrophic dinoflagellates) autotrophs was significantly (91 ± 31% of PP) impacted by nano (2-20 µm) and microzooplankton (20-200 µm) grazing, throughout a wide range in light (from 56% to 0.3% I_o) and nutrient (0 to >10 µM) conditions. Our results indicate that the microbial food web (including large phytoplankton as prey of protistan grazers) in this coastal upwelling system is complex and temporally dynamic, but with strong trophic couplings that generally lead to efficient carbon cycling in the upper layer.

Keywords: dilution method, carbon flux, phytoplankton growth rate, phytoplankton grazing rate, ENSENADA station.

1. - INTRODUCTION

Many productive and seasonal systems, as coastal upwelling systems involve multivorous food webs, where both classical (herbivorous food chains) and microbial trophic components (small eukaryotic algae and cyanobacteria as well as heterotrophic bacteria, microzooplankton) play significant roles in the carbon fluxes (Legendre and Rassoulzadegan, 1995). The balance between microbial and herbivore pathway determine the ability of the ecosystem to recycle carbon within the upper layer or export it to the ocean interior (Legendre and Le Fevre, 1989, 1995). Particularly, microzooplankton (here defined as nano- to micro-sized grazers <200 µm) is ubiquitous component in the microbial food web as major consumer of small and large primary producers, as well as heterotrophic bacteria (Sherr and Sherr, 2002; Calbet, 2008). To quantify this trophic pathway, relevant assessments of phytoplankton growth and microzooplankton grazing have been systematically conducted in a variety of oceanic habitats (including very productive coastal areas) by the dilution technique (Landry and Hasset, 1982), which have estimated that on average microzooplankton consumption accounts for 67% of phytoplankton daily production (Calbet and Landry, 2004). Most of remaining production is grazed by mesozooplankton that has been estimated to be on an average of only 10% of the primary production (Calbet, 2001), leaving a small fraction to be lost by direct sinking from the euphotic zone (Wasmann, 1998).

Because of the high production of upwelling regions and their importance for carbon fluxes from continental shelves to slopes (Walsh *et al*. 1981), more knowledge on the magnitude and variability of microbial food web activity in these regions is needed. Several coastal upwelling systems have been characterized by multivorous food web structures (Neuer and Cowles, 1994; Vargas and González, 2004; Vargas *et al.*, 2007; Landry *et al.*, 2009; Texeira *et al.*, 2010). Particularly, evidences recently found in the coastal region off western Baja California (WBC), have suggested that picoplankton temporal dynamics is strongly influenced by the seasonal oceanographic conditions, and that play a significant role in the carbon fluxes as integral part of the microbial structure from this upwelling system (Linacre *et al.*, 2010a).

The coastal region off WBC is the southern limit of the California Current System (CCS) and, has shown to be modulated by seasonal and interannual fluctuations that occur in this eastern boundary upwelling system (Durazo, 2009; Durazo *et al.*, 2010). Recently, it was suggested that a coastal monitoring observatory located off Ensenada, México (ENSENADA station) is representative of physical and chemical conditions of the coastal region off WBC (Linacre *et al.*, 2010b). Marked seasonal variability at ENSENADA station have been related to fluctuations in the predominant flows (equatorward surface California Current and poleward subsurface California Undercurrent) throughout the water column, as well as, to coastal upwelling events whose magnitude and frequency increases towards spring–summer. Besides, interannual variability is related to warm and/or cold ENSO phases that modify the characteristics of the water column in this coastal region (Linacre *et al.*, 2010b). Thus, this coastal site involves contrasting environmental situations that would be influencing the temporal dynamic of the carbon flux through a complex microbial food-web.

The aim of the present study was to assess the temporal dynamics of carbon transference through the microbial food web in the coastal upwelling system off northern WBC, by means of taxon-specific phytoplankton production estimates and carbon losses by microzooplankton grazing on the whole community and on major autotrophic groups, carried out in a coastal station (ENSENADA station) under contrasting seasonal oceanographic conditions.

2. - METHODS

2.1. Sampling and experimental set up

Experimental studies of phytoplankton growth and protistan grazing were conducted at the ENSENADA station (31°40.105’ N, 116 °41.596’ W) at the northern region off WBC (Fig.1), as part of the FLUCAR (*Carbon Sources and Sinks in the Continental Margins of the Mexican Pacific Waters*) project. During the period from 24

September 2007 to 11 November 2008, six sets of experiments were incubated *in situ* for 24-h at a fixed coastal station. Following the experimental approach of Landry *et al.* (2008), an abbreviated 3-treatment dilution protocol was applied in this site, which is described in detail by Linacre *et al.* (2010a). Routine station activities included CTD/rosette casts to 100 m depth with continuous measurements of pressure, temperature, conductivity, dissolved oxygen, chlorophyll fluorescence and PAR light, as well as, seawater collection with 5-L Niskin bottles for nutrient analyses (NO_3^- + NO_2^- and $Si(OH)_4$) at ten depths which were variable among cruises. Seawater dissolved inorganic nutrients (NO_3, NH_4, PO_4 and H_4SiO_4) were measured. Water samples were filtered in the field through Whatman 25 mm GF/F pre-combusted filters onto 30 mL polycarbonate vials and frozen until analyzed. Nutrient analyses were performed with colorimetric methods using a Skalar SAN^{plus} segmented-flow nutrient analyzer. NO_3, PO_4 and H_4SiO_4 determinations were based on the World Ocean Circulation Experiment protocols described by Gordon *et al.* (1993). Precision and accuracy were determined by repeated measurements of intermediate calibration standards and a Seawater Certified Reference Material for Nutrients (MOSS-1; National Research Council Canada). Based in the *in situ* fluorescence profiles, seawater was collected within euphotic zone for experimental initial conditions with 5-L Niskin bottles at the Deep Chlorophyll Maximum (DCM) and one level above and one level below the DCM. For each set of experiments, three treatments were prepared in clear polycarbonate bottles (2.0 L) with 100% (undiluted), 30% and 10% of whole seawater (diluted with 0.1-µm filtered seawater) at each depth. All dilution treatments were done filtering directly from the Niskin bottles using a peristaltic pump, silicone tubing and an in-line Suporcap filter capsule that had previously been acid washed (10% trace-metal grade HCl followed by distilled water and seawater rinses). Each bottle was subsampled for FCM analysis to confirm initial concentrations and volume dilutions. The bottles were tightly capped, then placed into net bags and secured with snap hooks to a weighted line hanging from surface floats and attached to a fixed buoy at the depths of initial sample collection. All experiments were started in the early morning and deployed prior to sunrise; the total elapsed time from Niskin sampling to array deployment was about 2.0 h.

2.2. Picoplankton analyses

Samples were taken for FCM analyses at the start and end of each experiment to determine initial abundances to compute carbon biomass and cell-specific growth and grazing loss rates in the dilution incubations. For enumeration of picophytoplankton and heterotrophic bacteria, 2-ml samples were collected, preserved (0.5% paraformaldehyde, final concentration), flash frozen and stored in liquid nitrogen until analysis on the flow cytometer. Samples were then analyzed following the laboratory approach described in detail by Linacre *et al.* (2010a). Cell abundances of heterotrophic bacteria (H-Bact), *Prochlorococcus spp*. (PRO), *Synechococcus spp*. (SYN) and PicoEukaryotes (Pico-Euks) were converted to carbon biomass based on carbon per cell conversions estimated for each category by cruise and depth where the dilution experiments were done. The carbon biomass estimations were computed from Forward Angle Light Scattering (FALS) as a proxy of cell size and, from carbon per cell conversion factors used for coastal waters of the CCS as a starting point (Linacre *et al.*, 2010a).

2.3. Pigment analysis

Seawater samples (1-L) were collected for HPLC pigment analysis at the start and end of each experiment to determine initial and final dilution concentrations to compute pigment-specific phytoplankton growth and grazing loss rates by heterotrophic protists in the dilution incubations. The pigment analysis was performed following the procedures modified by Almazán and García (2008).The samples were filtered through 25-mm GF/F filters and frozen immediately in liquid nitrogen until analysis. Extraction of the pigments was done by mechanical disruption (Bead Beater, Biospec Inc.) of the filters placed in 2-mL capped tubes with 0.5-mm diameter zirconia/glass beads in 1.0-mL of acetone (100%), vortexed at 100 rpm x 10 s and stored at 4°C x 5 min, process repeated 3 times. Cleaning of the samples was done by centrifugation (3000 rpm × 1.5 min x 2 times). A second cleaning of a 500 µL-subsample was done by centrifugation (13,000 rpm × 5 min, 2ºC). Pigment quantification was performed by high performance liquid chromatography (HPLC) as in Van Heukelem and Thomas (2001) modified according to

Colombo-Pallota *et al.* (2006) in the solvent delivery profile (%B, min): 5%, 0 min; 5%, 5 min; 95%, 22 min; 95%, 27 min; 5%, 30 min. The HPLC instrument was a Shimadzu AV-10 series equipped with a Zorbax Eclipse XDBC-8 reverse phase column (150 mm × 4.6 internal diameter, 3.5-μm size particles, 60°C). An absorption detector was set up at 436 nm. Pigments peaks in the chromatograms were identified by comparison of retention times with those of pure standards and extracts prepared from algal cultures of known pigment composition. This protocol achieves baseline separation of monovinyl chlorophyll *a* (MVChl *a*) and divinyl chlorophyll *a* (DVChl *a*), and was calibrated with 16 pigment standards (DHI Inc., Sweden). Standard purity determination and the calibration protocol were as in Wright and Mantoura (1997).

Taxonomic assignments for major pigments found in this study were based on known pigment compositions (Jeffrey and Vesk, 1997; Wright and Jeffrey, 2006). Significant peaks of chlorophyllide *a* (Chlide *a*), a chlorophyll derivate, were seen in the chromatograms during September 2007 and April 2008 cruises, even higher than MVChl *a* peaks, likely due to the damage caused by filtration of numerous and large diatom-chains that were observed microscopically during those seasons (Wright and Mantoura, 1997). Thus, the total chlorophyll *a* (TChl*a*), a proxy of total autotrophic community, was comprised by MVChl *a* + DVChl *a* + Chlide *a* (for Sep'07 and Apr'07 cases), following the approach of Latasa and Bigidare (1998). MVChl *a* is found in all eukaryotic phytoplankton, as well as *Synechococcus*, a prokaryote photosynthetic. DVChl*a* is found only in the *Prochlorococcus*, a photo-prokaryote weakly detected by HPLC analysis. Instead, it was found moderately by FCM analysis. 19'-hexanoyloxyfucoxanthin (Hex-Fuco) and 19'-butanoyloxyfucoxanthin (But-Fuco), are found in both prymnesiophytes and pelagophytes, but Hex-Fuco is found in prymnesiophytes in higher concentrations, while But-Fuco that was weakly detected in the samples, is the dominant accessory pigment of pelagophytes. Fucoxanthin (Fuco) was assumed in this study as mostly indicative of diatoms, although may also be found in prymnesiophytes and pelagophytes. Prasinoxanthin (Pras) is found in some types of prasinophytes and alloxanthin (Allo) is unambiguous markers for cryptophytes. Both

pigments were moderately detected in the samples. Peridinin (PERID) occasionally detected in this study, is found only in dinoflagellates, although it is absent in some taxa, thus likely the contribution from this group was minimum (Jeffrey and Vesk, 1997; Wright and Jeffrey, 2006).

2.4. Microscopical assessments of nano and microplankton

Estimations of carbon biomass for autotrophic and heterotrophic eukaryotes (grazers) divided by size-classes and functional groups were made by digitally enhanced epifluorescence microscopy on two slide preparations, after freezing and storage at -30°C, using the methodology described by Taylor *et al.* (2010). Cells <10 µm in size were enumerated in 50-mL of seawater samples, preserved with paraformaldehyde (0.5% final concentration), stained with proflavin (0.33%w/v) and DAPI (10 mg mL^{-1}) and mounted onto black 0.8-mm black Nuclepore filters. Larger cells were enumerated on 500-mL samples, preserved with 260µL of alkaline Lugol's solution followed by 10 mL of buffered formalin and 500 µL of sodium thiosulfate (modified protocol from Sherr and Sherr, 1993), and then stained with proflavin (0.33% w/v) and DAPI (10 µg mL^{-1}), and mounted onto 8-µm black Nucleopore filters. The slides were imaged and digitized at 630X (50 mL) and 200X (500mL) using a Zeiss AxioVert 200M inverted epifluorescence microscope equipped with an AxioCam HR black/white digital camera (Landry's Lab, SIO-UCSD). Cell biovolume (BV; μm^3) were determined from length (L) and width (W) measurements using the formula for a prolate sphere (BV=0.524 x L x W x H), where cell height (H) on the filters was empirically determined to be 0.5W for naked flagellates (including dinoflagellates). Carbon(C; pg $cell^{-1}$) biomass was computed from BV from the equations of Menden-Deuer and Lessard (2000): $C=0.216 \times BV^{0.939}$ for non-diatoms, and $C=0.288 \times BV^{0.811}$ for diatoms.

Additionally for each cruise, samples (250 mL) were collected, fixed with 5% acid Lugol's solution for biomass estimation of ciliates, which were sub-optimally preserved and rarely counted on the slides. Depending on the abundance found in each

cruise, subsamples of 10mL (for Sep'07 and Apr'08) and 50mL (for Nov'07/08, Jan'08 and Aug'08) were settled in Utermöhl sedimentation chambers for at least 24-h, counted, sorted by size-class in >20 µm and <20 µm, and measured at 400X with a Zeiss AxioVert 200 inverted microscope equipped with an AxioCam HRc color digital camera (Microbiology Department, CICESE). BV (μm^3) estimations were based on measured L and W dimensions and the closest geometric shapes for individual cells (50-100 cells) collected only from the DCM. To convert cell BV estimates to carbon, was used the equation, C (µg) = 0.12 + 0.19 BV (μm^3) for naked ciliates (Putt and Stoecker, 1989) and C (pg) =44.5 + 0.053 lorica volume (μm^3) for loricate ciliates (Verity and Langdon, 1984). The carbon per cell estimations for each cruise were also sorted by size-class in cells >20 and <20 µm, and computed the medians, as representative values of carbon per cell, to be used in the estimations of ciliates carbon biomass for each depth level.

Microzooplankton grazers in this coastal system were mainly represented by mixotrophic ciliates and heterotrophic and mixotrophic flagellates (included dinoflagellates). Thus, to represent the potential grazing contribution of all mixotrophic groups, we added to heterotrophic flagellates (included dinoflagellates) carbon biomass, half of autotrophic flagellates (included dinoflagellates) carbon biomass, assuming that around 50% of this group can be primarily autotrophic but capable of phagotrophy, following the approach done by Landry *et al.* (2010).

2.5. Growth and grazing estimates

Instantaneous rates of phytoplankton growth (µ) and mortality loss (m) by protistan grazers were estimated from dilution incubations according to Landry and Hassett (1982), using an abbreviated 3-treatment dilution protocol (Linacre *et al.*, 2010a). Initial pigment concentrations and population abundances from HPLC and FCM analyses (C_o) were determined for each dilution treatment from measured concentrations in the unfiltered seawater (100%) and the proportion of unfiltered (D_i) seawater in the treatment. Final concentrations (C_t) were measured in each bottle at the end of the 24-h incubations (t). Daily specific-net rates of change (d^{-1}) were determined as k_i =

$\ln(C_t/C_o)/t$, for picoplankton populations and for major phytoplankton groups from changes in abundances and concentration of pigment markers at each dilution, respectively. The typical linear relationship between k_i and D_i allowed estimation of m and μ daily rates from the slope and intercept of the trendline, respectively. Based on SYN, and PRO cell changes were estimate growth and grazing rates for picoautotrophic groups. TChl*a*, Fuco and Hex-Fuco were used to trace total autotrophic, diatoms and prymnesiophytes dynamics, respectively. Unfortunately, the signal from other minor pigments as Allo (cryptophytes), But-Fuco (pelagophytes) and Pras (prasinophytes) were too weak for rate analysis. However, based on the relative concentration of these minor pigments, as well as, on the low ratios lutein to chlorophyll *b* (Lut:Chl*b* = 0-0.04) two pigments also detected in the chromatograms (Wright and Jeffrey, 2006), we assume that prasinophytes dominated most of small green algae group. Thus, Pico-Euks rates flow cytometrically determined were used to estimate the dynamics of Prasinophytes, due to Pico-Euks category likely included some cells > 2μm. Similarly, estimates based on FCM data were done for *Prochlorocccus* due to its unambiguous marker DVChl *a* was detected in extremely low concentrations at initial and final samples. Although autotrophic dinoflagellates we seen microscopically, growth and grazing rates based on its biomarker PERID could not be computed, due to undetectable concentrations at the most of the initial and final samples.

Although the responses between k_i and D_i were linear in the most of experiments, on a few occasions (mainly in the taxon-specific pigments data) were found deviations to the linearity. Sometimes, k_i estimates from the most diluted treatment (10%) were lower than the 30% treatment, typically toward the base of the euphotic zone where the net rates and the population concentrations were both low and difficult to measure, and perhaps a feeding threshold response occurred (Frost, 1972). In these cases, μ and m rates were estimated following the two-treatment dilution approach of Landry *et al.* (2008, 2009), using two equations: $m = (k_d - k)/(1 - 0.30)$ and $\mu = k + m$, where k_d and k are the daily net rates of change in the 30% and undiluted (100%) treatments, respectively. Besides, saturated-increased responses were seen when k_i estimates for

undiluted treatment exceeded the estimates for 30% and 10% treatments, as was described by Texeira and Figueiras (2009). In this case, μ was obtained by linear relationship between 10% and 30% treatments, and m was calculated by the difference between μ and the net growth rate in the undiluted treatment (Texeira and Figueiras, 2009). However, an extreme of this situation was found on two instances, when a positive relationship (against theory) between Di and k_i was displayed. Following the approach of Landry *et al*. (2008) for these cases, μ was set as the measured rate of change in the undiluted bottle, which was assumed to represent a minimal reliable estimate of μ since it involved no experimental manipulation and had a higher measurement signal than the dilute bottle, and, in consequently, m was set as zero. The lack of nutrient-added treatments in the experimental design may mean that the computed rates are underestimates. However, a systematic bias was not observed in comparing the FCM results from 3-bottle *in situ* experiments to several full dilution experiments with nutrient treatments (data not shown) that were done in the laboratory during the same period of this work.

Mortality rates estimates were assumed to be unaffected by changes in phytoplankton physiological condition during the experimental incubations. However, pigment-specific phytoplankton growth rate estimates could be affected by physiological adjustments. We attempted to correct the growth rates based on changes in pigment concentrations using an approximation modified from Gutiérrez *et al.* (2010) for the photoacclimation response during the incubation. Based FCM measurements for Pico-Euks, as a proxy of the eukaryotic phytoplankton community, we used the ratios of red fluorescence (F1) to forward scatter (FS) per cell (a proxy for the Chl*a*/C ratio), to reflect the proportion of change in pigment concentration due to changes in pigment content not related to changes in phytoplankton carbon biomass (i.e. by changes on light conditions). We used the change in F1/FS from initial and final whole seawater measurements to compute daily instantaneous rates of change for the 24-h (t) incubations as a correction factor, i.e., $C_{factor}=\ln[(F1/FS)_f/(F1/FS)_i]/t$. These computations were applied to μ based on measured TChl*a* changes, as a correction factor for pigment photo-adaptation for total

autotrophic community, as well as, to μ based on measured of each pigment-specific phytoplankton changes to account for photoacclimation in diatoms (μ Fuco) and prymnesiophytes (μ Hex-Fuco). Thus, the corrected growth rates were calculated as, $\mu_{TChl\textit{a}/pigment\text{-}specific} - C_{factor}$.

2.6. Production and grazing losses estimates

Experimental values of μ and m were combined with carbon biomass estimates to compute total autotrophic community (TChl*a* based) and taxon-specific (cell and pigment based) rates of production and grazing losses according to Landry *et al.* (2000). Production estimates (PP, μg C L^{-1} d^{-1}) and the biomass consumption by protistan grazers (G, μg C L^{-1} d^{-1}) were calculated as:

$$PP = \mu (C_o [e^{(\mu-m)\, t} -1]/ (\mu-m)\, t), \text{ and}$$

$$G = m (C_o [e^{(\mu-m)\, t} -1]/ (\mu-m)\, t)$$

where C_o is initial carbon biomass expressed in carbon term (μg C L^{-1}) and t=time (~24-h).

Particularly, production and grazing losses rates for diatoms, prymnesiophytes, *Synechoccoccus* and *Proclorococcus* were estimated using their C-based standing stocks and specific-rates based on Fuco, Hex-Fuco pigments, SYN and PRO cell abundances, respectively. To determine PP and G for prasinophytes was assumed that this category and also pelagophytes were the major components of autotrophic flagellates (A-Flag) determined microscopically. Then, based on their relative specific-pigment contributions (But-Fuco for pelagophytes and Pras for prasinophytes) to total A-Flag carbon biomass and, on Pico-Euks rates estimated from FCM analysis, PP and G for prasinophytes were computed. In addition, production and grazing losses rates for other autotrophic eukaryotes (Other A-Euks) that cannot be attributed to a taxon-specific phytoplankton group (included mostly autotrophic dinoflagellates), were computed from rate estimates

based on Chl*a* (Chl*a*=MVChl*a*+Chlide*a*) and total biomass for all Chl*a* containing autotrophs (=Total Biomass – PRO biomass), following the approach used by Landry *et al.* (2010). After total production of Chl*a* taxa was determined, the production rates for diatoms, prymnesiophytes, prasinophytes and SYN were subtracted to yield the contribution of Other A-Euks by difference (Landry *et al.*, 2010).

Therefore, the ratios of grazing losses to production rates (G:PP=m:μ) were estimated as a measure of daily protistan grazing impact on the production of phytoplankton community (TChl*a* based) and of taxon-specific phytoplankton groups (FCM and specific-pigment based). For average-estimates purposes the G: PP ratios for each cruise and depth level were arctangent transformed as in Calbet and Landry (2004). This has the effect of reducing the impact of large ratios (i.e., large G relative to PP) on computed values and making the data distribution more normal.

2.7. ^{14}C-uptake primary production

As a basis of comparison to population production estimates from dilution experiments, we also measured primary productivity by the standard ^{14}C-bicarbonate-uptake technique (Steemann Nielsen, 1952). The ^{14}C methods and details results were presented in Linacre *et al.* (2010a). Seawater samples collected on the same hydrocast as dilution experiments were screened through a 150-μm net to exclude macrozooplankton, and inoculated with ~5 μCi $NaH^{14}CO_3$ in 250-ml polycarbonate bottles. Replicated light and dark bottles were placed into net bags on the array line together with dilution bottles and deployed at the initial collection depth for 24-h. After incubation, the labeled particulate matter was filtered onto 0.45-μm pore Millipore HA filters. To purge $NaH^{14}CO_3$ that was not fixed by photosynthesis, filters were placed in 20-ml scintillation vials with 0.5 ml of 10% HCl for 3 hours. Scintillation cocktail (10 ml Ecolite) was added to each vial, and the radioactivity was determined with a Beckman LS-6500 scintillation counter. Primary production rates were calculated from these radioactivity counts according to Parsons *et al.* (Parsons *et al.*, 1984), subtracting the carbon uptake of the dark bottles.

3. - RESULTS

3.1. Environmental conditions

Seasonal and interannual variability in the physical and chemical conditions at ENSENADA station are described in detail by Linacre *et al.* (2010b). An historical analysis on the 11 years oceanographic data of northern coastal waters off WBC, have revealed a marked seasonal variability in the thermohaline conditions associated with fluctuations in the surface flow of the equatorward California Current and the subsurface flow of the poleward California Undercurrent, as well as with coastal upwelling events whose magnitude and frequency increase towards spring–summer. Also, interannual variability has been related to warm and/or cold ENSO phases that modify the characteristics of the water column in this coastal region (Linacre *et al*, 2010b).

Six-hourly (Fig. 2a) and monthly (Fig. 2b) of Bakun Upwelling Indices at 31.6°N 116.8°W were directly downloaded from NOAA/PFEL webpage, and illustrated to represent the temporal variability of upwelling events at ENSENADA station for the sampling period (Sep'07- Nov'08). No six-hourly data was recorded for October and November 2007 (Fig. 2a). However, the monthly upwelling index was obtained for those months also obtained from NOAA/PFEL webpage (Fig. 2b). In figure 2b, the months when the dilution experiments were done at ENSENADA station were emphasized as light-grey bars. Also, in figure 2a was highlighted in enlarged gray circles the daily average of upwelling index corresponding to the incubation's day. Generally the values were neutral to positive in this region (excepting some a few values in Jan'08), indicating that the upwelling events are a semi-permanent feature in this region. The six-hourly Upwelling Index values oscillated from 0 to >1,000 m^3 s^{-1} per 100 m of coastline. The highest index value (518 m^3 s^{-1} per 100 m of coastline) occurred during the Apr'08 experiments, while the lowest value (17 m^3 s^{-1} per 100 m of coastline) was found during Nov'08. We can also assume that for Nov'07 the values were low, as was indicated by its monthly index (56 m^3 s^{-1} per 100 m of coastline; Fig. 2b).

Water column physical and chemical conditions at ENSENADA station are displayed in figure 3. The most contrasting changes in density occurred in the layer 2-35 m of depth, where the dilution where done, as was indicated by the light-grey area. The vertical distributions of seawater density (σ_t, kg m^{-3}) showed a strong and marked pycnocline around 10 m during warm periods (Sep'07 and Aug'08), in contrast to a more mixed water column during cold periods (Nov'07-08, Jan'08 and Apr'08) (Fig. 3a). The density values for all periods ranged between 24.5 to > 25.7 kg m^{-3} throughout 0-100 m of depth, being remarkable the anomalous denser waters found in April 2008, which were associated to new-upwelled cold and salty seawater. In addition, the normal seasonal intensification of upwelling was enhanced in our station during spring 2008 by La Niña condition reported from early 2007 until early summer 2008 in the northern region off WBC (McClatchie *et al.*, 2008; Durazo, 2009). This cold event was detected at ENSENADA station, trough the presence of seawater at euphotic zone with high salinity (~33.8), low temperature (~12°C) (consequently high density values), as well as waters depleted in dissolved oxygen (dO_2 ~150 µmol L^{-1}) but rich in dissolved inorganic carbon (DIC ~2,115 µmol kg^{-1}) (Linacre *et al.*, 2010b).

The figure 3b showed highest values *in situ* fluorescence (µg *Chl* L^{-1}) in the first 30 m of the water column during all periods, ranging from 0 to >16 µg *Chl* L^{-1}. The DCM was in general above 15 m of depth, except for Jan'08, when it was notably deeper (~20 m), likely associated to small-size autotrophic cells. The most striking higher concentrations (>16 µg *Chl* L^{-1}), were found above 15 m of depth in April 2008 when a dense layer of cells was formed at euphotic zone; while the lowest values (< 2 µg *Chl* L^{-1}) were observed in Nov'07, when the fluorescence profile was homogeneous throughout water column (Fig. 3b). The depth of the euphotic zone is defined here by 0.1% surface light penetration (%I_o relative to the average measurement for the first meter) and it varied from 37 m of depth in Jan'08 to 63 m of depth in Nov'07.

The profiles of some nutrients (NO_3^- + NO_2^- and silicates) required for phytoplankton growth, are displayed in figures 3c and 3d, and they was also reported in Linacre *et al.* (2010). Theirs vertical distributions are only shown for the first 40 m of the

water column, the layer where the dilution experiments where done in all cruises and where the most contrasting changes of nutrients occurred. Overall, the first 10 m of column water showed low concentrations (~1 µM of NO_3^- + NO_2^- and < 5 µM of silicate) likely due to phytoplankton uptake, while at deeper levels the values were higher (> 6 µM of NO_3^- + NO_2^- and silicate) associated to the input into the region of water masses rich in nutrients from equatorial origin. Despite of the depth euphotic layer variability among cruises, it was always deeper than the base of pycnocline, allowing upwelled water with high nutrients to penetrate into euphotic depths during all cruises (Figs. 3a, 3c and 3d). Because of high winds, station operations were abandoned in April 2008 before the hydrographic cast for nutrient sampling. Thus, the nutrients values showed in figure 3c and 3d were collected 5 days later. In spite of this difference in the time sampling, NO_3^- + NO_2^- and silicates showed during Apr'08 a notable decreasing above 15 m depth, coincidently with the highest fluorescence values (>16 µg *Chl* L^{-1}) detected 5 days before, suggesting a strong phytoplankton uptake during this season.

3.2. Autotrophic and heterotrophic carbon biomasses

Total autotrophic (Auto-C), heterotrophic (Hetero-C) carbon biomasses and theirs relative contributions by size-classes are shown in figure 4. Total plankton carbon biomass for cells <200µm reached the highest carbon biomass values (>120 µgC L^{-1}) in Sep'07 and Apr'08, while the lowest (<50 µgC L^{-1}) in November's cruises (Fig.4a). Considering all the samplings, the Auto-C contribution to total carbon biomass was 48%, while the Hetero-C fraction was slightly higher (52%). However, large proportion of Hetero-C is attributed to heterotrophic bacteria (H-Bact, Table I). Thus, if they are removed from Hetero-C group, the fraction of this component would reduce to 22%, while the Auto-C contribution would increase to 78% of total carbon biomass.

Overall, the major contribution to total Auto-C and Hetero-C were small cells (pico and nanoplankton) in all cruises and depths, except during April 2008, when total carbon was mostly due to nano and micro-sized cells (Fig. 4b and c). Particularly, A-Pico biomass was mostly dominated by *Synechococcus* (SYN) cells, while H-Pico was

comprised totally by H-Bac cells (Table I). Estimates of picoplankton carbon biomass ranged from 0.3 to 15 μg C L^{-1} for A-Pico (PRO and SYN) and from 9 to 70 μg C L^{-1} for H-Bact. A-Nano biomass was mainly represented by autotrophic nanoflagellates (A-Flag) and small diatoms (<20μm) chains-forming especially during Sep'07 and Apr'08, while H-Nano biomass by heterotrophic nanoflagellates (H-Flag) and some small heterotrophic dinoflagellates (H-Dino<20μm). Estimates of nanoplankton carbon biomass ranged from 1.6 to 58 μg C L^{-1} for A-Nano and from 0.4 to 7 μg C L^{-1} for H-Nano. Auto-C for micro-sized cells was dominated by diatoms and dinoflagellates, whereas Hetero-C was represented mainly by ciliates and also, H-Dino especially in Aug'08 (Table I). Estimates of microplankton carbon biomass ranged from 0.2 to 128 μg C L^{-1} for A-Micro and from 0.3 to 24 μg C L^{-1} for H-Micro.

For most of the sampling periods, Hetero-C: Auto-C ratios were higher than 1, except during Apr'08 when a more autotrophic trophic system (ratios <1) was found at ENSENADA station (Fig. 5). It also was noted by a positive and significant relationship between initial autotrophic and the heterotrophic carbon biomass (R^2 = 0.76, $p<0.0001$) found for all data excluding Apr'08 (data not shown).

A similar tendency is shown between Auto-C and concentrations of total chlorophyll *a* (TChl*a*) throughout the study period (Fig 6a). The Auto-C and TChl*a* values were highly variable in the euphotic zone, ranging from 3 to 186 μgC L^{-1} and from 0.4 to 12.5 μg Chl*a* L^{-1}, respectively. Extraordinary bloom levels of Auto-C and TChl*a* were found in Apr'08 associated to strong upwelling and La Niña conditions reported during this season at ENSENADA station (Fig. 6a). Positive relationship between all Auto-C and TChl*a* values was found (Fig. 6b); however this association was strong and significant (R^2 = 0.74, $p<0.0001$), only when Apr'08 data was excluded (Fig. 6b inset). From the slope of this significant correlation a C: TChl*a* ratio = 12.83 for all periods was obtained. This value is close to the average value of 14.83± 7.99 computed from C: TChl*a* ratios based on each cruise and depth levels (Fig. 6c).

3.3. Experimental rate estimates

Autotrophic community (TChl*a*) and major group estimates of growth (μ) and grazing mortality (m) rates were computed from the measured net changes in TChl*a* (Total Auto), cell carbon biomass of picoplankton and taxon-specific pigments (Fig. 7). Significant growth and grazing rates (i.e., > 0) for TChl*a* ranged from 0.24 to 1.62 d^{-1}, and from 0.34 to 2.64 d^{-1}, respectively. Additionally, significant estimates for major autotrophic groups showed similar tendency to total community in some cruises and depths. Growth rates for diatoms, *Synechococcus* and Prasinophytes (Pico-Euks based) varied from 0.06 to 2.05 d^{-1}, 0.05 to 2.11 d^{-1} and 0.11 to 1.51 d^{-1}, respectively. Also, protistan grazing rates for the same functional groups ranged from 0.16 to 2.77 d^{-1}, 0.16 to 1.36 d^{-1} and 0.13 to 1.21 d^{-1}, respectively (Fig. 7).

Overall, higher growth rates (μ >1 d^{-1}) of TChl*a* were found in the DCM, except in Jan'08 when a maximum μ value was found at 30 m of depth, i.e., below the maximum concentration of fluorescence measured *in situ* during this cruise (Figs. 7a and 3b). The growing of autotrophic cells toward low light levels (<1% I_o, Table I) in Jan'08, was also observed for diatoms and prasinophytes (Fig. 7b and 7d), as well as, moderately for *Synechococcus* (Fig. 7c), likely due to high nutrient concentrations in this depth (Fig. 3c and d). Similar μ and m increase toward deeper waters was found in Aug'08 for *Synechococcus* and prasinophytes (Figs. 7c and d). This behavior was similar for other small cells, as *Prochlorocccus* or H-Bact (data not shown). In general the grazing was lower than growth rates for all cells. However, in some cruises and depth levels the instantaneous grazing rates showed higher values than growth rates. Notable was the circumstance observed in Sep'07 at 7 m of depth, when a m value > 2.5 d^{-1} was detected for TChl*a* and diatoms (7a and b).

3.4. Carbon biomass production - loss estimates

Primary carbon biomass production (PP) and losses by protistan consumption (G) based on TChl*a* growth (μ) and grazing (m) estimates and, C: TChl*a* ratios for total

phytoplankton community (Total Auto-C) measured at each depth level by cruise had a marked seasonal variability throughout the euphotic zone at ENSENADA station (Fig. 8a). Significant (i.e., > 0) daily PP rates ranged from 3 to 272 µg C L^{-1} d^{-1} and, G estimates from 2 to 77 µg C L^{-1} d^{-1}. Highest biomass production and grazing losses were found in Sep'07 and Apr'08 within the mixed layer, while lowest during Jan'08 (first 20 m of depth) and Nov'07 cruises. Generally, protistan consumption was lower than primary production biomass, thus net production (=PP-G) was mostly positive in this coastal system (Fig. 8a). Also, production rates estimated from the dilution experiments (TChl*a* based) showed similar tendency with the standard measurements of primary production done simultaneously *in situ* by net ^{14}C- uptake (Fig.8a). Overall these two methods was significantly associated (R^2=0.51, p<0.0001) and ^{14}C-uptake primary production measurements were variable among seasons and depth levels, ranging from 0.24 to 217 µg C L^{-1} d^{-1}.

Similarly, taxon-specific PP and G, estimated from measured µ and m rates for cell and specific-pigment and microscopically estimated specific-carbon biomasses, registered a contribution seasonally relative to major autotrophic functional groups along the sampling period (Figs. 8b-8e). The most fraction of community PP and G was due to diatoms (mostly nano-sized cells) and Other A-Euks (Fig. 8b). Although A-Dino production and grazing losses cannot be estimated directly from its rates (PERID concentrations scarcely detected by HPLC), according to A-Dino contribution to total Auto-C biomass we can assume that a considerable fraction of A-Dino is included as part of Other A-Euks daily rates. Contributions of those functional groups were seasonally marked. Mostly in Apr'08 and also in Sep'07, higher not only carbon production but also losses by grazing were observed for diatoms and Other A-Euks (Fig. 8b), likely favored by upwelling conditions in the euphotic zone during those seasons (Fig. 2). Although PP and G attributed to small-sized cells had a more moderate contribution to total community, it was emphasized in other than Apr'08 samplings (Figs. 8c, d and e). *Synechococcus* and Prasinophytes followed the same tendency observed for total Auto-C in Sep'07; highest PP coupled with highest G estimates were found in the first 10m depth

during this cruise. Remarkable high grazing losses were found during cold seasons (Novs'07/08 and Jan'08), being even higher than production carbon rate, as was seen mainly in Jan'08 (Figs. 8c and d). Minor autotrophic groups as Prymnesiophytes and *Prochlorococcus* contributed modestly to total phytoplankton rates; however striking high PP and G rates were found in Aug'08 and mostly in Nov'08 cruises in these groups (Fig. 8e).

3.5. Grazing impact assessments

With the exception of a pair of occasions (Sep'07 and Aug'08) when instantaneous growth and/or grazing rate for TChl*a* and consequently PP and or G could not be estimated from the dilutions experiments, the microzooplankton grazing impact over to daily total primary production (Auto-C Impact), showed a substantial protistan removal (G close or higher to PP) on autotrophic cells in this coastal station throughout the year (Fig 9). Overall, G: PP averaged (±SD) 0.91± 0.31 for total Auto-C (n = 17; these and other G: PP data were arctangent transformed, averaged , then tangent back-converted, as in Calbet and Landry, 2004). This result indicates that protistan grazers consumed more than two-thirds of phytoplankton production in this coastal area. Higher predatory pressure was mostly observed during early autumn-winter cruises (Sep'07-Jan'08) and at DCM level in Apr'08, when G: PP ratios > 1 (=G> PP) were found. During more eutrophic periods (Sep'07 and Apr'08) the high impact on autotrophic community was mostly related with large consumers, mainly mixotrophic ciliates >20 µm (Micro_CIL), while in winter cruises (Nov'07/08, Jan'08), significant impact (G>PP) was associated with not only large consumers but also small (<20 µm) mixotrophic ciliates (Nano_CIL) and flagellates (Nano_Flag), including dinoflagellates (Fig. 9a).

Similar grazing impact tendency observed for total Auto-C was found for some major phytoplankton groups (Fig. 9b). On average for whole study period, taxon-specific percentage losses of primary production by microzooplankton grazing were highest for prasinophytes (Pras =96 ± 25%), followed by *Synechococcus* (SYN = 93± 23%), and diatoms (75± 43%). Highest impact value on diatoms was observed in Apr'08 at 10 m of

depth when large mixotrophic ciliates (>20µm) reached a high biomass (21 µgC L^{-1}). Otherwise, small mixotrophic ciliates and flagellates (included dinoflagellates) seem to prefer pico/nano-sized preys. In Jan'08, the highest impact on prasinophytes (Pras) observed at 20 m depth can be was associated with the dominance of small mixotrophic ciliates and flagellates. Similarly, *Synechococcus* were mostly impacted on periods when small consumer comprised an important fraction of total microzooplankton group, as was seen in Jan'08 (Fig. 9b).

4. - DISCUSSION

During six contrasting periods at a coastal site (ENSENADA station) which is representative of physical and chemical conditions for the northern coastal region off WBC (Linacre *et al.* 2010b), we caught different trophic scenarios that were modulated by changing environmental circumstances, representing thus an advance for studies of carbon flux dynamics in this region.

The upwelling events that are more frequent and stronger during spring-summer in BC region (Durazo *et al.*, 2010), were the most important environmental feature of this coastal station, being associated with the high nutrient delivery into the euphotic zone and consequently, with the increase of primary production. Based on similar results found with dilution-based estimates of autotrophic production and, with ^{14}C estimates of primary production that were reported previously for the same coastal area (Linacre *et al.*, 2010a), it were defined two more productive periods at ENSENADA station: Sep'07 and Apr'07 (Fig. 8a). During those samplings, 6-hourly upwelling indices showed strong increases during (Apr'08) or a few days before (Sep'07) the dilution incubations were conducted (Fig. 2a), bringing nutrients from deeper waters that are subsequently incorporated into phytoplankton. In regards to, in Apr'08 no nutrients were measured at the same time when dilution experiments were done, so we assumed a high nutrient concentrations in this site by the presence of saltier and colder (i.e., denser) waters at

surface depth layers (Fig. 3a). However, measurements done 5 days later, showed undetectable concentrations of nutrients (NO_3^- + NO_2^- and $Si(OH)_4$) in the first 10 m depth, evidencing strong phytoplankton uptake in the euphotic layer after a period of favorable environmental conditions (high nutrient input) to phytoplankton growth (Figs. 3b, c and d). Between these two eutrophic conditions seem to be that the contrasting stratification/mixed conditions among other factors played an important role in the autotrophic community structure. While turbulence and the upward displacement of water associated with upwelling (as was seen in Apr'08) would help to increase the residence time of large primary producers in the euphotic layer (Rodriguez *et al.*, 2001), a more stratified water column would increase the sinking of larger cells, keeping mainly smaller within euphotic layer (as was seen in Sep'07). It could explain the largest diatoms observed microscopically (some cells > 50 µm) in the euphotic layer of our station during Apr'08, in contrast to smaller mainly represented by SYN and Prasinophytes during Sep'07 (Figs. 3a, 4b and Table I).

Additionally, the most part of our samplings were made during La Niña condition reported from early 2007 until early summer 2008 in the northern region off WBC (McClatchie *et al.*, 2008; Durazo, 2009). This cold ENSO phase brings the pycnocline and nutricline closer to the ocean surface, allowing an easier entrainment into upper euphotic zone by upwelling favorable winds. In fact, during spring of 2008 this cold event was strongly detected at ENSENADA station, when anomalous colder and salty seawater as well as, poor in dissolved oxygen and rich in dissolved inorganic carbon was detected in the first 30 m of depth (Linacre *et al*, 2010b). Thus, the normal seasonality of phytoplankton community was especially intensified in Apr'08 in terms of autotrophic biomass (Fig. 6a), community structure and production (Fig. 8a).

4.1. Carbon Production versus Carbon Losses by Grazing

Under the seasonal and interannual variability found in the physical-chemical characteristics of water column at ENSENADA station and that was widely described in

Linacre *et al.* (2010b), phytoplankton community and its major functional groups displayed a spatial-temporal dynamics variable in their carbon fluxes based on production and consumption (losses) by microzooplankton grazing estimates. Overall, the mean production estimated for whole autotrophic populations (TChl*a* based) was closer to mean carbon losses by daily microzooplankton grazing (PP= 39 ± 60 µg C L^{-1} d^{-1} and G= 26 ± 26 µg C L^{-1} d^{-1}), yielding in a high microzooplankton grazing impact (overall mean 91 ± 31%) exerted on daily production of phytoplankton community. These results indicated that protistan grazers consumed more than two-thirds of total phytoplankton production in this coastal area, a higher fraction than global estimates done for temperate (61-69%) and coastal systems (57-60%) (Calbet and Landry, 2004). However, our estimates evidenced a close coupling between daily production and consumption of phytoplankton in this site, as has been previously reported for other coastal systems (García-Pámanes and Lara-Lara, J.R., 2001; Strom *et al.*, 2001; McMannus *et al.*, 2007; Gutiérrez *et al.*, 2010; Texeira *et al.*, 2010). Also, the seasonal variability of the grazing impact measured in this study is in agreement with other results found at mixed-layer of upwelling regions with contrasting trophic conditions along the year (Neuer and Cowles, 1994; Böttjer and Morales, 2005; Landry *et al.*, 2009; Texeira *et al.*, 2010). It was related to temporal fluctuations in standing stock and rates of autotrophic populations that contributed relatively to total pool of carbon biomass and production.

Picoplankton autotrophic and heterotrophic comprised an important component of community during the study period at this coastal station (Fig.4b and c), as had been reported previously for this same coastal site (Linacre *et al.*, 2010a). Overall (including Apr'08), pico-sized cells contributed to total autotrophic and of heterotrophic carbon biomass about 19% and 74%, respectively (Fig. 4a and b). Their main autotrophic populations (PRO and SYN) represented only 12% of total autotrophic production and 15% of total autotrophic losses throughout several light and nutrients conditions found within the euphotic zone of this coastal site. Thus, a close net balance between growth and grazing losses processes was found for this size-category, leading to a high grazing

impact by micrograzers (Figs. 8c, 8e and 9b). *Synechococcus* for example showed along whole period G: PP ratios close to 1 and sometimes higher, evidencing the strong top-down control (overall mean >90% of daily PP) exerted on this population (Fig. 9b). This dynamics was also reported for microbial community from equatorial Pacific waters, where particularly a strong coupling between growth and grazing rates was found for *Prochlorococcus* populations throughout euphotic zone (Landry *et al.* 2010). Also, in other coastal systems coupling between picoplancton growth and grazing rates has been reported (Putland, 2000; Strom *et al.*, 2001; Worden *et al.*, 2004; Strom *et al.*, 2007; Chen *et al.*, 2009). For example, for coastal waters of the Southern California Bight, *Prochlorococcus* growth and mortality rates were nearly balanced, as well as, carbon consumed: produced ratios for A-Pico populations were seasonally variable, ranging from 23 to >100% per day (Worden *et al.*, 2004). Similarly high percentages of A-Pico production grazed per day (83 ± 57% for *Prochlorococcus* and 61 ± 25% for *Synechococcus*) have been reported for the western South China Sea (Chen *et al.*, 2009). In addition, prasinophytes have been reported for California Current (CC) waters by microscopic (Thomsen and Buck, 1998) and molecular analysis (Worden *et al.*, 2004; Worden, 2006) as an important group of small green algae. Some forms of this group belong to pico-sized cells like the picoprasinophyte *Ostreococcus* reported for CC coastal waters and, they can contribute significantly to biomass, carbon production, and trophic transport of carbon (Worden *et al.*, 2004). In our case, Prasinophytes estimates were based on rates computed from Pico-Euks FCM data due to this category included some cells that are larger than formal 2-µ diameter cut-off. Thus, some of the balance attributed strictly to prokaryotic cells was also due to pico and nanoprasinophytes, as was seen by the general association between C-production and C-losses by grazing for this small-sized group (Fig. 8d).

On the other hand, diatoms and other autotrophic-eukaryotes (assumed mostly autotrophic dinoflagellates) represented by nano and micro-sized cells, showed a marked seasonal contrast modulated by the physical and chemical characteristics found in the euphotic zone of this coastal site. Overall, they showed a major contribution than

picoplankton populations to total autotrophic carbon biomass (41% for diatoms and 24% for A-Dino), primary production (38% for diatoms and 45% for Other A-Euks) and grazing losses (31% for diatoms and 47% for Other A-Euks), as have been reported for other coastal upwelling systems (Vargas and González, 2004; Vargas *et al.*, 2007; Gutiérrez *et al.*, 2010; Texeira *et al.*, 2010). Most part of this contribution occurred in Apr'08, associated with the intrusion into euphotic layer of rich-nutrients waters that produced exceptionally high carbon biomass accumulation (PP >100 µg C L^{-1} d^{-1}) in this coastal site (Fig. 8b). Specifically, diatoms relative to small autotrophic cells, had lower predatory pressure (overall mean= 75± 43%) in this zone, leaving a fraction (25%) of diatom production that escapes consumption by microzooplankton. Then, it could be lost to direct sinking from the euphotic zone, consumed by mesozooplankton and exported by lateral advection, or even, attacked by viral infection and/or cellular death, although maybe these last loss-processes would be undetected with our experimental design and incubations technique used in our study.

Besides other than microzooplankton grazing loss processes, the vertical flux of biogenic carbon derive from fecal pellets could have a high contribution to carbon exported, in comparison to a small fraction of PP originated from the aggregation of diatoms into large, rapidly sinking particles, as was reported at the coastal upwelling system of Humboldt Current (Vargas *et al.*, 2007). Similarly, it could likely be the case for ENSENADA station during Apr'08, when anomalous denser water (Fig. 3a), could be a physical mechanism that kept large and heavy diatoms (some of them >50 µm) into the euphotic zone, decreasing its sinking far-away favorable-light conditions to grow. It is supported by results from an empirical model that indicate an increase of relative proportion of large cells with the upward velocity magnitude (Rodriguez *et al.*, 2001). Besides, excepting Apr'08 when the nutrients were sampled 5 days later, the relative high nutrients concentrations (>3µm NO_3^- + NO_2^- and $Si(OH)_4$) in the euphotic zone, could be indicating the dominance of healthy cells with few probabilities for the aggregates formation (Landry *et al.*, 2009). Other option is that mesozooplankton consumption would be high in our zone. Indeed, unexpectedly high and variable mesozooplankton

grazing rates were observed at nearshore waters of upwelling system off Southern California, which leaded important temporal fluctuations in phytoplankton dynamics (Landry *et al.*, 2009). However, estimates of overall impact of mesozooplankton across a wide spectrum of marine ecosystems revealed that the average percentage of PP consumed daily for this group is only 22.6%, which decreases exponentially with increasing productivity (Calbet, 2001). Some examples are found for highly productive coastal upwelling regions of the Humboldt Current System, where there have been reported that only 1-6% PP is consumed per day by mesozooplankton populations (Vargas *et al.*, 2007), or specifically small copepods and appendicularians can be removed only 0.6 to 5%, and 0.08 to 0.6% of PP per day, respectively (Vargas and González, 2004). Similarly, in an upwelling filament off Galicia, based on a carbon flux model elaborated with field measurements, Halvorsen *et al.* (2001) concluded that heterotrophic nanoflagellates were the most important group of carbon transference by grazing in relation to other microbial and mesozooplankton components. Even under highly concentrated phytoplankton blooms (harmful algal blooms, HABs) that are frequent in some coastal systems, it has been observed a low grazing impact by mesozooplankton components as copepods, in contrast to high grazing by microzooplankton components, which can be a substantial loss-factor for HABs (Calbet *et al.*, 2003). It is also possible that a fraction of diatoms produced in Apr'08 had been moved offshore by upwelling-induced advection, a process that have been reported as dominant over vertical export flux, local grazing and flux of zooplankton-derived detritus in the upwelling system off Monterey Bay, California (Oliviere and Chavez, 2000). However, independently of other losses that were not estimated in this study, our results indicated that microzooplankton grazing was the most significant process that controlled small and large autotrophic fraction of primary production in our coastal site.

In consequence, the results discussed above suggest that large fraction of carbon produced by several autotrophic functional groups into euphotic zone would be efficiently recycled within upper layer mainly by microzooplankton consumption and likely, in minor proportion by mesozooplankton feeding, leaving thus, only a minimum

fraction that would be exported by passive (sinking/fecal pellets) and/or active (diel vertical migration of zooplankton; Hays *et al.*, 2001) carbon flux into the ocean interior.

4.2. Trophic status and plankton community structure

It is also important to consider in the estimations of carbon fluxes produced and consumed by several components of pelagic food web, the trophic status and community structure of these upwelling coastal ecosystems. Overall, plankton biomass (< 200 µm) in this study showed a close balance between autotrophic and heterotrophic components (Auto-C mean=33 ± 42 µgC L^{-1}, Hetero-C mean=37 ± 21 µgC L^{-1}; Fig. 4a). However, seasonally these ratios were unbalanced, as was observed by the dominance of heterotrophic (H-Bact+H-Flag+H-Dino+CIL) over autotrophic components (Hetero:Auto>1) during all periods, except in Apr'08 when the carbon biomass was mainly comprised by chain-forming diatoms and large single-celled forms (Fig. 5, Table I). This seasonal change in the trophic status observed was mainly modulated by intensified upwelling conditions that were reported in our site in Apr'08 (Linacre *et al.*, 2010b). Our results were agreement with estimations done by Gasol *et al.* (1997) for open ocean and coastal communities that indicated declined trends of heterotrophic: autotrophic ratios with increased phytoplankton biomass and primary production. Similar results have been reported for other coastal upwelling ecosystems, where the major variations in plankton biomass are due to seasonal variations in autotrophic biomass that contribute significantly during upwelling periods (Vargas *et al.*, 2007; Texeira *et al.*, 2010).

Size-structure of the community is other important factor to analyze in the carbon flux dynamics in pelagic food web. In general, the autotrophic carbon biomass to total chlorophyll *a* ratios (C:TChl*a*) used for the estimations of total carbon production and losses in our coastal site, showed constant values throughout the periods and depths, ranging around a mean ratio of 15± 8 when it was calculated for each particular experiment done at specific depth and cruise (Obayashi and Tanoue, 2002, Gutiérrez *et al.*, 2010), or 13±2 when was used the slope of the relation between carbon and TChl*a*

(Latasa *et al.*, 2005), excluding the most outlier points corresponding to Apr'08 data (Figs. 6b and c). Both means were similar between them, and fall within the ranges reported for coastal waters with relative high nutrients concentrations in the euphotic layer and similar light conditions (Eppley, 1968; Arin *et al.*, 2002; Gutiérrez *et al.*, 2010). According to Eppley (1968) in his work carried out in coastal waters off La Jolla, California, low ratios (mean=30) are attributed to nutrient-rich waters (>1µM) while higher (mean=90) to nutrient-depleted or high light intensities surface waters. C:Chl*a* ratios have also been related directly to the cell size, with a tendency to increase with size-fraction (Arin *et al.*, 2002). Remarkable was the highest C:TChl*a* ratio found in Apr'08 at 15 m (Fig. 6c), likely related with the high contribution to total autotrophic biomass of large autotrophic dinoflagellates (>50% of cells>20µm) during this period.

Additionally, composition of plankton community (< 200 µm) not only of the main autotrophic groups but also the microzooplankton that consume actively on phytoplankton community should be also considered in carbon transfer through the pelagic food web. From many works found in the literature about microzooplankton feeding on phytoplankton community, it is doubtless the high importance that microzooplankton has as key component of marine foodwebs due to strong impact exerted by this group on primary production in several ecosystems (Calbet and Landry, 2004). However, the trophic role of the major consumers (nano and micro-sized grazers) of microzooplankton group has been scarcely recognized (Calbet, 2008). Microzooplakton composition has apparently been related to the productivity of the ecosystems (Calbet, 2008). Pico and nano-sized grazers are the main consumers of phytoplankton in oligotrophic waters (Calbet *et al.*, 2001, 2008; Sherr and Sherr, 2002), while heterotrophic and mixotrophic dinoflagellates and ciliates are potential candidates in productive waters, as have been seen in several upwelling coastal systems (Neuer and Cowles, 1994; Aberle *et al.*, 2007; Sherr and Sherr *et al.*, 2007; Texeira *et al.*, 2010). Higher phytoplankton community grazing impact where found during more productive periods (Sep'07 and Apr'08) and during Jan'08, when potential grazers were relatively more abundant in this ecosystem. This predatory pressure seems to be differential among

the major autotrophic groups and also, relative to consumer biomass that predominates in this coastal site under contrasting oceanographic conditions recorded along the year (Fig. 9). Thus, it is observed for example a high top-down control on diatom production when ciliates contributed significantly to total grazers biomass, especially in Apr'08 at 10 m depth, when the highest diatom impact (G: PP=7) was found coincidently with a high carbon biomass (21µgC L^{-1}) of large ciliates (cells >20µm). It is important to remark here, that many marine planktonic ciliates are mixotrophic, i.e., combine phagotrophy and phototrophy as feeding strategies (Stoecker, 1998). In coastal surface waters of temperate systems more than 50% of the ciliates (mostly oligotrich) have been reported as mixotrophic (Stoecker *et al.*, 1989). Thus, large fraction of high ciliate biomass observed in our coastal site during Apr'08, may be associated with ciliates phototrophic, which likely are growing sustained by the input into euphotic layer of nutrient-rich waters by intensified upwelling events. Similar feeding combination has been identified for the flagellates, including dinoflagellates (Sherr and Sherr, 1994, 2002). For this reason, we represented in Figure 9a the potential grazing contribution of all mixotrophic groups, following the approach done by Landry *et al.* (2010) for heterotrophic flagellates (included dinoflagellates; see methods for details). In spite of these considerations, large ciliates have been reported as significant consumers on diatom chains and large single-celled diatoms in coastal waters (Aberle *et al.*, 2007; Texeira *et al.*, 2010). However, diatoms could also be consumed by heterotrophic dinoflagellates, which in comparison with ciliates can consume prey cells as large as themselves, or even larger (Lessard 1991, Hansen 1992, Strom and Strom 1996, Saito *et al.* 2006; Vargas and González, 2004; Sherr and Sherr, 2007). It is possible that the high predatory pressure on diatoms found in the most productive periods (Sep'07 and Apr'07) could be associated not only with ciliates but also with large flagellates (mostly dinoflagellates) (Fig. 9b). Particularly, gymnodinoids, a heterotrophic dinoflagellate commonly found in coastal waters of CCS and, that was also observed by microscopy in our coastal site during Apr'08, was reported as a significant consumer on chain-forming diatoms in other coastal systems (Neuer and Cowles, 1994; Strom and Strom 1996; Texeira *et al*., 2010).

Conversely, the strong grazing impact on small algae appears to be related to occurrence of smaller grazers in this coastal station. Particularly, higher grazing impact on *Synechococcus* and Prasinophytes that were found at the first 20 m depth in Jan'08, were associated with the significant presence of small ciliates and flagellates (Fig. 9). It was in agreement with modeling approaches done for coastal upwelling ecosystems at the Humboldt Current System where heterotrophic nanoflagellates seem to ingest a high fraction of PP due to small autotrophic cells (0.7-5µm) in several sampling occasions (Vargas and González, 2004) and, also with the higher grazing impact exerted on autotrophic nanoflagellates by microzooplankton during winter and autumn seasons (25-49% PP), in contrast to lower grazing impact (0.1-1%PP) in spring-summer seasons (Vargas *et al.*, 2007).

5. – CONCLUSION

On the frame of contrasting seasonal oceanographic conditions found at ENSENADA station, our results indicated that for the most of the year this coastal system is dominated by heterotrophic over autotrophic components (Hetero-C:Auto-C>1), except in periods of stronger and more frequent upwelling events, which to lead to a shift in system toward the autotrophy due to substantial improvement in the environmental nutrient-conditions that favor phytoplankton growth within the euphotic zone. Thus, a close net balance trophic is expected to be found along the year. Also, large fraction of primary production attributed to small (mostly SYN and PRAS) and large (mostly diatoms and A-Dino) autotrophic cells, was impacted significantly (91 ± 31% of PP) by nano (2-20 µm) and microzooplankton (20-200 µm) grazing, throughout the wide light (from 56% to 0.3%I_o) and nutrients (0 to >10 µM) conditions recorded in our coastal site. It suggest that microbial food web (included large phytoplankton cells as prey of protistan grazers) is a significant component in this coastal upwelling system of WBC that coexist with the classical short food chains commonly found in the highly

productive upwelling systems (Ryther, 1969). This complex food web structure appears to prevail in several coastal upwelling systems (Neuer and Cowles, 1994; Vargas and González, 2004; Böttjer and Morales, 2005; Vargas *et al.*, 2007; Landry *et al.*, 2009; Texeira *et al.*, 2010) and, confers to the ecosystem the ability to recycle carbon efficiently within upper layer.

***Acknowledgements*:** We gratefully acknowledge all students, technicians and scientists whose efforts facilitated and contributed to our results, as well as, the captain and crew of R/V *Francisco de Ulloa* and the boat *GENUS* for their help during the hard work at the sea. We are also grateful to PhD. student, Andrew Taylor (SIO, UCSD) and technician Daniel Wick for theirs valuable training and help in the epifluorescence microscopy analysis and software data processing. Also we appreciate the valuable help received for the undergraduate student Patricia García (FC, UABC) in ciliates counting and Dr. Víctor Camacho-Ibar (IIO-UABC) for the nutrient analysis. This study was supported by FLUCAR project from CONACyT grants SEP-2004-C01-45813/A-1 and 25339.

REFERENCES

Aberle, N., Lengfellner, K., Sommer, U., 2007. Spring bloom succession, grazing impact and herbivore selectivity of ciliate communities in response to winter warming. Oecologia 150: 668-681.

Almazán-Becerril A, García-Mendoza E. 2008. Photosystem II maximum efficiency of charge separation of the phytoplankton community in the Eastern Tropical North Pacific (ENTP) off Mexico: A nutrient stress diagnostic tool? Ciencias Marinas 34: 29‑43.

Arin, L., Moran, X.A.G., Estrada, M., 2002. Phytoplankton size distribution and growth rates in the Alboran Sea (SW Mediterranean): short term variability related to mesoscale hydrodynamics. Journal of Plankton Research 24, 1019–1033.

Armstrong, F.A., Stearns, C.R., Strickland, J.D. 1967. The measurement of upwelling and subsequent biological processes by means of the Technicon AutoAnalyzer and associated equipment. Deep-Sea Research, 14, 381–389.

Böttjer, D. and Morales, C. E., 2005. Microzooplankton grazing in a coastal embayment off Concepción, Chile, (~36°S) during non-upwelling conditions. Journal of Plankton Research 27, 383–391.

Calbet, A. 2008. The trophic roles of microzooplankton in marine systems. ICES Journal of Marine Science 65, 325-331.

Calbet, A. and Landry, M., 2004. Phytoplankton growth, microzooplankton grazing, and carbon cycling in marine systems. Limnology and Oceanography 49, 51–57.

Calbet A, Vaqué D, Felipe J, Vila M, Sala MM, Alcaraz M, Estrada M., 2003. Relative grazing impact of microzooplankton and mesozooplankton on a bloom of the toxic dinoflagellate *Alexandrium minutum.* Marine Ecology Progress Series 259:303–309

Calbet, A., Landry, M.R., Nunnery, S., 2001. Bacteria-flagellate interactions in the microbial food web of the oligotrophic subtropical North Pacific. Aquatic Microbial Ecology 23, 283-292.

Chen, B., Liu, H., Landry, M.R., Dai, M., Huang, B., Sune J., 2009. Close coupling between phytoplankton growth and microzooplankton grazing in the western South China Sea. Limnology of Oceanography 54:1084-1097.

Colombo-Pallota M.F., García-Mendoza E, Ladah L.B., 2006. Photosynthetic performance, light absorption, and pigment composition of *Macrocystis pyrifera* (Laminariales, Phaeophyceae) blades from different depths. Journal of Phycology 42: 1225–1234.

Durazo, R., 2009. Climate and upper ocean variability off Baja California, Mexico: 1997–2008. Progress in Oceanography 83, 361-368.

Durazo, R., Ramírez, A.M., Miranda, L.E., Soto-Mardones, L.A., 2010. Climatología hidrográfica de la Corriente de California frente a Baja California. In: Durazo, R., Gaxiola, G. (eds.). Dinámica del Ecosistema Pelágico frente a Baja California, 1997-2007. Published by Instituto Nacional de Ecología (INE)/ Centro de Investigación Científica y de Educación Superior (CICESE), México, 20 pp.

Eppley, R.W. 1968. An incubation method for estimating the carbon content of phytoplankton in natural samples. Limnology of Oceanography 13: 574–582.

Frost, B.W., 1972. Effect on size and concentration of food particles on feeding behavior of the marine planktonic copepod Calanus pacificus. Limnology of Oceanography 17, 805-815.

García-Pámanes, J., Lara-Lara, J.R., 2001. Microzooplankton grazing in the Gulf of California. Ciencias Marinas 27, 73-90.

Gasol, J. M., P. A. Del Giorgo, C. M. Duarte. 1997. Biomass distribution in marine planktonic communities. Limnology of Oceanography 42: 1353–1363.

Gordon, L., Jennings Jr., J., Ross A., Krest J., 1993. A Suggested Protocol for Continuous Flow Automated Analysis of Seawater Nutrients (Phosphate, Nitrate, Nitrite and Silicic Acid) in the WOCE Hydrographic Program and the Joint Global Ocean Fluxes Study. WHP Operations and Methods - November 1993. WOCE Hydrographic Program Office, Methods Manual, 91-1, 55pp.

Gutiérrez-Rodríguez A., Latasa M., Estrada M., Vidal M., Marrasé C., 2010. Carbon fluxes through major phytoplankton groups during the spring bloom and post-bloom in the Northwestern Mediterranean Sea. Deep-Sea Research I 57:486–500

Halvorsen, E., Pedersen, O. P., Slagstad, D., K.S. Tande, E.S. Fileman, S.D. Batten. 2001. Microzooplankton and mesozooplankton in an upwelling filament off Galicia: Modelling and sensitivity analysis of the linkages and their impact on the carbon dynamics. Progress of Oceanography 51: 499–513.

Hansen, P. J. 1992. Particle size selection, feeding rates and growth dynamics of marine heterotrophic dinoflagellates, with special emphasis on *Gyrodinium spirale*. Marine Biology 114: 327–334.

Hays GC, Harris RP y Head RN. 2001. Diel changes in the near-surface biomass of zooplankton and the carbon content of vertical migrants. Deep-Sea Research II 48: 1063-1068

Jeffrey S.W., Vesk M., 1997. Introduction to marine phytoplankton and their pigment signatures. In: Jeffrey S.W., Mantoura R.C.F., Wright S.W. (eds) Phytoplankton pigments in oceanography: guidelines to modern methods. UNESCO Publishers, Paris, p 37–82

Landry, M.R. and Hassett, R.P., 1982. Estimating the grazing impact of marine micro-zooplankton. Marine Biology 67, 283–288.

Landry, M.R., Constantinou, J., Latasa, M., Brown, S.L., Bidigare, R.R., Ondrusek, M.E., 2000. Biological response to iron fertilization in the eastern equatorial Pacific (IronEx II). III. Dynamics of phytoplankton growth and microzooplankton grazing. Marine Ecology Progress Series 201, 57–72.

Landry, M.R., Brown, S.L., Rii, Y.M., Selph, K.E., Bidigare, R., Yang, E.J., Simmons, M.P., 2008. Depth-stratified phytoplankton dynamics in Cyclone Opal, a subtropical mesoscale eddy. Deep-Sea Research II 55, 1348-1359.

Landry, M.R., Ohman, M.D., Goericke, R., Stukel, M.R., Tsyrklevichet K., 2009. Lagrangian studies of phytoplankton growth and grazing relationships in a coastal upwelling ecosystem off Southern California. Progress in Oceanography 83, 208-216.

Landry, M.R., Selph K.E., Taylor A.G., Décima, M., Balch, W.M., Bidigare, R.R., 2010. Phytoplankton growth, grazing and production balances in the HNLC equatorial Pacific. Deep-Sea Research II, doi:10.1016/j.dsr2.2010.08.011

Lessard, E. J. 1991. The trophic role of heterotrophic dinoflagellates in diverse marine environments. Marine Microbial Food Webs 5:49–58.

Latasa, M., Moran, X., Scharek, R., Estrada, M., 2005. Estimating the carbon flux through main phytoplankton groups in the northwestern Mediterranean. Limnology and Oceanography 50, 1447–1458.

Legendre L, Le Fevre J., 1989. Hydrodynamic singularities as controls of recycled versus export production in oceans. In: Berger WH, Smetacek VS, Wefer G (eds) Productivity of the ocean: present and past. Wiley, Chichester, p 49-63.

Legendre L, Le Fevre J., 1995. Microbial food webs and the export of biogenic carbon in oceans. Aquatic Microbial Ecology 9:69-77.

Legendre, L. and Rassoulzadegan, F., 1995. Plankton and nutrient dynamics in marine waters. Ophelia, 41, 153–172.

Linacre, L.P., Landry, M.R., Lara-Lara, J.R., Hernández-Ayón, J.M., Bazán-Guzmán, C., 2010a. Picoplankton dynamics during contrasting seasonal oceanographic conditions at a coastal upwelling station off Northern Baja California, México. Journal Plankton Research 32(4):539-557.

Linacre, L., Hernández-Ayón, J.M., Durazo, R., Delgadillo-Hinojosa, F., Cervantes-Díaz, G., Lara-Lara, J.R., Camacho-Ibar, V., Siqueiros-Valencia, A., Bazán-Guzmán, C., 2010b. Temporal variability of the physicochemical water characteristics at a coastal monitoring observatory: Station ENSENADA.", Continental Shelf Research, 30:1730-1742.

Menden-Deuer, S., Lessard, E.J., 2000. Carbon to volume relationships for dinoflagellates, diatoms, and other protist plankton. Limnology and Oceanography 45, 569–679.

McClatchie, S., Goericke, R., Koslow, J.A., Schwing, F.B., Bograd, S.J., Charter, R., Watson, W., Lo, N., Hill, K., Gottschalk, J., L'Heureux, M., Xue, Y., Peterson, W.T., Emmett, R., Collins, C., Gaxiola-Castro, G., Durazo, R., Kahru, M., Mitchell, B.G., Hyrenbach, K.D., Sydeman, W.J., Bradley, R.W., Warzybok, P., Bjorkstedt, E., 2008. The state of the California current, 2007–2008: La Nin˜a conditions and their effects on the ecosystem. California Cooperative Oceanic Fisheries Investigation Reports 49, 39–76.

McManus, G.B., Costas, B.A., Dam, H.G., Lopes, R.M., Gaeta, S.A., Susini , S.M., Rosettaet, C.H., 2007. Microzooplankton grazing of phytoplankton in a tropical upwelling region. Hydrobiology 575, 69-81.

Neuer, S. and Cowles, T. J., 1994. Protist herbivory in the Oregon upwelling system. Marine Ecology Progress Series 113, 147–162.

Obayashi, Y., Tanoue, E., 2002. Growth and mortality rates of phytoplankton in the northwestern North Pacific estimated by the dilution method and HPLC pigment analysys. Journal Expimental Marine Biological Ecology 280, 33–52.

Olivieri, R.A., Chavez, F.P., 2000. A model of plankton dynamics for the coastal upwelling system of Monterey Bay, California. Deep-Sea Research II 47: 1077–1106.

Parsons T.R., Maita, Y. and Lalli C.M., 1984. A manual of chemical and biological methods for seawater analysis. Pergamon Press, Oxford, p. 173.

Putland, J.N., 2000. Microzooplankton herbivory and bacterivory in Newfoundland coastal waters during spring, summer and winter. Journal of Plankton Research 22 (2): 253–277

Putt, M., Stoecker, D.K., 1989. An experimentally determined carbon: volume ratio for marine ''oligotrichous'' ciliates from estuarine and coastal waters. Limnology and Oceanography 34, 1097–1103.

Rodríguez, J., Tintoré, J., Allen, J., Blanco, J.M., Gomis, D., Reul, A., Ruiz, J., Rodriguez, V., Echevarría, F., Jimenez-Gómez, F., 2001. Mesoscale vertical motion and the size structure of phytoplankton in the ocean. Nature, 410, 360–363.

Ryther, J. H., 1969. Photosynthesis and fish production in the sea. Science, 166: 72–76.

Saito, H., Ota, T., Suzuki, K., Nishioka, J., and Tsuda, A. 2006. Role of heterotrophic dinoflagellate *Gyrodinium sp.* in the fate of an iron induced diatom bloom. Geophysical Research Letters, 33: L09602, doi:10.1029/2005GL025366.

Sherr, E.B., Sherr, B.F., 1993. Preservation and storage of samples for enumeration of heterotrophic protists. In: Kemp, P.F., Cole, J.J., Sherr, B.F., Sherr, E.B. (Eds.), Handbook of Methods in Aquatic Microbial Ecology. CRC Press, Boca Raton, Florida, pp. 207–212.

Sherr EB and Sherr BF., 1994. Bacterivory and herbivory: key roles of phagotrophic protists in pelagic food webs. Microbial Ecology 28: 223–235.

Sherr E.B. and Sherr B.F., 2002. Significance of predation by protists in aquatic microbial food webs. Antonie van Leeuwenhoek, 81, 293–308.

Sherr, E.B., Sherr, B.F., 2007. Heterotrophic dinoflagellates: a significant component of microzooplankton biomass and major grazers of diatoms in the sea. Marine Ecology Progress Series 352, 187–197.

Steemann Nielsen, E., 1952. The Use of Radio-Active Carbon (^{14}C) for Measuring Organic Production in the Sea. J. Cons. Int. Mer., 18, 117-140.

Stoecker, D. 1998. Conceptual model of mixotrophy in planktonic protists and some ecological and evolutionary implications. European Journal of Protistology 34: 281-290.

Stoecker, D., Taniguchi A., Michaels, A., 1989. Abundance of autotrophic, mixotrophic and heterotrophic planktonic ciliates in shelf and slope waters. Marine Ecology Progress Series 50:241-254.

Strom, S.L., Strom, M.W., 1996. Microplankton growth, grazing, and community structure in the northern Gulf of Mexico. Marine Ecology Progress Series 130, 229-240.

Strom, S.L., Brainard, M.A., Holmes, J.L., Olson, M.B., 2001. Phytoplankton blooms are strongly impacted by microzooplankton grazing in coastal North Pacific waters. Marine Biology, 138, 355–368.

Strom, S.L., Macri, E.L., Olson, M.B., 2007. Microzooplankton grazing in the coastal Gulf of Alaska: Variations in top-down control of phytoplankton. Limnology of Oceanography 52(4): 1480–1494

Taylor, A.G., Landry, M.R., Selph, K.E., Yang, E.J., 2010. Biomass, size structure and depth distributions of the microbial community in the eastern equatorial Pacific. Deep-Sea Research II, doi:10.1016/j.dsr2.2010.08.017.

Teixeira, I.G., Figueiras, F.G., 2009. Feeding behaviour and non-linear responses in dilution experiments in a coastal upwelling system. Aquatic Microbial Ecology 55: 53-63.

Teixeira I.G., Figueiras F.G., Crespo B.G., Piedracoba S., 2010. Microzooplankton feeding impact in a coastal upwelling system on the NW Iberian margin: The Ría de Vigo. Estuarine, Coastal and Shelf Science, doi:10.1016/j.ecss.2010.10.012.

Thomsen, H., Buck, K.R., 1998. Nanoflagellates of central California waters: taxonomy, biogeography and abundance of primitive, green flagellates (Pedinophyceae, Prasinophyceae). Deep-Sea Research II 45: 1687-1707.

Van Heukelem L, Thomas C.S. 2001. Computer-assisted high performance liquid chromatography method development with application to the isolation and analysis of phytoplankton pigments. Journal of Chromatography 910: 31–49.

Verity, P.G., Langdon, C., 1984. Relationship between lorica volume, carbon, nitrogen, and ATP content of tintinnids in Narragansett Bay. Journal of Plankton Research 66, 859–868.

Wright S.W., Jeffrey S.W., 2006. Pigment Markers for Phytoplankton Production. In: Volkman J.K. (ed.), Marine Organic Matter: Biomarkers, Isotopes and DNA. The Handbook of Environmental Chemistry, Volume 2N, doi: 10.1007/698_2_003, pp. 71-104

Wright S., Mantoura R.F.C. 1997. Guidelines for collection and pigment analysis of marine samples. In: Jeffrey S.W., Mantoura R.F.C., Wright S. (eds.), Phytoplankton Pigments in Oceanography: Guidelines to Modern Methods. UNESCO, Paris, pp. 429–445.

Vargas, C.A., González, H.E., 2004. Plankton community structure and carbon cycling in a coastal upwelling system. II. Microheterotrophic pathway. Aquatic Microbial Ecology 34, 165-180.

Vargas, C.A., Martínez, R.A., Cuevas, L.A., Pavez, M.A., Cartes, C., González, H.E., Escribano, R., Daneri, G., 2007. The relative importance of microbial and classical food webs in a highly productive coastal upwelling area. Limnology and Oceanography 52, 1495-1510.

Walsh J.J., Row G.T., Iverson R.L., McRoy C.P., 1981. Biological export of shelf carbon is a sink of the global CO2 cycle. Nature 291:196–201

Wassman, P., 1998. Retention versus export food chains: processes controlling sinking loss from marine pelagic systems Hydrobiologia 363: 29–57.

Worden, A.Z., Nolan, J.K. and Palenik, B., 2004. Assessing the dynamics and ecology of marine picophytoplankton: The importance of the eukaryotic component. Limnology and Oceanography 49, 168–179.

Worden, A.Z. 2006. Picoeukaryote diversity in coastal waters of the Pacific Ocean. Aquatic Microbial Ecology 43: 165–175

Figure captions

Figure 1. Location of experimental station in the coastal waters off WBC, México.

Figure 2. (a) Six-hourly Bakun upwelling index (m^3 s^{-1} per 100 m of coastline) and, (b) monthly upwelling mean (m^3 s^{-1} per 100 m of coastline) from NOAA/PFEL data for 31.6°N 116.8°W, for the period from September 2007 to November 2008, when 19 dilution experiments were conducted in the euphotic zone at ENSENADA station in the northern region off WBC, Mexico. The (a) panel shows gray and enlarged circles that indicate the index value for the day when incubation dilutions were done. The (b) panel shows light-grey bars that indicate the six periods when the dilution experiments were done.

Figure 3. Profiles of (a) water density (σ_t ; kg m^{-3}), (b) *in situ* fluorescence (µg Chl L^{-1}), (c) nitrite+nitrate and, (d) silicates measured at the time of the seawater collection for the dilution experiments conducted in the euphotic zone from September 2007 to November 2008 at ENSENADA station in the northern region off WBC, Mexico. For nutrients, the vertical distribution was represented only for the surface layer (0- 40 m) when the dilution experiments were done. In April 2008, seawater for nutrients analyses was collected 5 days later.

Figure 4. (a) Total autotrophic (Auto-C) and heterotrophic (Hetero-C) carbon biomass, (b) autotrophic carbon and (c) heterotrophic carbon by size-class, from initial conditions of 19 dilution experiments conducted in the euphotic zone from September 2007 to November 2008 at ENSENADA station in the northern region off WBC, Mexico. Note that heterotrophic pico-sized cells were totally comprised by heterotrophic bacteria.

Figure 5. Scatter plot the between heterotrophic to autotrophic carbon biomass ratios (Hetero: Auto Carbon) and autotrophic carbon biomass (Auto Carbon) from initial conditions of 19 dilution experiments conducted in the euphotic zone from September 2007 to November 2008 at ENSENADA station in the northern region off WBC, Mexico. The dashed line indicate when heterotrophic carbon biomass was equal to autotrophic carbon biomass (Hetero: Auto carbon ratio=1).

Figure 6. (a) Total autotrophic carbon biomass (TAuto-C) and total concentration of chlorophyll *a* (TChl*a*), (b) scatter plots between TChl*a* and total Autotrophic Carbon (Auto-C) and, (c) autotrophic carbon to chlorophyll *a* ratios, from initial conditions of 19 dilution experiments conducted in the euphotic zone from September 2007 to November 2008 at ENSENADA station in the northern region off WBC, Mexico. The top (b) panel show significant linear regressions from overall data, excluding April 2008 experiments. The dashed line on the figure c shows the overall average for the periods sampled.

Figure 7. Instantaneous rates of autotrophic growth (μ) and grazing mortality (m) for (a) total autotrophic community (TChl*a*), (b) Diatoms (Fucoxanthin rates), (C) *Synechococcus* (cells rates) and, (d) Prasinophytes (Pico-Euks rates), from 19 dilution experiments conducted in the euphotic zone from September 2007 to November 2008 at ENSENADA station in the northern region off WBC, Mexico.

Figure 8. Daily rates of primary production (PP) and grazing losses (G) by microzooplankton based on total concentration of chlorophyll *a* (TChl*a*) and cell or specific-pigments for (a) total autotrophic community, (b) diatoms and other autotrophic eukaryotes (Other A-Euks), (c) *Synechococcus*, (d) prasinophytes and, (e) prymnesiophytes and *Prochlorococcus* from 19 dilution experiments conducted in the euphotic zone from September 2007 to November 2008 at ENSENADA station in the northern region off WBC, Mexico. The (a) panel also show contemporaneous measurements of ^{14}C-uptake primary production done simultaneously at this coastal station.

Figure 9. (a) Relative contribution of initial carbon biomass for total grazers by size-class: ciliates < 20μm (Nano_CIL), ciliates > 20μm (Micro_CIL), flagellates (including dinoflagellates) < 20μm (Nano_Flag) and flagellates > 20 μm (Micro_Flag), in addition to grazing impact on total autotrophic carbon (Autotrophic community impact) and, (b) microzooplankton grazing impact on main phytoplankton groups: diatoms, *Synechococcus* (SYN) and prasinophytes (Pras), from 19 dilution experiments conducted in the euphotic zone from September 2007 to November 2008 at ENSENADA station in the northern region off WBC, Mexico. The dashed line in (b) panel, indicates the ratio when grazing losses are equal daily primary production (G=PP).

Table I: Estimations of initial carbon biomass (μgCL^{-1}) based on cell abundances of main autotrophic and heterotrophic functional groups found at ENSENADA station located in the northern region off WBC, México. Light ($\%I_o$) conditions were measured at midday CTD-cast. Temperature and initial abundances of cells were measured in pre-dawn CTD cast during the collection of seawater for in situ dilution experiments. Groups of picoplankton distinguished by flow cytometry were Prochlorococcus spp. (PRO), Synechococcus spp. (SYN) and Heterotrophic Bacteria (H-Bact). Groups of nanoplankton and microplankton distinguished by epifluorescence microscopy were autotrophic and heterotrophic flagellates (A-Flag and H-Flag), Prymnesiophytes (Prym), Cryptophytes (Cryp), autotrophic and heterotrophic dinoflagellates (A-Dino and H-Dino) and Diatoms. From Lugol' samples, ciliates were identified and counted by inverted microscopy.

				Autotrophic								**Heterotrophic**				
	Depth	Light	Temp	Carbon Biomass (μgCL^{-1})							**Total**	Carbon Biomass (μgCL^{-1})				**Total**
Cruise	(m)	%Io	(°C)	PRO	SYN	A-Flag	Prym	Cryp	A-Dino	Diatom	**Auto-C**	H-Bact	H-Flag	H-Dino	Ciliates	**Hetero-C**
Sept' 07	2	55.9	15.4	0.6	14.2	4.0	0.2	0.2	3.1	17.7	40.0	69.9	1.6	0.5	11.2	83.2
Sept' 07	7	23.4	14.6	0.8	13.4	7.4	0.9	0.3	4.6	16.9	44.4	54.6	3.3	0.3	21.1	79.3
Sept' 07	10	14.6	13.2	0.9	4.5	2.3	1.1	0.2	1.1	4.2	14.3	29.6	1.6	1.1	7.6	39.9
Sept' 07	35	1.1	11.9	0.1	1.0	9.0	0.4	0.2	0.8	1.8	13.2	25.2	0.3	0.5	2.5	28.6
Nov'07	10	13.5	15.2	0.7	4.5	2.9	0.3	1.3	0.8	1.4	12.0	23.9	1.6	0.9	3.2	29.6
Nov'07	20	6.1	14.0	1.2	3.2	2.0	0.7	0.8	0.2	0.4	8.6	15.4	1.7	0.2	5.9	23.1
Nov'07	30	2.3	12.8	1.8	2.4	6.5	0.3	0.6	2.5	0.2	14.3	13.4	2.5	0.1	10.9	26.9
Jan'08	5	24.9	13.8	1.2	14.3	4.1	1.4	0.3	1.3	1.5	24.2	56.0	5.8	2.4	1.7	65.9
Jan'08	20	1.7	13.2	0.5	9.6	2.8	0.8	0.3	2.0	5.6	21.6	40.3	0.9	1.0	9.4	51.5
Jan'08	30	0.3	12.9	0.2	3.1	3.0	0.3	0.2	3.5	0.9	11.3	24.8	0.9	0.6	3.6	29.9
Apr' 08	5	22.1	11.6	0.0	0.4	1.4	0.3	0.4	5.4	74.2	82.0	18.6	0.4	1.2	3.8	24.0
Apr' 08	10	8.0	11.3	0.0	0.3	1.0	0.6	0.4	16.3	45.1	63.6	11.6	0.7	3.0	20.6	35.9
Apr' 08	15	2.9	10.5	0.0	0.5	4.1	2.0	0.1	98.9	80.2	185.8	12.9	1.1	2.4	0.0	16.4
Aug'08	5	36.2	16.3	3.6	9.4	11.2	2.5	0.8	8.6	0.1	36.1	25.8	6.1	5.9	7.3	45.2
Aug'08	10	16.7	14.4	1.3	6.4	1.8	1.2	0.5	1.4	1.5	14.0	17.4	0.6	2.5	0.5	21.1
Aug'08	20	4.1	12.3	0.3	0.9	1.0	0.4	0.0	0.6	0.1	3.3	11.0	0.3	0.4	0.0	11.7
Nov' 08	5	47.2	16.0	3.0	7.6	1.5	3.0	1.1	1.2	10.2	27.5	26.2	2.0	2.8	0.1	31.0
Nov' 08	12	13.5	15.0	2.0	6.2	1.4	3.1	0.9	2.1	0.8	16.5	17.9	1.5	2.5	2.9	24.8
Nov' 08	30	1.1	13.9	0.4	0.5	0.6	0.3	0.2	0.2	0.5	2.7	9.2	1.3	0.7	0.0	11.2

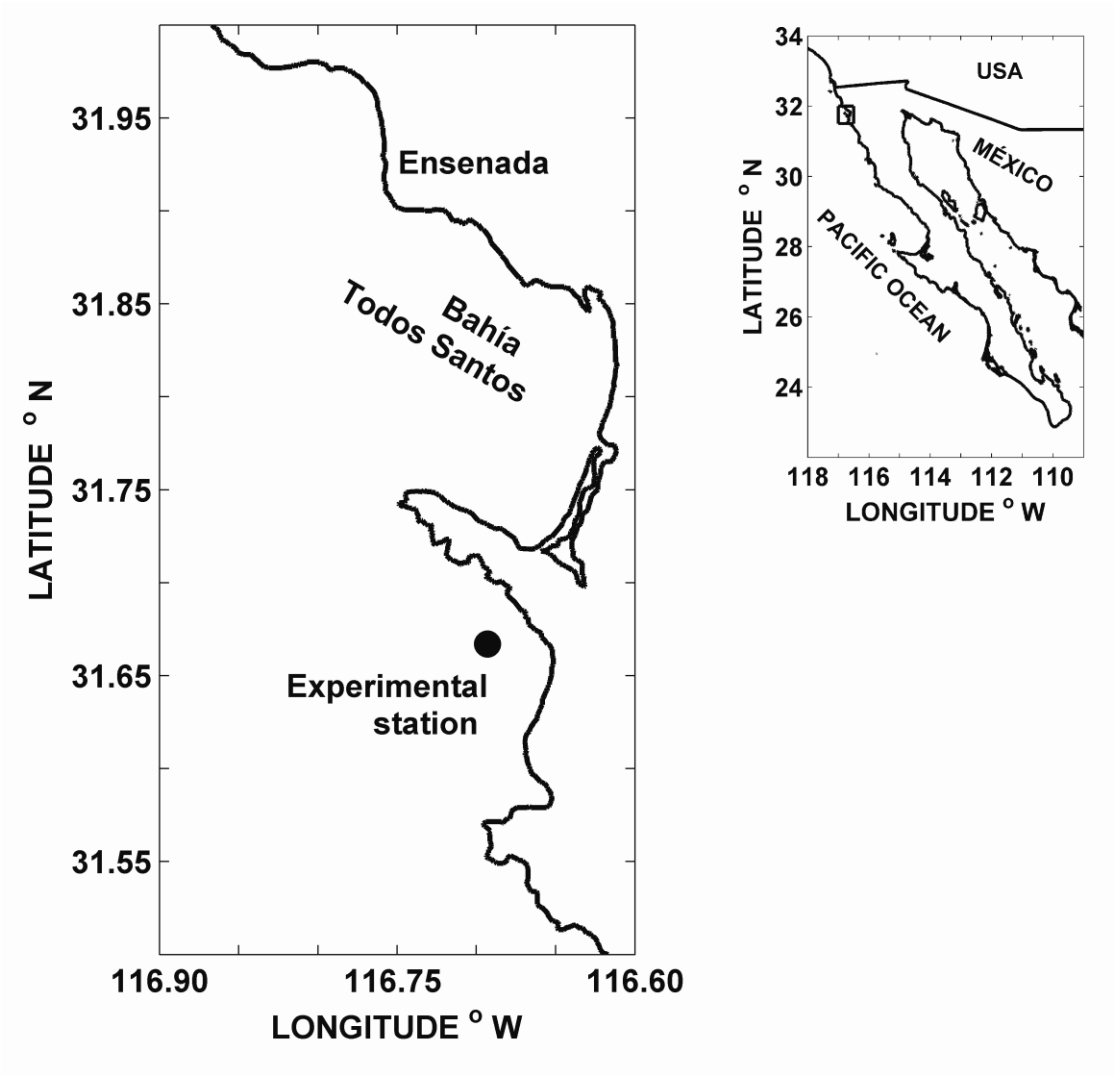
31.95
31.85
31.75
31.65
31.55
LATITUDE ° N
Ensenada
Bahía
Todos Santos
Experimental
station
116.90
116.75
116.60
LONGITUDE ° W
34
32
30
28
26
24
LATITUDE ° N
USA
MÉXICO
PACIFIC OCEAN
118
116
114
112
110
LONGITUDE ° W

Fig. 1

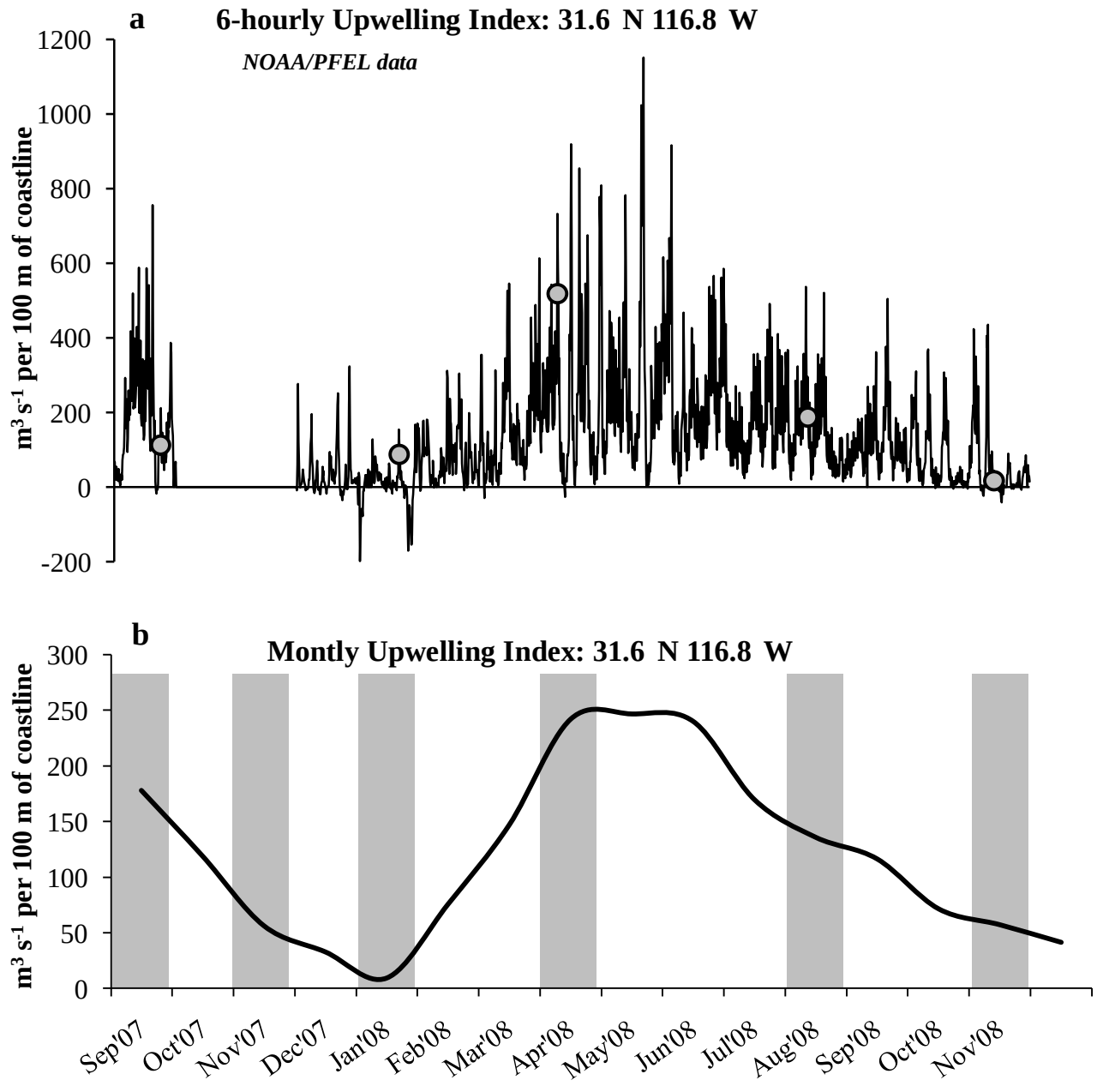
a
6-hourly Upwelling Index: 31.6 N 116.8 W
NOAA/PFEL data
m3 s-1 per 100 m of coastline
1200
1000
800
600
400
200
0
-200
b
Montly Upwelling Index: 31.6 N 116.8 W
m3 s-1 per 100 m of coastline
300
250
200
150
100
50
0
Sep'07
Oct'07
Nov'07
Dec'07
Jan'08
Feb'08
Mar'08
Apr'08
May'08
Jun'08
Jul'08
Aug'08
Sep'08
Oct'08
Nov'08

Fig.2

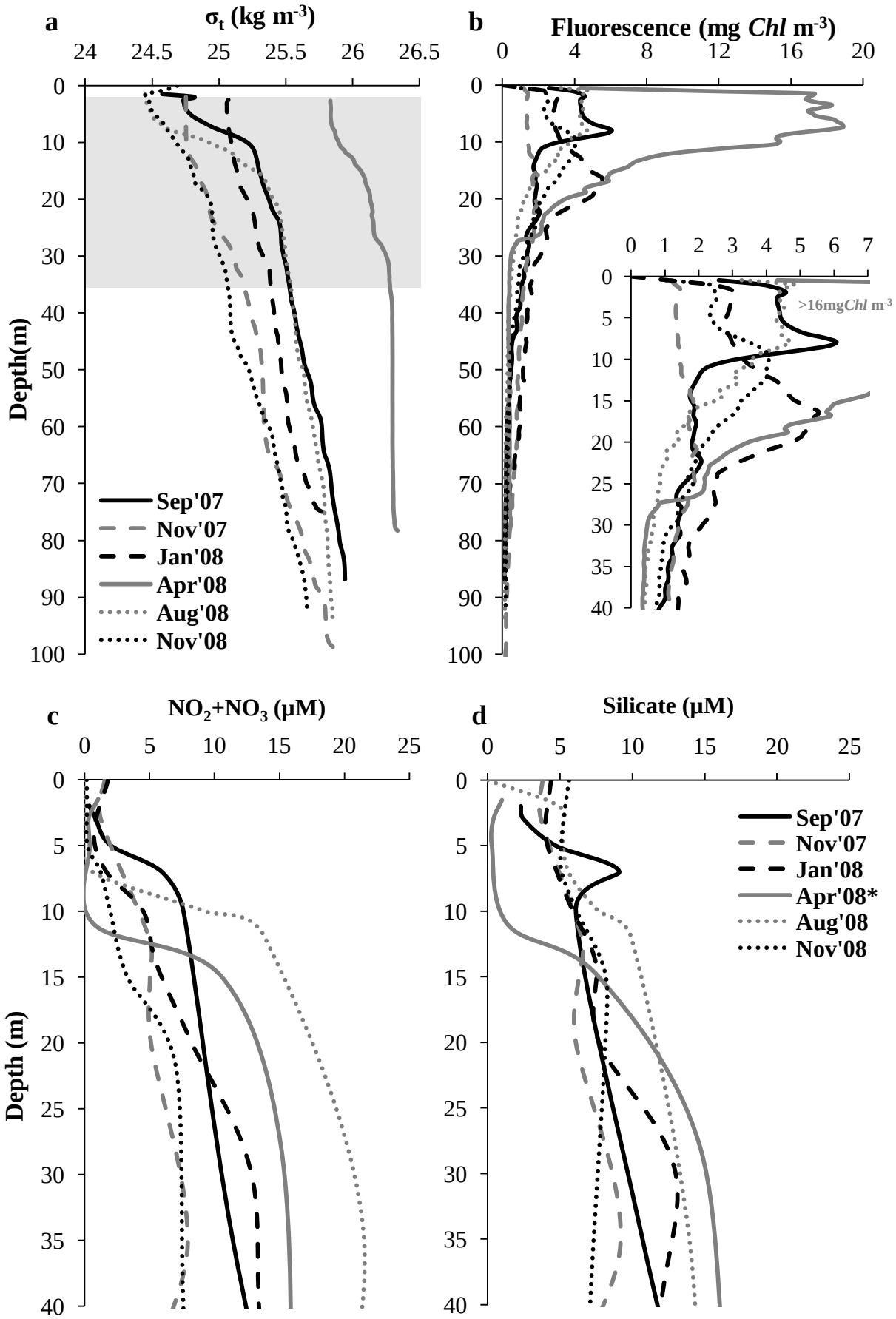

**Nutrients data collected 5 days after dilution incubations*

Fig. 3

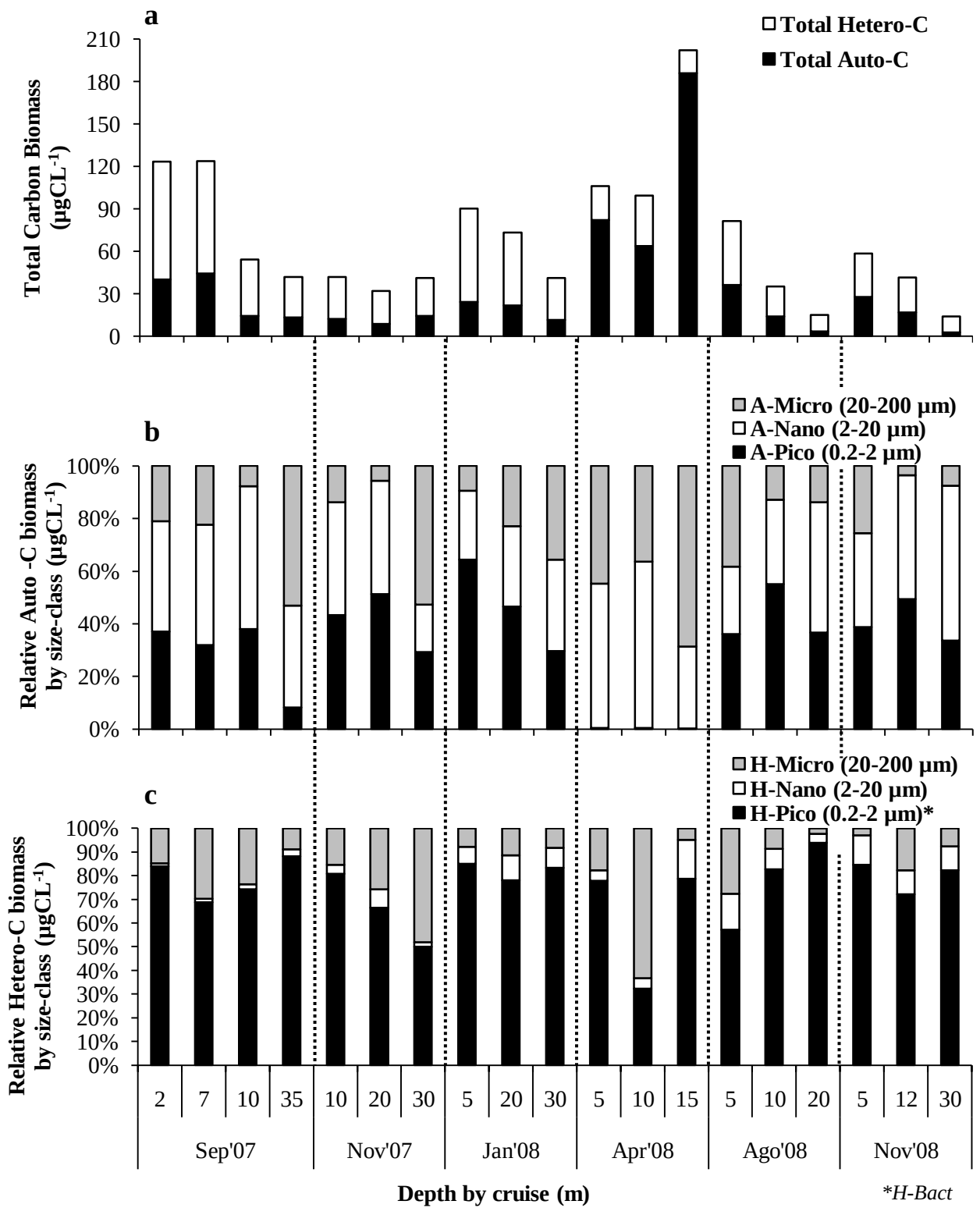
a
Total Hetero-C
Total Auto-C
Total Carbon Biomass (µgCL-1)
210
180
150
120
90
60
30
0
b
A-Micro (20-200 µm)
A-Nano (2-20 µm)
A-Pico (0.2-2 µm)
Relative Auto -C biomass by size-class (µgCL-1)
100%
80%
60%
40%
20%
0%
c
H-Micro (20-200 µm)
H-Nano (2-20 µm)
H-Pico (0.2-2 µm)*
Relative Hetero-C biomass by size-class (µgCL-1)
100%
90%
80%
70%
60%
50%
40%
30%
20%
10%
0%
2 7 10 35 10 20 30 5 20 30 5 10 15 5 10 20 5 12 30
Sep'07
Nov'07
Jan'08
Apr'08
Ago'08
Nov'08
Depth by cruise (m)
*H-Bact

Fig. 4

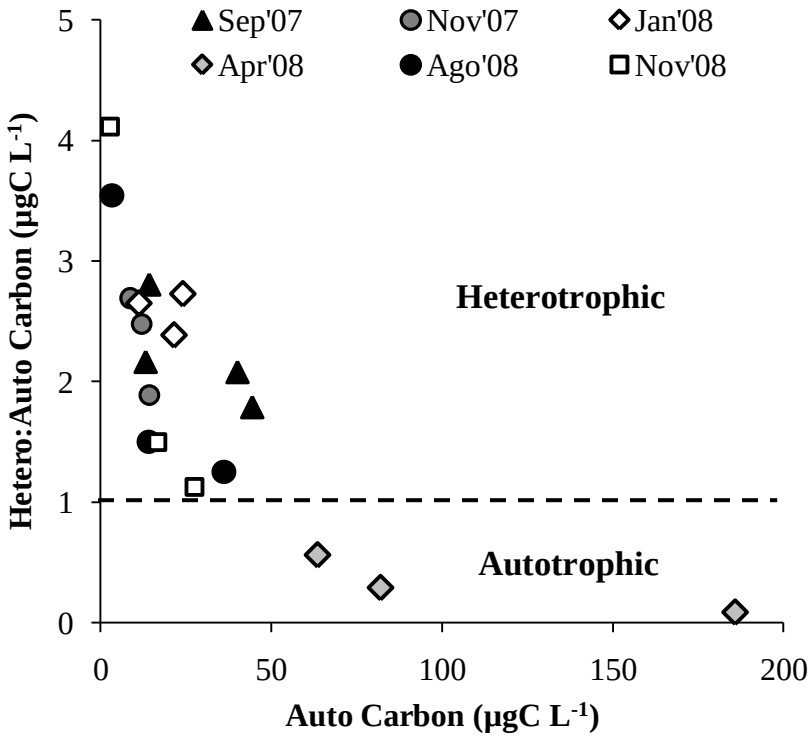
Sep'07
Nov'07
Jan'08
Apr'08
Ago'08
Nov'08
Heterotrophic
Autotrophic
Hetero:Auto Carbon (µgC L-1)
Auto Carbon (µgC L-1)
0
1
2
3
4
5
0
50
100
150
200

Fig. 5

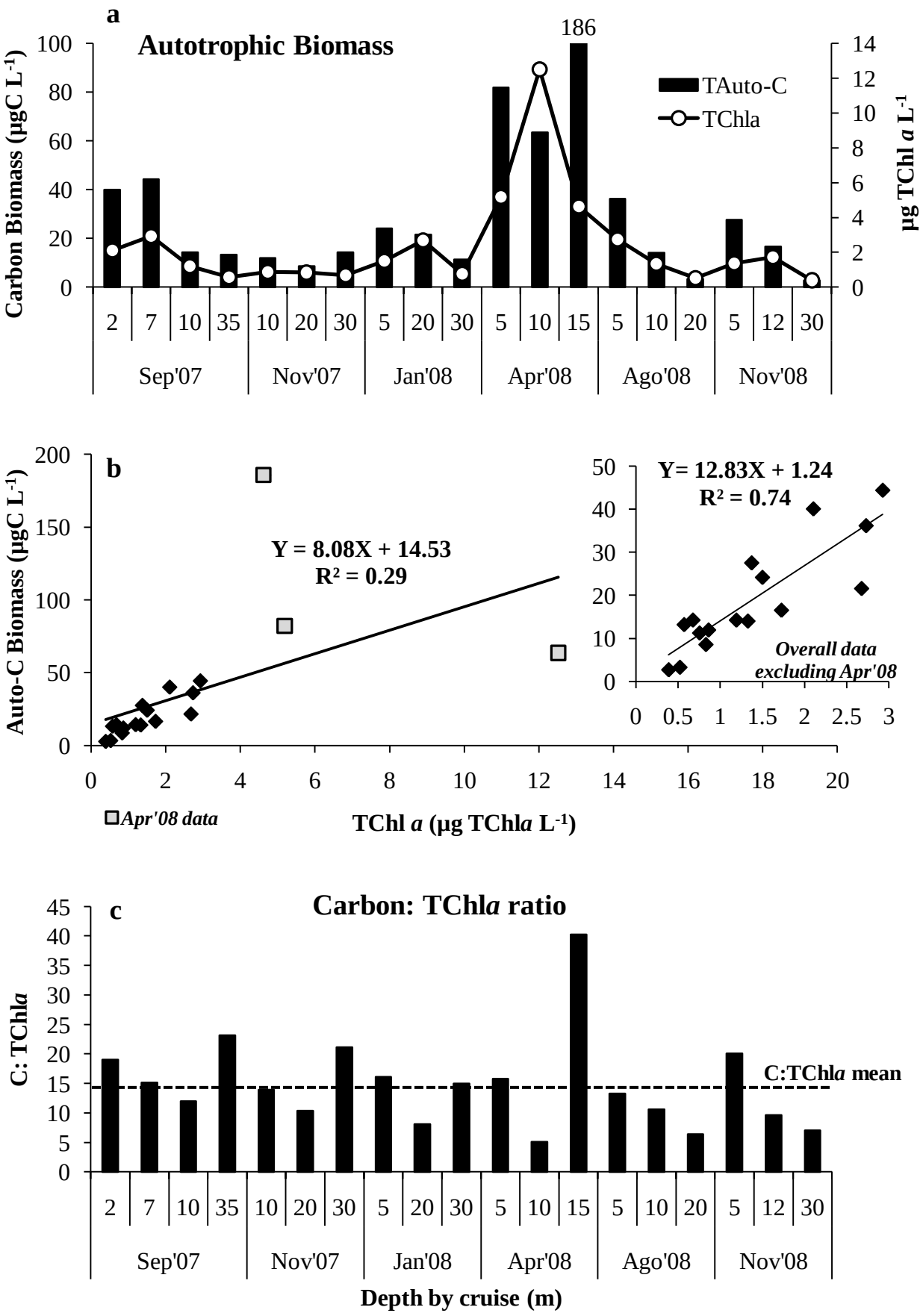
a
Autotrophic Biomass
186
TAuto-C
TChla
Carbon Biomass (µgC L-1)
µg TChl a L-1
2 7 10 35 10 20 30 5 20 30 5 10 15 5 10 20 5 12 30
Sep'07 Nov'07 Jan'08 Apr'08 Ago'08 Nov'08
b
Y = 8.08X + 14.53
R² = 0.29
Y= 12.83X + 1.24
R² = 0.74
Overall data excluding Apr'08
Auto-C Biomass (µgC L-1)
Apr'08 data
TChl a (µg TChla L-1)
c
Carbon: TChla ratio
C: TChla
C:TChla mean
Depth by cruise (m)

Fig. 6

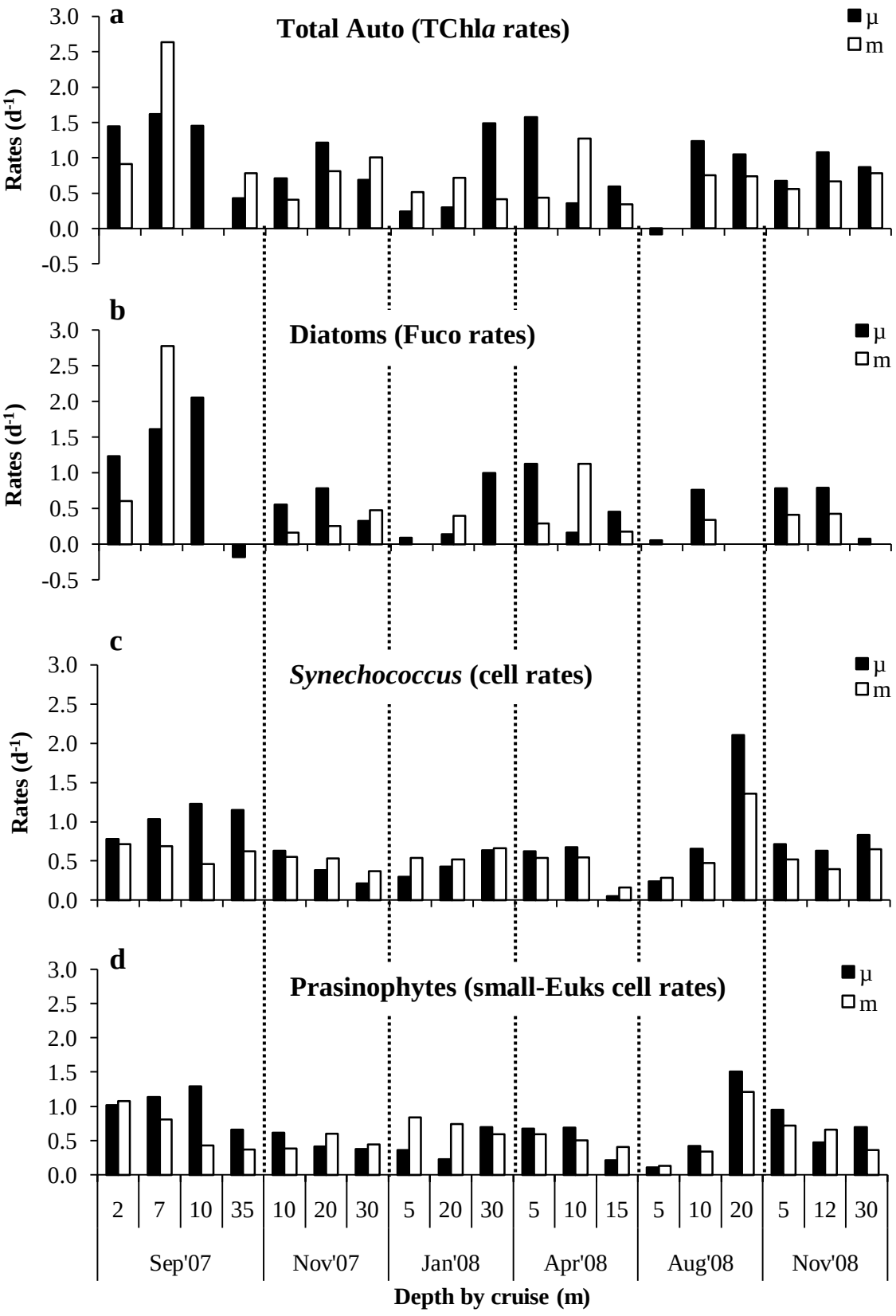
a
Total Auto (TChl*a* rates)
b
Diatoms (Fuco rates)
c
Synechococcus (cell rates)
d
Prasinophytes (small-Euks cell rates)
μ
m
Rates (d-1)
3.0
2.5
2.0
1.5
1.0
0.5
0.0
-0.5
2 7 10 35 10 20 30 5 20 30 5 10 15 5 10 20 5 12 30
Sep'07 Nov'07 Jan'08 Apr'08 Aug'08 Nov'08
Depth by cruise (m)

Fig. 7

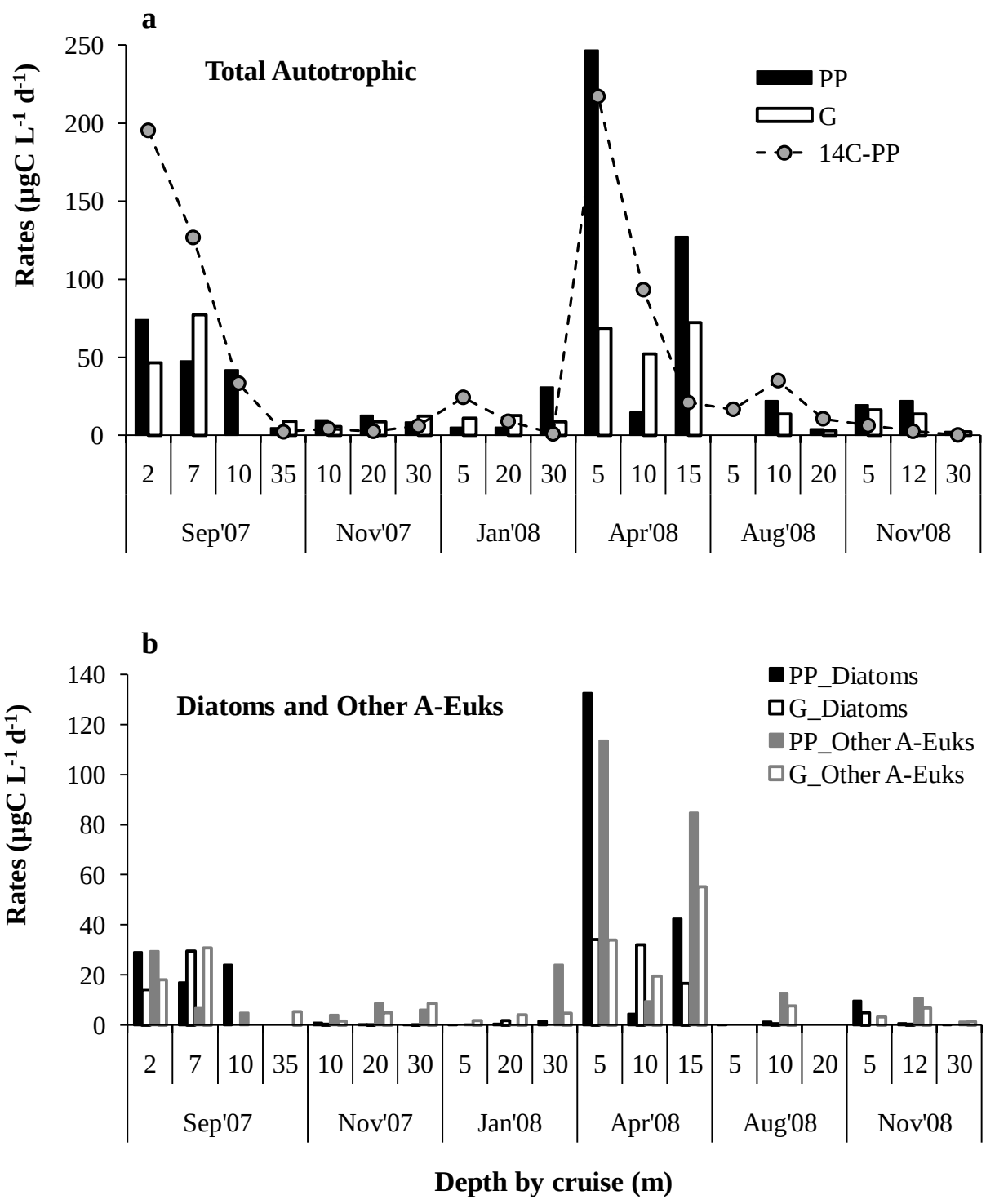
a
Total Autotrophic
PP
G
14C-PP
Rates (µgC L-1 d-1)
250
200
150
100
50
0
2 7 10 35 10 20 30 5 20 30 5 10 15 5 10 20 5 12 30
Sep'07
Nov'07
Jan'08
Apr'08
Aug'08
Nov'08
b
Diatoms and Other A-Euks
PP_Diatoms
G_Diatoms
PP_Other A-Euks
G_Other A-Euks
Rates (µgC L-1 d-1)
140
120
100
80
60
40
20
0
2 7 10 35 10 20 30 5 20 30 5 10 15 5 10 20 5 12 30
Sep'07
Nov'07
Jan'08
Apr'08
Aug'08
Nov'08
Depth by cruise (m)

Fig. 8

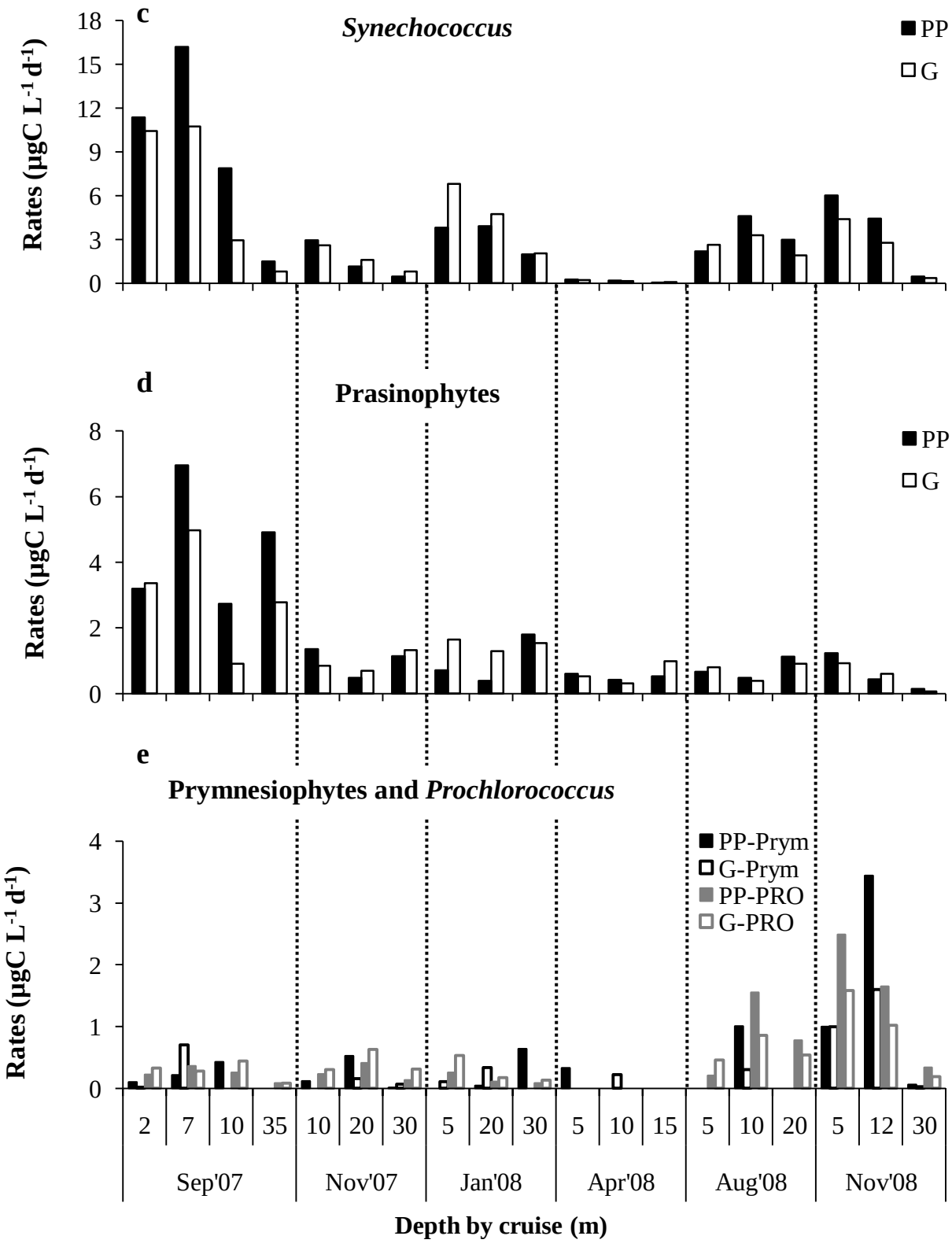
c
Synechococcus
PP
G
Rates (µgC L-1 d-1)
18
15
12
9
6
3
0
d
Prasinophytes
PP
G
Rates (µgC L-1 d-1)
8
6
4
2
0
e
Prymnesiophytes and Prochlorococcus
PP-Prym
G-Prym
PP-PRO
G-PRO
Rates (µgC L-1 d-1)
4
3
2
1
0
2 7 10 35 10 20 30 5 20 30 5 10 15 5 10 20 5 12 30
Sep'07 Nov'07 Jan'08 Apr'08 Aug'08 Nov'08
Depth by cruise (m)

…Cont. Fig. 8

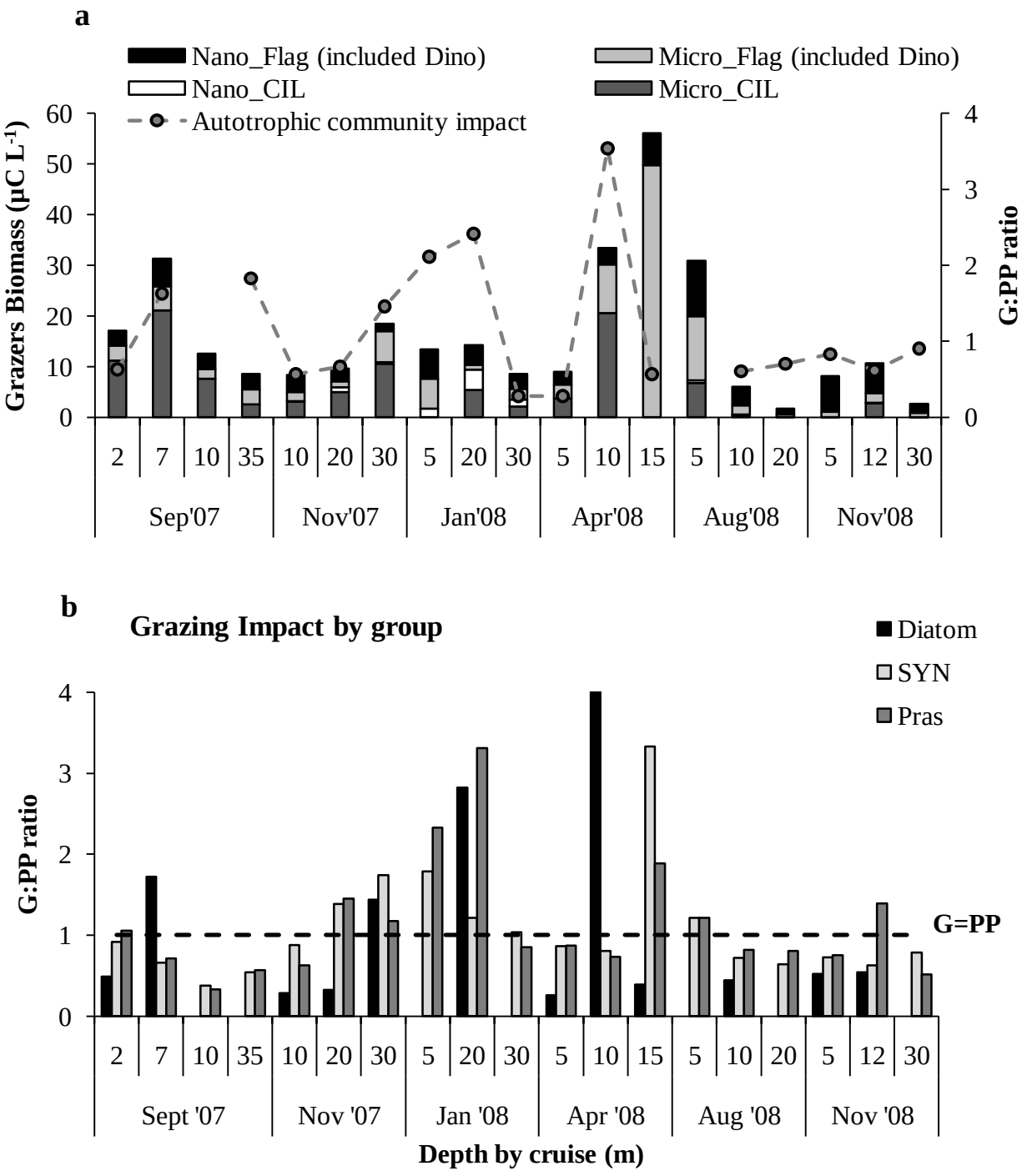
a
Nano_Flag (included Dino)
Micro_Flag (included Dino)
Nano_CIL
Micro_CIL
Autotrophic community impact
Grazers Biomass (µC L-1)
G:PP ratio
0
10
20
30
40
50
60
0
1
2
3
4
2 7 10 35 10 20 30 5 20 30 5 10 15 5 10 20 5 12 30
Sep'07
Nov'07
Jan'08
Apr'08
Aug'08
Nov'08
b
Grazing Impact by group
Diatom
SYN
Pras
G:PP ratio
G=PP
0
1
2
3
4
2 7 10 35 10 20 30 5 20 30 5 10 15 5 10 20 5 12 30
Sept '07
Nov '07
Jan '08
Apr '08
Aug '08
Nov '08
Depth by cruise (m)

Fig. 9

CONCLUSIONES

Derivado del trabajo de ésta tesis, se puede establecer que la zona costera frente a Ensenada, Baja California (México), presenta una marcada variabilidad temporal en las condiciones físico-químicas de la columna de agua. Esta variabilidad es en parte modulada por fluctuaciones estacionales en el intercambio de calor océano-atmósfera y los patrones de vientos (a lo largo de la costa y en el rotacional ciclónico del viento), los cuales controlan los eventos de surgencia costera, la estratificación de la columna de agua y los patrones de circulación superficial (Corriente de California) y subsuperficial (ContraCorriente de California). Adicionalmente, la zona es modulada por fluctuaciones interanuales asociadas a eventos cálidos y fríos de mayor escala, como El Niño y la Niña, respectivamente. Particularmente, la estación ENSENADA, un observatorio de monitoreo localizado en esta zona costera frente a Ensenada, ha demostrado ser un sitio costero sensible a estos cambios físico-químicos estacionales e interanuales y representativo de estas aguas costeras, por lo que bajo circunstancias ambientales fuertemente variables, resulta ser además, una localidad conveniente para la evaluación del papel que cumplen las comunidades planctónicas en el ciclo del carbono.

Además, a lo largo de este estudio se ha sugerido que la dinámica del ciclo del carbono en la región se encuentra relacionada a la variabilidad temporal descrita en los parámetros físico-químicos, donde las comunidades planctónicas microbianas desempeñan un papel fundamental en la producción y en la transferencia del carbono hacia los niveles tróficos superiores. El enriquecimiento de nutrientes inorgánicos incorporados a la zona eufótica desde estratos subsuperficiales por los frecuentes e intensos eventos primaverales de surgencia costera, alternado con periodos de estratificación en la columna de agua, han demostrado ser los mecanismos físicos principales que modulan la dinámica ecológica de las comunidades de esta región costera y consecuentemente, el flujo del carbono dentro de la trama trófica microbiana, y hacia los eslabones alimenticios superiores.

Las condiciones oceanográficas que fueron registradas esporádicamente a lo largo de un año, en conjunto a los experimentos biológicos realizados *in situ* en la estación ENSENADA, mostraron que generalmente las aguas costeras de esta región son

dominadas por componentes heterótrofos, principalmente bacterias heterotróficas, sugiriendo un papel preponderante del enlace microbiano como vía de canalización del carbono hacia el resto de la trama trófica. Esto, aunado a las estimaciones del porcentaje de producción primaria (PP) generada mayormente por componentes autótrofos pico y nanoplanctónicos (*Synechococcus* y Prasinofitas), que es activamente pastoreada (~90% de la PP) por organismos microzooplanctónicos (flagelados y ciliados <200 µm), se sugiere que esta zona costera recicla eficientemente el carbono en los estratos superficiales de la columna de agua a través de los componentes planctónicos autótrofos y heterótrofos menores a 200 µm, dejando solo una pequeña fracción que puede ser consumida directamente por organismos mesozooplanctónicos (200-2,000 µm), ó ser exportada al océano profundo, por el hundimiento de grandes y pesadas células fitoplanctónicas (grandes diatomeas) o indirectamente, a través de la migración vertical de sus consumidores.

Aunque la dominancia heterotrófica del ecosistema fue encontrada la mayor parte del tiempo de observación en la zona, una deriva hacia la autotrofía es registrada ante condiciones ambientales extremas causadas por la surgencia costera, tal como fue el caso de abril del 2008 cuando el fitoplancton estuvo mayormente representado por grandes células de largas cadenas de diatomeas y dinoflagelados autótrofos (>50 µm), en comparación a los pequeños picoautótrofos que durante los otros periodos del año contribuyeron significativamente a la comunidad (>30% del total de la biomasa fitoplanctónica). Así, ante la mayor riqueza de nutrientes aportados por el afloramiento desde aguas subsuperficiales hacia la zona eufótica, se sugiere que la respuesta biológica de este ecosistema fue una sucesión fitoplanctónica, donde los pequeños productores primarios son reemplazados principalmente por grandes diatomeas, aparentemente por factores físicos (advección fuera de costa de pequeñas células e incremento del tiempo de residencia en capas superficiales de grandes autótrofos a causa de la surgencia), fisiológicos (mayor aprovechamiento de las altas concentraciones de nitratos por células más grandes y/o influencia de las bajas temperaturas en la capacidad funcional de las células picoplanctónicas), o incluso ecológicos (mayor impacto sobre la producción primaria del picofitoplancton por pastoreo del nano/microzooplancton). Sin embargo, a pesar del evidente cambio en la estructura comunitaria fitoplanctónica, al igual que en los

periodos más oligotróficos la producción primaria fue activamente consumida por organismos microzooplanctónicos, tales como ciliados y dinoflagelados mixotróficos, los cuales aparentemente también fueron favorecidos en su crecimiento (mayores biomasas) ante el enriquecimiento ambiental detectado en la zona. En consecuencia, se sugiere que en esta zona costera la trama trófica microbiana, incluyendo a las grandes células fitoplanctónicas como presas de consumidores microplanctónicos, es una componente bastante significativa en la dinámica del carbono, la cual coexiste con la clásica vía trófica herbívora (grandes células fitoplanctónicas → consumidores herbívoros → peces pelágicos) que comúnmente caracteriza a los sistemas productivos de surgencia costera.

Por lo tanto, este estudio sugiere que el ciclo del carbono en esta zona costera, no solo es influenciado por la variabilidad temporal en las condiciones físico-químicas de la columna de agua sino además, por la estructura trófica y relaciones ecológicas existentes entre las comunidades planctónicas microbianas que trasfieren el carbono incorporado al océano. Las fluctuaciones estacionales y/o interanuales en las condiciones abióticas de esta zona costera son moduladas por mecanismos físicos, tales como la surgencia costera, que favorecen el intercambio océano-atmósfera y en consecuencia la determinación de la dirección entrante o saliente del flujo de carbono. Sin embargo, dentro de este esquema ambiental y a una menor escala, se puede concluir que las tramas tróficas microbianas pueden influenciar significativamente a los flujos del carbono entre el océano y la atmósfera, a través del cambio temporal en la abundancia, composición y biomasa de sus componentes comunitarios, como también en la dinámica del crecimiento y mortalidad por consumo de sus poblaciones autótrofas y heterótrofas. Aunque estas conclusiones son basadas en un marco temporal esporádico de un sitio costero particular, pueden servir como fundamento inicial para futuros estudios y modelos biogeoquímicos que provean un entendimiento más global del ciclo del carbono en sistemas de surgencia costera de México, ante el patente cambio climático de la atmósfera y sus océanos adyacentes.

LITERATURA GENERAL CITADA

Azam, F., Fenchel, T., Field, J., Gray, J., Meyer-Reil, L., Thingstad, F. 1983. The ecological role of water-column microbes in the sea. Mar. Ecol. Prog. Ser., 10: 257-263.

Alvarez, M., Fernández, E., Pérez F. 1999. Air-sea CO_2 fluxes in a coastal embayment affected by upwelling: physical versus biological control. Oceanologica Acta, 22(5): 499-515.

Borges, A. 2005. Do we have enough pieces of the jigsaw to integrate CO_2 fluxes in the coastal ocean?. Estuaries, 28(1): 3-27.

Bottjer, D., Morales, C. 2005. Microzooplankton grazing in a coastal embayment off Concepción, Chile, (~36°S) during non-upwelling conditions. J. Plankton Res., 27(4): 383–391.

Calbet, A. 2001. Mesozooplankton grazing effect on primary production: A global comparative analysis in marine ecosystems. Limnol. Oceanogr., 46(7): 1824-1830.

Calbet, A. 2008. The trophic roles of microzooplankton in marine systems. ICES Journal of Marine Science 65, 325-331.

Calbet, A., Landry M. 2004. Phytoplankton growth, microzooplankton grazing, and carbon cycling in marine systems. Limnol. Oceanogr., 49(1): 51-57.

Chisholm, S. 2000. Oceanography: Stirring times in the Southern Ocean. Nature 407, 685-687, doi:10.1038/35037696.

Landry, M.R., Hassett, R.P. 1982. Estimating the grazing impact of marine micro-zooplankton. Marine Biology 67, 283–288.

Landry, M.R., Ohman, M.D., Goericke, R., Stukel, M.R., Tsyrklevichet K. 2009. Lagrangian studies of phytoplankton growth and grazing relationships in a coastal upwelling ecosystem off Southern California. Prog. Oceanogr., 83, 208-216.

Legendre, L., Rassoulzadegan, F. 1995. Plankton and nutrient dynamics in marine waters. Ophelia, 41, 153–172.

Legendre, L., Rassoulzadegan, F. 1996. Food-web mediated export of biogenic carbon in oceans: hydrodynamical control. Mar. Ecol. Prog. Ser., 145:179–193.

Legendre, L., Rivkin, R. B. 2002. Fluxes of carbon in the upper ocean: regulation by food-web control nodes. Mar. Ecol. Prog. Ser., 242, 95–109.

Legendre, L., Rivkin, R. B. 2005. Integrating functional diversity, food web processes, and biogeochemical carbon fluxes into a conceptual approach for modeling the upper ocean in a high-CO2 world. Journal of Geophysical Research, 110, C09S17, doi:10.1029/2004JC002530.

Linacre *et al., in prep*. Taxon-specific phytoplankton production and microzooplankton grazing impact dynamics during contrasting seasonal oceanographic conditions at a coastal upwelling station off Northern Baja California, México.

Neuer S., Cowles, T. 1994. Protist herbivory in the oregon upwelling system. Mar. Ecol. Prg. Ser., 113 (1-2): 147-162.

Pennington, J., Castro, C., Collins, C., Evans, W., Friederich, G., Michisaki, R., Chavez, F. 2007. A carbon budget for the northern and central California coastal upwelling system. Continental Margins Task Team, The Synthesis Book. Chapter 2.2, California Current System. Springer-Verlag, New York. 32 pp.

Rivkin, R.B., Legendre, L. 2002. Roles of food web and heterotrophic microbial processes in upper ocean biogeochemistry: Global patterns and processes. Ecol. Res., 17: 151–159.

Ryther, J. H. 1969. Photosynthesis and fish production in the sea. Science, 166: 72–76.

Sarmiento, J., Gruber, N. 2002. Sinks for anthropogenic carbon. *In* Physics Today 55(8), p30-36.

Sherr E. y B. Sherr. 1988. Role of microbes in pelagic food webs: A revised concept. Limnol. Oceanogr., 33(5): 1225-1227.

Sherr, E., Sherr, B. 1994. Bacterivory and herbivory: key roles of phagotrophic protists in pelagic food webs. Microb. Ecol. 28: 223–235.

Sherr, E., Sherr, B. 2002. Significance of predation by protists in aquatic microbial food webs. Antonie van Leeuwenhoek, 81: 293-308.

Sherr, E., Sherr, B. 2007. Heterotrophic dinoflagellates: a significant component of microzooplankton biomass and major grazers of diatoms in the sea. Mar. Ecol. Prog.Ser., 352:187-197.

Teixeira I.G., Figueiras F.G., Crespo B.G., Piedracoba S. 2010. Microzooplankton feeding impact in a coastal upwelling system on the NW Iberian margin: The Ría de Vigo. Estuarine, Coastal and Shelf Science, doi:10.1016/j.ecss.2010.10.012.

Torres, R., Turner, D., Rutland, J., Sobarzo, M., Antezana T., González, H. 2002. CO_2 outgassing off central Chile (31-30ºS) and northern Chile (24-23 ºS) during austral summer 1997: the effect of wind intensity on the upwelling and ventilation of CO_2 – rich waters. Deep Sea Res., I, 49: 1413-1429.

Vargas, C.A., González, H.E. 2004. Plankton community structure and carbon cycling in a coastal upwelling system. II. Microheterotrophic pathway. Aquat. Microb. Ecol., 34, 165-180.

Vargas, C.A., Martínez, R.A., Cuevas, L.A., Pavez, M.A., Cartes, C., González, H.E., Escribano, R., Daneri, G. 2007. The relative importance of microbial and classical food webs in a highly productive coastal upwelling area. Limnol. Oceanogr., 52, 1495-1510.

Wassman, P. 1998. Retention versus export food chains: processes controlling sinking loss from marine pelagic systems Hydrobiologia 363: 29–57.

ANEXO 1. Tabla con la abundancia (células por litro) de los principales grupos funcionales autótrofos y heterótrofos registrados en la estación ENSENADA, localizada en la región costera nororiental de Baja California, México. Los grupos de picoplancton fueron identificados mediante citometría de flujo y fueron, *Prochlorococcus spp.* (PRO), *Synechococcus spp.* (SYN) y Bacterias Heterotróficas (H-Bact). Los grupos de nanoplancton y microplancton fueron identificados mediante microscopía invertida de epifluorescencia y fueron, flagelados autótrofos (Flag-A) y heterótrofos (Flag-H), Prymnesiofitas (Prym), Criptofitas (Cryp), dinoflagelados autótrofos (Dino-A) y heterótrofos (Dino-H) y diatomeas (Diat.). De muestras fijadas con Lugol fueron identificados los ciliados por microscopía invertida.

				Abundancia de células (# cél. L^{-1})										
				Autótrofos							**Heterótrofos**			
	Prof.	Luz	Total Fito	PRO	SYN	Flag-A	Prym	Cryp	Dino-A	Diat.	Flag-H	Dino-H	Ciliados	H-Bact
Crucero	(m)	%Io	(µgChl*a* L^{-1})	(cél. L^{-1} x 10^4)							(cél. L^{-1} x 10^4)			(cél. L^{-1} x 10^6)
Sep' 07	2	55.9	2.10	1,508	18,664	122	4	4	10	31	26	9	3	3,026
Sep' 07	7	23.4	2.93	1,832	15,960	255	44	7	24	27	31	8	6	2,320
Sep' 07	10	14.6	1.19	2,083	4,911	168	52	9	29	19	27	6	2	1,239
Sep' 07	35	1.1	0.57	146	1,112	199	49	10	39	14	52	29	1	1,052
Nov'07	10	13.5	0.86	1,752	7,046	265	32	83	3	6	47	9	0	1,121
Nov'07	20	6.1	0.83	3,170	4,628	168	60	43	0	1	67	0	1	720
Nov'07	30	2.3	0.68	4,641	3,473	148	40	43	23	0	24	14	1	629
Ene'08	5	24.9	1.50	3,305	22,323	238	36	23	26	2	48	18	1	2,569
Ene'08	20	1.7	2.67	1,232	13,968	297	83	23	69	13	21	52	2	1,810
Ene'08	30	0.3	0.75	486	4,161	211	29	23	42	1	46	26	1	1,117
Abr' 08	5	22.1	5.19	0	333	138	13	22	15	163	69	52	1	1,105
Abr' 08	10	8.0	12.52	0	277	90	29	13	38	92	46	55	8	686
Abr' 08	15	2.9	4.62	0	394	199	107	12	57	172	111	96	0	765
Ago'08	5	36.2	2.73	9,936	12,005	425	103	47	2	0	419	81	1	1,559
Ago'08	10	16.7	1.33	3,579	7,959	214	112	18	25	2	34	22	0	1,013
Ago'08	20	4.1	0.52	668	1,175	176	46	3	1	1	31	0	0	628
Nov' 08	5	47.2	1.37	8,812	10,493	44	190	65	14	17	140	83	0	1,613
Nov' 08	12	13.5	1.72	5,637	8,000	97	221	37	9	2	24	2	2	1,081
Nov' 08	30	1.1	0.39	1,131	631	82	40	18	3	1	58	19	0	537

ANEXO 2. Tabla con la biomasa (microgramos de carbono por litro) de los principales grupos funcionales autótrofos y heterótrofos registrados en la estación ENSENADA, localizada en la región costera nororiental de Baja California, México. Los grupos de picoplancton fueron identificados mediante citometría de flujo y fueron, *Prochlorococcus spp.* (PRO), *Synechococcus spp.* (SYN) y Bacterias Heterotróficas (H-Bact). Los grupos de nanoplancton y microplancton fueron identificados mediante microscopía invertida de epifluorescencia y fueron, flagelados autótrofos (Flag-A) y heterótrofos (Flag-H), Prymnesiofitas (Prym), Criptofitas (Cryp), dinoflagelados autótrofos (Dino-A) y heterótrofos (Dino-H) y diatomeas (Diat.). De muestras fijadas con Lugol fueron identificados los ciliados (Cil.) por microscopía invertida.

				Biomasa en Carbono (µgC L^{-1})												
				Autótrofos							**Total**	**Heterótrofos**				**Total**
Crucero	Prof. (m)	Luz %Io	Tot. Fito (µgChl*a* L^{-1})	PRO	SYN	Flag-A	Prym	Cryp	Dino-A	Diat.	**C-Auto**	H-Bact	Flag-H	Dino-H	Cil.	**C-Hetero**
Sep' 07	2	55.9	2.10	0.63	14.20	4.03	0.20	0.18	3.14	17.67	**40.05**	69.89	1.62	0.48	11.21	**83.20**
Sep' 07	7	23.4	2.93	0.77	13.37	7.44	0.91	0.31	4.60	16.95	**44.36**	54.56	3.32	0.26	21.14	**79.28**
Sep' 07	10	14.6	1.19	0.91	4.50	2.26	1.08	0.17	1.12	4.22	**14.25**	29.65	1.58	1.08	7.64	**39.95**
Sep' 07	35	1.1	0.57	0.07	1.02	8.99	0.37	0.16	0.81	1.79	**13.21**	25.19	0.31	0.51	2.55	**28.55**
Nov'07	10	13.5	0.86	0.66	4.51	2.91	0.30	1.34	0.80	1.44	**11.96**	23.93	1.56	0.93	3.23	**29.65**
Nov'07	20	6.1	0.83	1.20	3.21	2.03	0.72	0.80	0.19	0.44	**8.59**	15.37	1.68	0.15	5.92	**23.13**
Nov'07	30	2.3	0.68	1.78	2.38	6.48	0.34	0.61	2.49	0.18	**14.26**	13.43	2.52	0.06	10.92	**26.93**
Ene'08	5	24.9	1.50	1.25	14.29	4.11	1.36	0.29	1.32	1.54	**24.16**	56.01	5.80	2.39	1.71	**65.91**
Ene'08	20	1.7	2.67	0.49	9.57	2.85	0.84	0.30	1.97	5.57	**21.58**	40.25	0.91	0.96	9.40	**51.52**
Ene'08	30	0.3	0.75	0.21	3.13	3.05	0.30	0.23	3.45	0.89	**11.26**	24.84	0.91	0.55	3.55	**29.86**
Abr' 08	5	22.1	5.19	0.00	0.36	1.37	0.26	0.36	5.45	74.23	**82.02**	18.64	0.41	1.16	3.75	**23.97**
Abr' 08	10	8.0	12.52	0.00	0.27	1.02	0.58	0.36	16.26	45.09	**63.58**	11.57	0.67	3.00	20.63	**35.87**
Abr' 08	15	2.9	4.62	0.00	0.47	4.07	2.00	0.14	98.90	80.22	**185.80**	12.90	1.08	2.40	0.00	**16.39**
Ago'08	5	36.2	2.73	3.65	9.37	11.18	2.46	0.82	8.60	0.07	**36.14**	25.83	6.14	5.88	7.33	**45.18**
Ago'08	10	16.7	1.33	1.34	6.39	1.77	1.17	0.48	1.40	1.48	**14.02**	17.43	0.59	2.51	0.53	**21.06**
Ago'08	20	4.1	0.52	0.27	0.95	0.99	0.44	0.01	0.58	0.07	**3.31**	11.00	0.30	0.40	0.03	**11.73**
Nov' 08	5	47.2	1.37	3.02	7.64	1.47	2.97	1.10	1.17	10.15	**27.52**	26.20	1.96	2.77	0.06	**30.98**
Nov' 08	12	13.5	1.72	1.98	6.20	1.39	3.12	0.92	2.09	0.83	**16.54**	17.91	1.54	2.51	2.86	**24.82**
Nov' 08	30	1.1	0.39	0.42	0.50	0.63	0.30	0.20	0.18	0.51	**2.73**	9.24	1.28	0.70	0.03	**11.24**

ANEXO 3. Tabla con las tasas instantáneas diarias de crecimiento y de mortalidad por pastoreo ejercido por el nano y microzooplancton de los principales componentes autótrofos y heterótrofos registrados en la estación ENSENADA localizada en la región costera nororiental de Baja California, México. Las tasas de la comunidad picoplanctónica es decir de las poblaciones de *Prochlorococcus spp.* (PRO), *Synechococcus spp.* (SYN), picoeucariontes (PEUK) y Bacterias Heterotróficas (H-Bact), fueron basadas en cambios temporales de su abundancia celular. Las tasas de prymnesiofitas y diatomeas fueron basadas en los cambios de los pigmento específicos, Hex-fucoxantin (Hex-Fuco) y Fucoxantin (Fuc), respectivamente. Las tasas de la comunidad total de fitoplancton fueron basadas en los cambios temporales del total de clorofila *a*.

			Tasas instantáneas de crecimiento (μ) y de mortalidad (m) (día^{-1})										**Tot.Fito**			
	Prof.	Luz	PRO		SYN		PEUK		Prymnesiofitas		Diatomeas		**Total Chl*a***		H-Bact	
Crucero	(m)	%Io	μ	m	μ	m	μ	m	μ	m	μ	m	**μ**	**m**	μ	m
Sep' 07	2	55.9	0.39	0.57	0.78	0.71	1.02	1.07	0.44	0.09	1.24	0.60	**1.45**	**0.91**	0.65	0.67
Sep' 07	7	23.4	0.45	0.35	1.04	0.69	1.13	0.81	0.32	1.04	1.61	2.77	**1.62**	**2.64**	0.67	0.55
Sep' 07	10	14.6	0.31	0.54	1.23	0.46	1.29	0.43	0.34	0.00	2.05	0.00	**1.46**	**0.00**	0.45	0.36
Sep' 07	35	1.1	1.29	1.26	1.15	0.62	0.66	0.37	-0.04	0.00	-0.18	0.00	**0.43**	**0.78**	0.32	0.27
Nov'07	10	13.5	0.37	0.50	0.63	0.55	0.61	0.38	0.33	0.00	0.55	0.16	**0.71**	**0.41**	0.76	0.52
Nov'07	20	6.1	0.38	0.59	0.38	0.53	0.42	0.60	0.58	0.17	0.78	0.25	**1.22**	**0.81**	0.41	0.36
Nov'07	30	2.3	0.08	0.19	0.21	0.37	0.38	0.44	0.00	0.24	0.33	0.47	**0.69**	**1.01**	0.19	0.21
Ene'08	5	24.9	0.23	0.49	0.30	0.54	0.36	0.84	-0.01	0.09	0.09	0.00	**0.24**	**0.52**	0.74	0.60
Ene'08	20	1.7	0.24	0.39	0.43	0.52	0.22	0.74	0.07	0.50	0.14	0.40	**0.30**	**0.72**	0.53	0.40
Ene'08	30	0.3	0.45	0.74	0.64	0.66	0.70	0.59	1.12	0.00	1.00	0.00	**1.49**	**0.41**	0.35	0.51
Abr' 08	5	22.1			0.62	0.54	0.68	0.59	0.82	0.00	1.12	0.29	**1.57**	**0.44**	1.71	1.39
Abr' 08	10	8.0			0.68	0.54	0.69	0.50	-0.18	0.55	0.16	1.12	**0.36**	**1.27**	1.10	0.84
Abr' 08	15	2.9			0.05	0.16	0.22	0.41	-0.03	0.00	0.46	0.18	**0.60**	**0.34**	0.93	0.67
Ago'08	5	36.2	0.06	0.13	0.24	0.29	0.11	0.13	-0.26	0.00	0.06	0.00	**0.09**	**0.00**	0.54	0.42
Ago'08	10	16.7	0.93	0.52	0.65	0.47	0.42	0.34	0.68	0.21	0.76	0.34	**1.24**	**0.75**	0.54	0.50
Ago'08	20	4.1	2.10	1.45	2.11	1.36	1.51	1.21					**1.05**	**0.74**	1.43	1.53
Nov' 08	5	47.2	0.72	0.46	0.71	0.52	0.95	0.72	0.34	0.34	0.78	0.41	**0.67**	**0.56**	0.79	0.51
Nov' 08	12	13.5	0.72	0.45	0.63	0.39	0.47	0.66	0.86	0.40	0.79	0.43	**1.08**	**0.66**	0.46	0.39
Nov' 08	30	1.1	0.68	0.38	0.83	0.65	0.70	0.36	0.20	0.08	0.07	0.00	**0.87**	**0.78**	0.20	0.09

ANEXO 4. Protocolo del experimento de dilución abreviado a 3 tratamientos (10%, 30% y 100% de agua de mar sin diluír) realizado *in situ* en 3 niveles de profundidad en la estación ENSENADA, localizada en la región costera nororiental de Baja California, México. Técnica original modificada de Landry y Hassett (1982).

1) En las primeras horas de la madrugada (entre 2 y 3 AM aprox.) para evitar el contacto de las muestras con la luz solar, se procede a colectar agua de mar desde 3 niveles de profundidad que se basan en mediciones previas de la fluorescencia *in situ* en la columna de agua. Utilizando el perfil de bajada de fluorescencia *in situ*, se colecta agua de mar desde el nivel del máximo de clorofila y dos niveles a elegir sobre y bajo éste máximo, utilizando 3 botellas Niskin (15- L en total) por cada nivel de profundidad.

2) El volumen de agua de mar correspondiente a 2 Niskin (10- L) es utilizado para el llenado de las *"botellas de dilución"* con 3 tratamientos: 10%, 30% y 100% de agua de mar sin diluír, y para el llenado de las *"botellas de producción primaria"* (2 claras y 2 oscuras). La tercera botella Niskin (5- L), es utilizada para colectar directamente las muestras biológicas iniciales de cada experimento, las cuales solo provienen del agua de mar sin filtrar (100% de dilución). Estas muestras iniciales son para la determinación de: la concentración de clorofila *a* (Chl*a*) mediante fluorometría, la concentración de Chl*a* y otros pigmentos accesorios mediante High-performance liquid chromatography (HPLC), la abundancia y composición de células picoplanctónicas autótrofas (*Prochlorococcus spp.*, *Synechococcus spp.* y picoeucariontes) y heterótrofas (bacterias heterotróficas) mediante citometría de flujo, la abundancia y composición de células del nano y microplancton autótrofos y heterótrofos mediante microscopía invertida de epifluorescencia, la abundancia de ciliados fijados con Lugol y contados por microscopía invertida. Las *"botellas de dilución"* consisten en botellas de policarbonato transparentes con una capacidad de 2.0 L cada una. Las *"botellas de producción primaria"* son botellas de policarbonato transparentes con una capacidad de 250 mL cada una.

3) Por cada nivel de profundidad se enjuagan 2 veces todas las botellas de dilución y las botellas de producción primaria.

4) De las 2 Niskin asignadas por nivel se procede primero a tomar las muestras de producción primaria, utilizando 2 frascos de 250 ml oscuros y 2 frascos claros. Estas muestras son trasladadas al laboratorio húmedo para su inoculación inmediata.

5) De las mismas 2 Niskin anteriores se procede a filtrar agua de mar utilizando un sistema de filtración consistente en una bomba peristáltica, mangueras de silicón para las conexiones y un filtro cerrado de 0.1µm tipo cápsula (Acropak) que ha sido previamente lavado con HCl al 10% y enjuagado varias veces con agua destilada. Luego se llenan cada una de las botellas de dilución con el volumen requerido por cada tratamiento (10% y 30% de agua de mar sin diluír, es decir, 90% y 70% de agua de mar diluída, respectivamente), el cual es marcado previamente en cada botella con un plumón indeleble. Es importante considerar que la filtración de agua de mar se debe iniciar desde la muestra más profunda (menos carga de partículas) hasta la más superficial (más carga de partículas).

6) Después de colocar el agua de mar filtrada, se procede a rellenar las botellas de dilución hasta el tope con agua de mar colectada directamente de la Niskin, según el tratamiento correspondiente (10%, 30% y 100%) por cada nivel de profundidad, y se almacenan momentáneamente hasta su anclaje en una caja protegida de la luz.

7) De la tercera Niskin asignada por nivel se procede a enjuagar 2 veces los frascos y luego tomar las muestras iniciales en el siguiente orden: clorofila *a* (3 réplicas de 250 mL c/u), HPLC (2 réplicas de 1 L c/u), microplancton (de 250 a 500 mL dependiendo de la biomasa planctónica de la zona y de la profundidad), nanoplancton (50 mL) y Lugol (250 a 125 ml dependiendo de la biomasa planctónica de la zona y de la profundidad).

8) Directamente desde las botellas de dilución se toman las muestras iniciales de picoplancton para cada uno de los 3 tratamientos de dilución.

9) Después, se procede a incubar en el mar las botellas de dilución junto con las de producción primaria por aproximadamente 24-h. Para ello se utiliza un sistema de anclaje que va fijado a la boya de monitoreo del CO_2, consistente en: bolsas hechas con redes por cada nivel de profundidad y que contienen a las botellas, boyas

superficiales que mantienen todo el sistema en la columna de agua, un peso muerto que permite el anclaje al fondo y una bandera de señalización. El lapso de tiempo desde la colecta de agua de mar al anclaje no debe ser mayor a 3 horas. Este sistema de incubación se esquematiza a continuación:

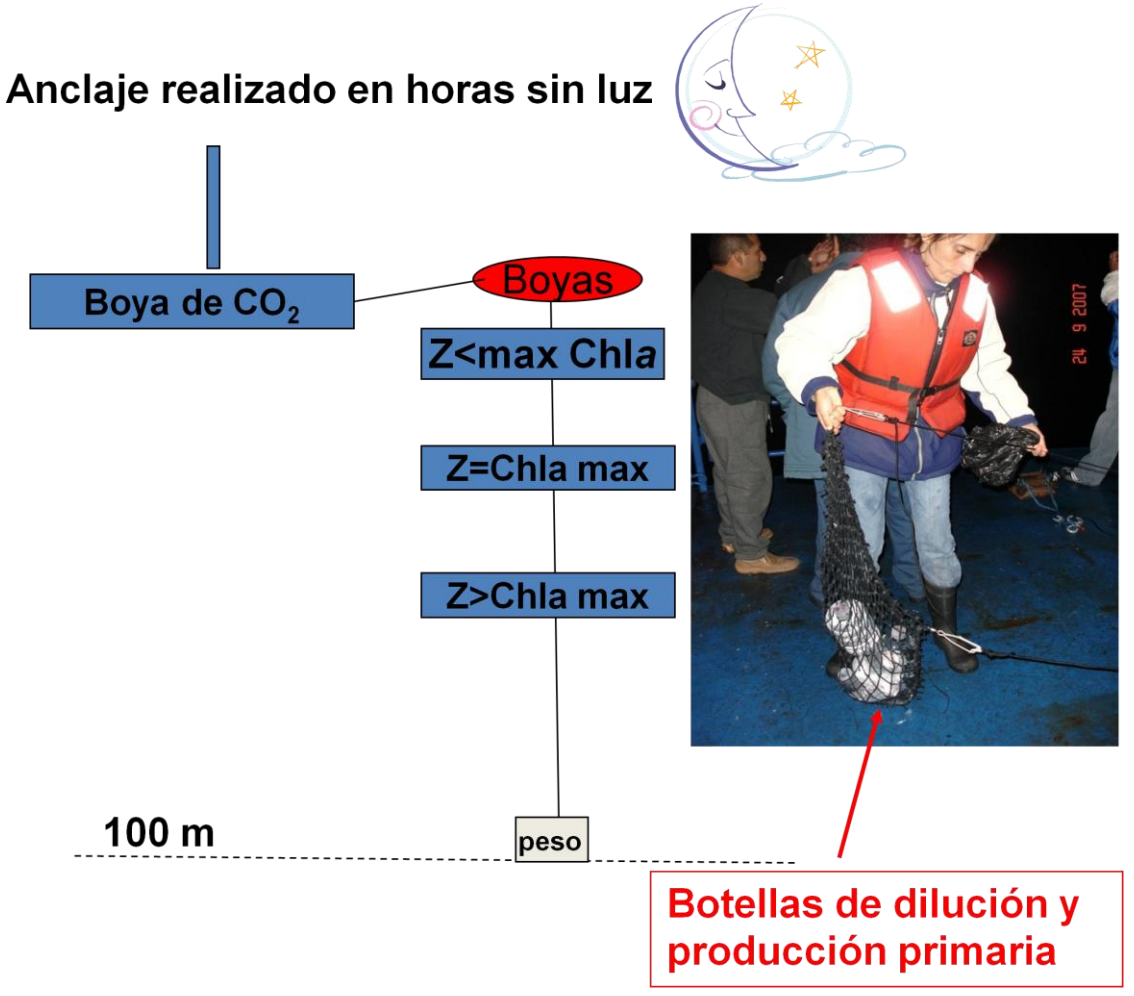

10) Posterior a la incubación en el mar por aproximadamente 24 horas, se procede a retirar el anclaje antes del amanecer para evitar el contacto de las muestras con la luz solar. Las botellas experimentales se almacenan momentáneamente para su traslado al laboratorio en una caja protegida de la luz.

11) En el laboratorio, se proceden a colectar directamente desde cada uno de los tratamientos de dilución, las muestras finales de cada experimento que fue realizado en cada uno de los 3 niveles de profundidad. Las muestras finales se colectan en el siguiente orden: clorofila (2 réplicas de 250 mL c/u), HPLC (1 L), picoplancton (2

mL), microplancton (de 250 a 500 mL dependiendo de la biomasa planctónica de la zona y de la profundidad), nanoplancton (50 mL) y Lugol (250 a 125 ml dependiendo de la biomasa planctónica de la zona y de la profundidad). Asimismo, todas estas muestras al igual que las colectadas al inicio de cada experimento son preservadas y analizadas utilizando las técnicas adecuadas para cada caso y que fueron descritas en las secciones metodológicas de los capítulos 2 y 3 de este documento de tesis.

12) Las concentraciones iniciales y finales de los pigmentos así como las abundancias iniciales y finales de los distintos organismos autótrofos y heterótrofos categorizados por tamaño (pico, nano, microplancton) se expresan en términos de biomasa de carbono utilizando conversiones de la literatura (picoplancton) y mediciones geométricas de las células (nano y microplancton). Asimismo, basado en el cambio temporal de estas mediciones durante la incubación en el mar, se realizan estimaciones de las tasas instantáneas de crecimiento y mortalidad por pastoreo siguiendo la ecuación dada por Landry y Hassett (1982): $k_i = \ln(C_t/C_o)/t$, donde k_i es la tasa de cambio neto, C_t y C_o la concentración o abundancia celular inicial y final, respectivamente y t es el tiempo de incubación expresado en días. Mayores detalles de la técnica y sus estimaciones pueden ser encontradas en las secciones metodológicas de los capítulos 2 y 3 de este documento de tesis.